Annual Report

2010

HELMHOLTZ | ASSOCIATION

Helmholtz Institute Jena

Helmholtz Institute Jena
Helmholtzweg 4
07745 Jena
www.hi-jena.de

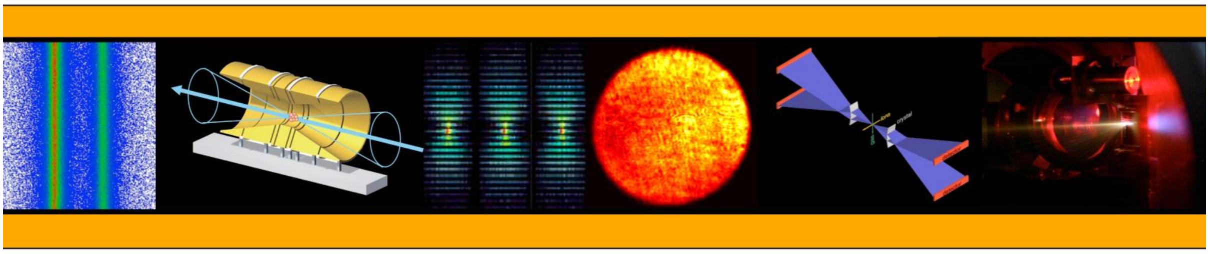

seit 1558

Helmholtz-Institute Jena

Annual Report 2010

Contents

Introduction

The objective of the recently established Helmholtz Institute Jena (HI-Jena) is excellence in fundamental and applied research, in particular research on structure of matter based on high-power lasers, accelerated particles, and x-ray science. Emphasis is on research at the interface of particle accelerators and lasers in order to harvest well-established and yet to discover synergies.

At the junction of these, to date, primarily independent research fields, HI-Jena is expected to create scientific and technical foundations for exploiting this enormous potential. As a consequence, research activities at the two large accelerator projects, the European X-FEL and the international FAIR facility, where the Helmholtz Association is strongly involved, are central to the HI-Jena.

The institute is located on the campus of the Friedrich Schiller University Jena (FSU) as a branch of GSI Helmholtz Center for Heavy Ion Research, with the Helmholtz-Centers DESY and HZDR, and FSU as partner institutions.

The Mission Statement of HI-Jena combines the following key aspects of activity:

- Within the Helmholtz Association the HI-Jena, in concert with the above partners, acts as a competence center for innovative high-power lasers, light sources, and for associated optical components.
- The HI-Jena serves as an interface for future advancements of conventional and laser based acceleration of electrons and ions.
- The HI-Jena will develop and advance innovative ideas in measurement techniques and diagnosis applicable to the investigation of light-matter interactions.
- The HI-Jena will develop new schemes for future experiments in the fields of the physics of extremely strong electromagnetic fields and of warm dense matter and will check their feasibility in pilot experiments at the existing facilities.

The Annual Report 2010 contains substantial contributions to all of these fields, which are ordered in context with the main Research Areas of the HI-Jena:

1 - Improving Petawatt Lasers

2 - Merging advanced solid-state laser technology with FEL sources

3 - Laser-driven particle acceleration, particle diagnostics

4 - X-ray science including high-resolution x-ray spectroscopy, polarimetry and laser-based x-ray generation

5 - Quantum field theory and relativistic ionization

Each section is introduced separately giving a summary of the main physical results and technical achievements.
A list of publications, which appeared in peer-reviewed journals during 2010, concludes the present report.
We would like to underline that most of the contributed work was performed in close cooperation with scientists from the partner institutions named above.

Research Area 1: Improving Petawatt Lasers

Research area 1 (RA1) is dedicated to the high-peak-power diode-pumped laser development, which includes the improvement of existing systems (PHELIX, POLARIS) as well as the development of future laser technology. In particular, RA1 deals with research for new laser materials, coatings, extraction schemes, chirp compensation and temporal contrast. The focus is also put on exploring beam quality improvements, high repetition rate and energy efficiency via advanced cooling schemes. Since the requirements for large laser systems in fundamental research are changing together with the development of the experiments for which they are used, a continuous work on laser improvement is demanded.

A foremost project (uOPA) is the development of a picosecond laser-pumped optical parametric amplifier (OPA) front-end for the PHELIX laser system. The replacement of traditional laser preamplifiers by OPAs, that are pumped by a rather short pulse, provides the advantage of a considerably increased pulse-to-background intensity contrast. The reason is that conventional amplifiers using stimulated emission always produce a background radiation called amplified spontaneous emission (ASE) in a time window of the radiation life time of excited states of the used material. In case of the preamplifiers of PHELIX, it is determined by the regenerative laser cavity round-trip time of ~10 ns. A contrast improvement in that time range is expected with the amount of amplification of the OPA, what can be about 10^5. The central issue of this solution gravitates around the pump laser that has advanced requirements not met by commercial lasers. The short pulse has to be stable within all parameters including the delay to the femtosecond pulse that has to be amplified by the OPA. The development of a diode-pumped regenerative amplifier following two fiber pre-amplifiers should solve this task, as optical synchronization is reached by the amplification of a spectral part from the main femtosecond pulse. Within the project, an innovative approach for chirped pulse amplification (CPA) lasers using a volume-bragg-grating for stretching and compression is examined. The pump laser system was so far developed in Jena and is actually transferred to Darmstadt. Calculations for the OPA are finished.

The second project (POLAR) includes all the work required in order to fully assemble and commission the final amplifier A5 of POLARIS. The increase in peak power by the higher energy of this amplifier turns the system into a world unique tool with certain parameters that could be especially used for laser ion acceleration. Nevertheless the design of the amplifier was made years ago, some technical problems have to be overcome. Electronics and mechanical parts were assembled last year and first amplification tests are actually going on.

The project CRYO summarizes all efforts in applying cryogenic techniques to Yb-doped materials. Cryogenic cooling allows an improved efficiency of quasi-three-level lasers, like that based on Yb^{3+}, because the low laser levels are less populated by thermal excitation. Consequently, the single-pass gain increases and energy extraction becomes easier. Additionally, the low temperature helps for heat removal from laser materials, since typically the thermal conductivity increases with lowering the temperature. In 2010, the project has developed around two lines: efforts are being made on reducing the heat dissipation in the host crystals (see the contribution to this report) and second, emphasis is put on heat removal at low and high thermal load levels. This results in building a laser amplifier with a high-pressure He-gas cryogenic cooling system, suitable for the POLARIS A4 amplifier, and allowing for a total heat load of the laser head of 1 kW, which needs to be dissipated at a temperature of 80K from a volume of only 36 ml. The development of this gas-cooled laser head can be seen as a demonstrator for short-pulse high energy production with lasers at much higher total power levels than those actually available. The status of this project in 2010 is that the design of the cryogenic system has been outsourced to CEA in France, where a strong expertise in cryogenics has been identified as a mandatory asset.

A hybrid fiber-Yb:KYW picosecond laser for optical parametric amplifier pumping

V. Bagnoud[1,2], C. P. João[3], J. Körner[4], J. Hein[4], T. Gottschall[5] and J. Limpert[2,5]

[1]GSI Helmholtzzentrum für Schwerionenforschung GmbH, Planckstraße 1, 64291 Darmstadt, Germany; [2]Helmholtz-Institute Jena, Jena, Germany; [3]Instituto de Plasmas e Fusão Nuclear, Lisbon, Portugal; [4]IOQ, Friedrich Schiller University, Jena, Germany; [5]IAP, Friedrich Schiller University, Jena, Germany

Introduction

Laser-plasma interaction studies clearly show that many processes are strongly influenced by the temporal contrast of the laser pulse used to initiate the plasma. This aspect has grown in interest in the past years, motivated by the ever-increasing on-target intensities achieved by short pulse lasers. One of the problems lies in the existence of a nanosecond-long pedestal that is created during the amplification process by amplified spontaneous emission (ASE). A novel solution relies on the use of time-gated laser amplifiers based on optical parametric amplification (OPA) rather than standard laser amplification[1]. In order to efficiently eliminate the pulse pedestal, the parametric amplifier[2] should operate with pump pulses at or below 1 picosecond pulse duration. Such a pump laser system, which we plan to implement on the PHELIX[3] laser facility at GSI is not commercially available and therefore must be developed.

Laser architecture

One of the main requirements of the parametric amplifier is the need for a precise, low-jitter timing between the pump and seed pulses. In an effort to reduce the temporal jitter to well below one picosecond, we use a single laser oscillator for generating both pump and seed pulses and additionally, we optimized the pump laser architecture to minimize its optical length.

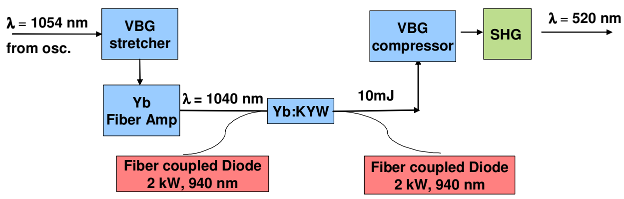

Figure 1: schematics of the OPA pump laser amplifier. VBG: Volume Bragg Grating, SHG: frequency doubling crystal

The OPA pump laser architecture depicted in figure 1 is that of a chirped-pulse amplifier. The laser pulses are generated by a commercial short pulse laser (Mira, Coherent) tuned at 1054 nm to match the gain bandwidth of PHELIX Glass amplifier. One part of the beam is then used to seed the OPA, while the other part is amplified in the OPA pump laser. The OPA pump amplifier exploits the broad amplification-spectrum properties of Ytterbium-doped KYW. Such a material exhibits the spectral bandwidth necessary to support sub-picosecond laser pulses. However, the gain spectrum of this material is not centered at the oscillator frequency but rather shifted by 14 nm at 1040 nm. To circumvent this problem, a fiber preamplifier is added to the laser, with the goal of shifting the oscillator frequency and also providing initial single-pass amplification to the microjoule level on two stages.

Achievements in 2010

The fiber amplifier is made of a 1.2 m long step index fiber which is pumped by 0.7 W of a CW laser diode. The amplifier is tuned to generate 300-mW output power at 1040 nm and 72 MHz repetition rate. After reducing the repetition rate to 1 MHz be means of an acousto-optical modulator, the pulse are further amplified in a 1.2-m-long double-clad fiber (Crystal Fibre, DC-135-15-PM). At the output, 1-W average power and 1-µJ pulse-energy are achieved.

At this point, we have successfully compressed the laser pulses to verify that nonlinear effects in the fiber were not degrading the temporal quality of the pulses.

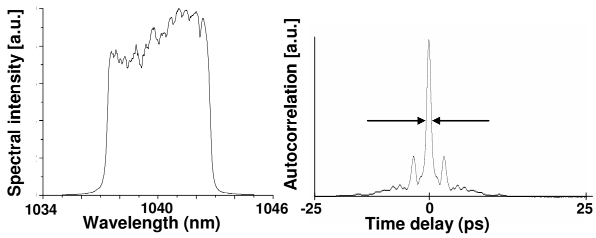

Figure 2: autocorrelation (left) and spectrum (right) of the pulse after amplification. The autocorrelation width is 1.17 ps.

The plots in figure 2 show the pulses and spectrum obtained after compression. Although the laser pulse is not fully compressed due to imperfections in the volume Bragg grating, the dependence of the pulse duration on the pulse energy demonstrate the negligible influence of the nonlinear effects.

In the next months, we will complete the Yb:KYW amplifier and incorporate it to the pump laser. The pump pulses will then be frequency doubled and used in the OPA setup.

[1] C. Dorrer et al., Optics Lett. **32**, 2143 (2007)
[2] J. Fils et al., this report
[3] V. Bagnoud et al., Appl. Phys. B **100** (1) 137 (2010)

Implementation of uOPA @ PHELIX: Mirò simulations and code validation

J. Fils[1,2], V. Bagnoud[1,2], T. Stöhlker[1,2]

[1] Helmholtz-Institute Jena, Jena, Germany; [2]GSI Helmholtzzentrum für Schwerionenforschung GmbH, Planckstraße 1, 64291 Darmstadt, Germany;

Introduction

Experiments with Petawatt lasers are often limited by the existence of a pre-pulse that is pre-heating the target before the high-power main pulse arrives[1]. One compact and simple way to improve the PHELIX laser front-end contrast to 10^{11} is to implement the new concept of Ultrafast Optical Parametric Amplification (uOPA)[2]. The amplification noise, responsible in a classical Chirped Pulse Amplification (CPA) scheme for contrast degradation, is in this case limited to the interaction time of some picoseconds during the pump-seed Optical Parametric Amplification (OPA).

The uOPA setup consists of a 100 fs front-end oscillator at 1054 nm divided into pump and seed pulses. The pump laser, described elsewhere[3], will provide 5-mJ pulses at 10-Hz repetition rate and 520-nm central wavelength. Both seed at 1054 nm and pump at 520 nm are then recombined in a second non linear crystal by difference frequency generation (DFG). Non linear crystal nature and geometry for second harmonic generation (SHG) and DFG are key points of the system. We performed with the Mirò[CEA, 4] software simulations to determine the optimal performances.

Crystal choice and performances

Crystals have to fulfill specific requirements such as a high damage threshold (input beams have intensity of some tens of GW/cm^2), high non linear coefficients for reducing the crystal thickness that produces unwanted walk-off effect and must remain cost-effective. Beta-Barium Borate (BBO) and Lithium Triborate (LBO) crystals used in type I configuration are good candidates.

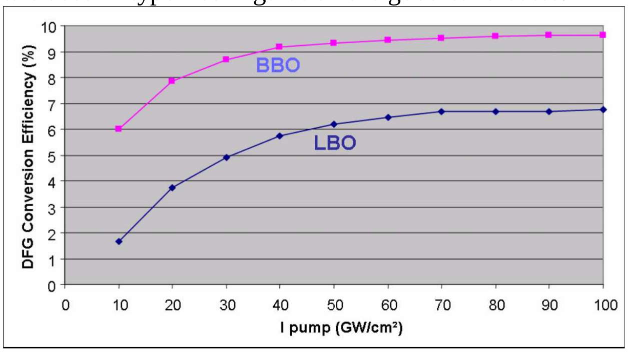

Figure 1: DFG Conversion Efficiency (in %) from 520-nm pump to 1054-nm signal vs. pump input intensity for both BBO and LBO crystals.

We compare crystals by simulating DFG conversion efficiencies from the 520-nm pump to the 1054-nm signal. The intensity is set to some tens of GW/cm² for the pump pulse and a few KW/cm² for the seed pulse; and the spectral widths are set to 4.5 and 16.5 nm respectively. Temporal and spatial profiles are Gauss-shaped. For discriminating purpose, the two beams make a 0.5° angle. Results in % are depicted in figure 1. BBO crystals offer obviously a higher conversion efficiency for the same pump intensity and are therefore recommended for this application.

Simulations using experimental beam parameters show that SHG conversion efficiency yields more than 62 % with a 1 mm-thick BBO crystal and a pump input at 1040 nm of 64 GW/cm². DFG is then optimal with a 2.9 mm-thick BBO crystal with a energy transfer reaching 12 %, which means a seed energy output of 0.9 mJ.

Code validation

To validate the previous Mirò simulations, we performed a SHG experiment with the PHELIX fs front-end at 1054 nm. Comparison between measurements and results given by Mirò are plotted in figure 2. Experimental spatial and temporal beam parameters have been used in the calculation. SHG Conversion Efficiency (in %) is drawn vs. input energy at 1054 mn. According to intensity measurement inaccuracies, simulation and experience matches quite well (± 5%).

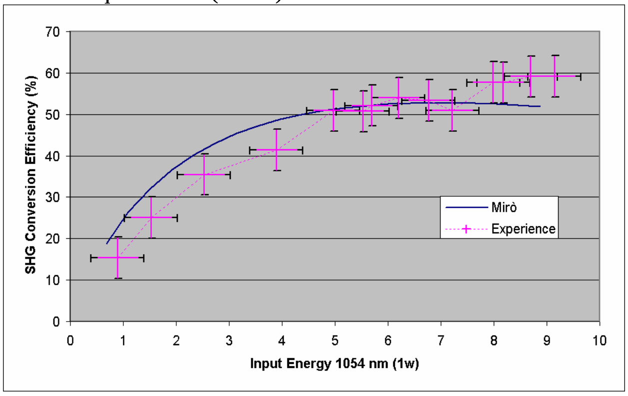

Figure 2: SHG Conversion Efficiency vs. input energy (in mJ). Experience (solid curve) and Mirò simulations (dashed curve) are compared.

Next steps will be to build and test the uOPA setup in coming year 2011.

[1] T. Wittmann et al., Rev. of Sc. Inst. 77, 083109 (2006)
[2] C. Dorrer et al., Opt. Lett. 32, 2143 (2007)
[3] V. Bagnoud et al., This report
[4] E. Bordenave, T. Chies, J. Phys. IV France **133** 661-663 (2006)

POLARIS - recent developments and current status.*

S. Keppler[1], R. Bödefeld[2], A. Sävert[1], M. Hornung[2], J. Hein[1], and M. C. Kaluza[1,2]

[1]Institute for Optics and Quantumelectronics, Jena; [2]Helmholtz Institute Jena

Performance of the Polaris laser system

The current status allows up to $8\,\mathrm{J}$, before the compressor, a mean pulse duration of $200\,\mathrm{fs}$ and a focal spot of $8.1\,\mu\mathrm{m}^2$ (FWHM) in a daily operational mode. This corresponds to a peak power of $25\,\mathrm{TW}$ and a peak intensity on target of $8 \times 10^{19}\,\frac{\mathrm{W}}{\mathrm{cm}^2}$ [1].

Frontend and multipass amplifiers

The frontend of Polaris consists of the oscillator, two regenerative amplifiers, A1 and A2, and a pulse stretcher. The amplifiers were improved in stability, by excluding turbulent air and reducing the output energy to $40\,\%$ of the maximum parameters achievable with each amplifier. The first regenerative amplifier A1 now operates with a gain of 10^4 and an output energy of $25\,\mu\mathrm{J}$. The A2 was reduced to a gain of 0.5×10^4 and has an output energy of $20\,\mathrm{mJ}$. Additionally the amplifiers were encased in tight boxes which improved the stability drastically. The spectral bandwidth of the frontend, affected by gain narrowing effects, was maximized by optimizing the bandwidth of each amplifier by the use of multi-order halfwaveplates. Finally, the Polaris frontend provides $20\,\mathrm{mJ}$ with an energy stability of $\pm 5\,\%$ and a spectral bandwidth of $15\,\mathrm{nm}$.

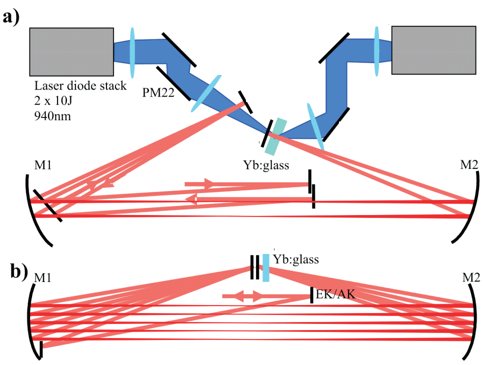

Figure 1: Outline of the amplifier A2.5 in top view (a) and side view (b). The amplifier is pumped with 2 10 J - laser diode stacks. The beam is imaged with the mirrors M1 and M2 with a focal length of $1.25\,\mathrm{m}$.

Due to the reduced output energy of the frontend and the reduction of the pass number of the amplifier A3 due to contrast issues, it was necessary to introduce an additional amplifier into the Polaris laser chain. The amplifier A2.5, a relay imaging multipass amplifier with a gain factor of 8, ensures the output energy of $8\,\mathrm{J}$ out of the amplifier A4 in the daily operational mode. The multipass amplifiers were also encased in tight boxes, which improves both the pointing stability and the energy stability. The amplifier A2.5 amplifies the beam up to $160\,\mathrm{mJ}$, A3 up to $960\,\mathrm{mJ}$ and finally the A4 output energy is $8\,\mathrm{J}$. Note that the specified values for the output energy are the daily ensured values and not the maximal values of the amplifiers.

* Work supported by BMBF (contract no: 03ZIK052 and 03ZIK445), and the EU (Laserlab Europe)

Contrast improvement

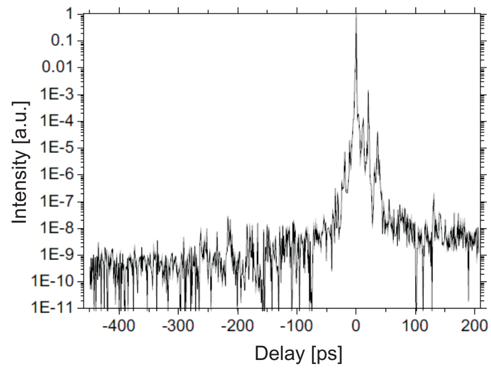

Figure 2: Contrast measurement after the contrast improvement with the Sequoia (Amplitude Technology). Negative time delays represents times before the main pulse.

A main issue in the last year was the improvement of the contrast ratio of the Polaris frontend. Existing prepulses on the ns- and ps-timescale were investigated and suppressed. For this, photodiodes only allow a high contrast measurement of up to 8 orders of magnitudes of more than $4\,\mathrm{ns}$ before the main pulse due to the ASE of the regenerative amplifiers. To investigate the time window of $4\,\mathrm{ns}$ before the main pulse, the Sequoia, a third order cross correlator, which scans the time before the main pulse with a replica of the main pulse itself, was extended in terms of the measurement range in time from $-450\,\mathrm{ps}$ to $-3.5\,\mathrm{ns}$. The result of the measurement were prepulses up to 10^{-5} corresponding to the time difference of the round trip time of A1 and A2 and a prepulse train with a period equal to the time difference of the round trip time of the oscillator and A1. By synchronizing the round trip times of the amplifier A1 to the A2 as well as both to the oscillator, the prepulses could be shifted in time under the main pulse [2]. The improved contrast ratio was measured to better than 10^{-7}.

References

[1] M. Hornung *et al.*, Appl. Phys. B, (2010) 101: 93102.

[2] S. Keppler *et al.*, to be submitted to Applied Physics B

Cryogenic Amplifiers*

M. Kahle[1], J. Hein[1], J. Körner[1], H. Liebetrau[1]

[1]Helmholtz-Institut Jena, Germany

A promising method to reduce the thermal load in the laser medium is the usage of cryogenic amplifiers. The cryogenic cooling is applied to change the spectra of the laser material and improve the laser performance. The changes in the spectra can be used to change the laser- and pump-wavelength and thus decrease the quantum defect and prevent heat from emergence. Yb^{3+}-doped gain-media are good candidates for such efficient lasers since they have a broad spectrum, a long fluorescence lifetime, a quantum efficiency close to one and they can be pumped directly by laser diodes.

In 2010 we analysed various Yb^{3+}-doped laser materials including CaF_2 and YAG with regards to their absorption- and emission-characteristics while adjusting the temperature between 300K and 100K with a liquid nitrogen cryostat. The samples were placed in a vacuum chamber to prevent condensation. Fluorescence spectra were measured by imaging the irradiated sample surface onto the spectrometer with high depth-discrimination to prevent reabsorption. For the laser wavelengths the fluorescence intensity was found to be increasing and the reabsorption is decreasing with lower temperatures. Also the absorption at certain pump wavelengths is increasing. For some materials including Yb:YAG there is an optimal temperature below witch further cooling is not useful.

Based on the results of these experiments simulations were performed to estimate the performance of a laser amplifier made of the respective material over the measured temperature range. The simulations include reabsorption effects, estimation of the optimal length of the material with certain doping level, and pump saturation effects.

For the materials of interest we also performed temperature dependent gain measurements in a multi-pass-amplifier. The temperature was again varied between 100K and 300K by transverse cooling. The amplifier itself is a mirror based 4-f relay imaging setup to provide a good beam quality. For example, with Yb:YAG we achieved an output energy of 1.1 J and an optical-to-optical-efficiency of more than 45%. The complete results are going to be published when they are fully analysed.

Another approach that we are working is to further increase laser efficiency by pumping Yb:CaF at 980nm and lasing at 992nm with a quantum defect of about 1%. Because of the otherwise to high reabsorption this is only possible at cryogenic temperatures. Due to the fact that the dynamics of the laser processes with reabsorption are not completely understood we decided to try the new concept at first on a cw-laser. The setup can easily be modified for amplifiers later. Because of the difficulties with wavelengths that are so close together a disc laser setup was chosen. The prototype is currently being tested and adjusted under vacuum conditions and cryogenic temperatures. Figure 1 shows the construction scheme of the disc laser witch had to be put upright to provide a symmetrical cooling of the disc with the nitrogen cryostat. During our preparations it was shown by another workgroup that lasing at 992nm with a tunable Yb:CaF-laser is possible [1] though their setup was not optimized for operation at 992nm.

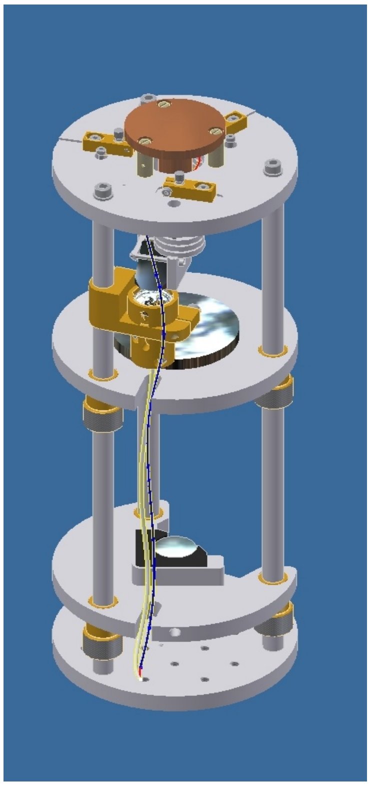

Figure 1: disc laser setup for operation under vacuum conditions at low temperature

Conclusion and Outlook

Various important Yb3+-doped laser materials were analysed with regards to their crosssections and gain in laser amplifiers at temperatures between 300 and 77K. The complete results are going to be published in 2011. The prototype for a highly efficient cryogenic disc laser is prepared for operation and is going to be finished in 2011.

References

[1] S. Ricauld, D. N. Papadopoulos, P. Camy, J. L. Dou-alan, R. Moncorgé, A. Coujaud, E. Mottay, P. Georges, and F. Duron, "Highly efficient, high-power, broadly tun-able, cryogenically cooled and diode-pumped Yb:CaF2", Optics Letters 35 (2010) p.3757

* Work supported by Laserlab Europe under Contract No. 228334; ELI-PP FP7 Grant Agreement No. 212105; and the OPTIMAL-Project of TMBWK under Project No. B715-09012 and B514-09050

Research Area 2: Merging advanced solid-state laser technology with FEL sources

The focus of this research area is the development and application of high-performance solid-state laser technology. For example high-repetition-rate phase-stabilized few-cycle lasers will be developed for seeding of the free-electron laser FLASH at DESY, for two-color pump-probe experiments and eventually for the generation of intense attosecond hard x-ray pulses at the European XFEL (X-Ray Free-Electron Laser). To meet the extreme laser requirements, novel innovative laser amplifier technologies have to be tested regarding their power handling capabilities and nonlinear limitations.

Especially, fiber-based laser systems are known for excellent beam quality, which is nearly independent of the emitted average power but also restricted by nonlinearities. In combination with the steady improvements in Chirped Pulse Amplification (CPA) technology and the increase in the available fundamental mode area, fiber-based ultra-short pulse amplifiers have been successfully developed. In order to extract the highest pulse energies and highest average powers from such amplifiers, novel Yb-doped fibers with ultra-large core diameters are developed and employed in femtosecond laser systems. Furthermore, optimized OPCPA technology is explored. It is known to be superior to conventional laser technology in terms of pulse contrast and amplification bandwidth. Even amplification of few-cycle laser pulses is feasible. However, thermo-optical limitations have to be investigated and evaluated to permit reliable operation of OPCPA-based lasers at high repetition rates and average powers. Furthermore, OPCPA-based, compact and robust front-end laser systems with exceptional pulse contrast are developed and will be employed at large scale laser facilities, such as PHELIX at GSI Darmstadt, in order to improve their performance and reliability.

Development of high repetition rate laser amplifier systems for applications at free electron laser sources*

F. Tavella[1], A. Willner[1,2], M. Schulz[2,4], R. Riedel[1], E. Seise[1,3], T. Gottschall[3], S. Hädrich[1,3], J. Rothhard[1,3], J. Limpert[1,3], H. Schlarb[1,2], S. Düsterer[1,2], A. Tünnermann[1,3], J. Feldhaus[1,2], M. Drescher[4], J. Rossbach[4]

[1]HI-Jena, Germany; [2]DESY, Hamburg, Germany, [3]IAP Jena, Germany, [4]Universität Hamburg, Germany

Several applications at Free Electron Laser (FEL) sources require laser amplifier systems. Applications such as an injector laser amplifier, optical pump-probe laser amplifiers and a laser amplifier system for FEL seeding, to name a few. A common requirement of these amplifier systems is the need of extreme reliability in operation with marginal downtime. Additionally, Free Electron Lasers such as the FLASH and the European XFEL require very high repetition rates, a MHz burst-mode in 10 Hz macro-pulses. The required pulse energy for FEL seeding is on the mJ-level, the pulse duration depends on the seeding mode. 20-30 fs pulse duration is required for High Gain Harmonic Generation and few-optical-cycle pulses with ~6-7 fs pulse duration are required for direct seeding of single longitudinal modes in the XUV region. Such laser parameters are not commercially available.

The first application of the planned laser amplifier development is seeding of the FLASH-II FEL. The planned parameters are few mJ pulse energy, ~7fs duration in a 10 Hz burst mode with burst repetition rate of 1MHz (100 kHz for the laser amplifier prototype) with 800 pulses in the burst. This laser amplifier needs a pump amplifier system with even more demanding parameters. The pump amplifier is based on a fiber amplifier front-end and an Yb:YAG booster amplifier. The central wavelength is 1030 nm, the pulse duration needed for the pumping of two Optical Parametric Amplifier (OPA) stages is <1ps and the total required pulse energy is >20 mJ which leads to a total burst average power of >20 kW for the 1 MHz final version of the amplifier system. While the first prototype will be operated at reduced repetition rate of 100 kHz, an upgrade to 1 MHz (4.5 MHz for the European XFEL) is already planned. The following two sections will explain the progress made for the prototype amplifier system and also the progress on the XUV seed source development.

Laser amplifier development

The functionality of the OPCPA concept with sub-ps pump pulses has been tested using a fiber CPA amplifier system. The fiber pump amplifier delivers up to 500 µJ of pulse energy at up to 100 kHz burst or continuous repetition rate. The second harmonic is used to pump an OPCPA stage (double passed) amplifying a broadband seed to several tens of micro-joules. The seed from a Ti:Sapphire oscillator is first stretched in a down-chirped strecher-compressor scheme consisting of a prism stretcher and spatial light modulator in 4-f geometry combined with a glass compressor. The pulses can be compressed to close to their transform-limited duration of 7 fs [2,3]. This system was also used to generate higher order harmonics at high repetition rates in a single gas-jet [4]. Further steps to reach the mJ amplification level include the development of the pump amplifier system. Two different techniques are pursued to further amplify the output of the fiber pump amplifier system. Slab amplifier technology offers the advantage of high average power and high gain with excellent beam quality. Thin-disk amplifier technology offers also the advantage of high average power but with a rather small single pass gain in multi-pass geometry. In recent experiments, the output of the fiber amplifier was further amplified with a slab amplifier (Amphos) to 200 W average power at repetition rate of (12.5-)100 kHz and the output pulses were recompressed to sub-ps duration.

* Work supported by Helmholtz Institut Jena, DESY, BMBF grant Förderkennzeichen 05 ES7GU1.

XUV source development

The XUV source development for FLASH-II seeding runs in parallel to the laser source development. The high average power of the planned laser amplifier system allows the use of free jet geometry only, in contrast to commonly used capillaries,. To enhance the conversion efficiency, the targets for high order harmonic generation are thus all based on multi-jet arrays. Two different target types are tested to boost the harmonic conversion efficiency with quasi-phase matching. First tests with a four nozzle array show promising results with harmonic a conversion efficiency of close to 10^{-6} in the region between 20-40 nm.

References

[1] B. Faatz, et al., "FLASH II: Perspectives and Challenges", Nucl. Instr. And Meth. A Proceedings D-10-00825R1, (2010).

[2] F. Tavella et al., "Fiber-amplifier pumped high average power few-cycle pulse non-collinear OPCPA", Opt. Express 5, 4689-4694 (2010).

[3] J. Rothhardt, et al., "High average and peak power few-cycle laser pulses delivered by fiber pumped OPCPA system", Opt. Express 12, 12719-12726 (2010).

[4] S. Hädrich et al., "High harmonic generation by novel fiber amplifier based sources" Optics Express, 18, 20242-20250 (2010).

High peak and average power few-cycle laser development

J. Rothhardt[1,2], S. Hädrich[1,2], T. Eidam[1,2], F. Jansen[2], F. Stutzki[2], C. Jauregui[2], S. Demmler[2], J. Limpert[1,2], A. Tünnermann[1,2]

[1]Helmholtz Institute Jena, Germany; [2]Institute of Applied Physics, Friedrich-Schiller-University Jena, Germany

High peak power laser pulses are required for a variety of applications. The generation of high order harmonics enables studies on extremely small length- and timescales. In order to improve back current studies and to enable new applications, such as seeding of free electron lasers, the driving laser system should provide high average output powers and shortest pulse durations.

In this regards, optical parametric chirped pulse amplifiers (OPCPAs) provide enormous potential. They support few-cycle pulse durations and can handle the highest average powers, due to negligible thermal load in the amplifier crystal. However, a high average power pump laser is needed to drive the OPCPAs. Chirped pulse fiber amplifiers are known for their high average output power capability, but their pulse energy has been limited to ~ 1 mJ in the past by the onset of nonlinear effects. To exploit the full potential of fiber based pump lasers for OPCPA, scaling to higher pulse energies and average output powers is required.

The following two sections present the latest results that have been achieved by fiber laser driven OPCPAs and recent achievement in power and energy scaling of fiber based pump lasers for OPCPA.

Few-cycle fiber driven OPCPA

The basic concept of a fiber driven few-cycle OPCPA laser system has been demonstrated in first experiments. The second harmonic of a FCPA system has been used to drive a two stage OPCPA. An optimized configuration revealed both a large amplification bandwidth (>300 nm) and a high pump to signal conversion efficiency (22 %). In summary, 8 fs pulse duration, 6 GW peak power and 6.7 W average power have been achieved at the OPCPA output [1, 2]. Furthermore, high harmonic generation has been demonstrated with this laser system revealing a cut-off wavelength of 20 nm and a conversion efficiency of ~10^{-7} (at 40 nm) [3].

Pump laser power and energy scaling

It is worth mentioning that the performance of the demonstrated OPCPA system is currently limited by the pump laser. Hence, scaling to higher average power and pulse energy is desirable. The pulse energy of FCPA systems can be increased if the nonlinear distortions are kept low or can be compensated for. Combining active phase shaping with an efficient reduction of the acquired nonlinear phase by using a Ytterbium-doped fiber with a mode field diameter of 105 µm as the main amplifier, the pulse energy of the FCPA systems has been increased significantly. Nearly transform-limited sub-500 fs pulses with 2.2 mJ pulse energy have been achieved at ~ 10 W average power [4].

However, the combination of high average output power and high pulse energy from a femtosecond fiber amplifier still remains a challenging task. In this context, novel fiber designs, which allow for stable single mode operation and high average power and large mode field diameters will play an important role. Currently, a special large pitch photonic crytal fiber is developed and characterized. A microscope image of this fiber is shown in fig. 1. Up to 250 W average output power have been achieved and frequency doubled to 135 W [5]. This novel fiber provides a mode field diameter as large as 50 µm, is therefore suitable for mJ-FCPA systems and will be implemented in the next generation OPCPA pump laser in the near future. Consequently, a significant increase in the average output power can be expected.

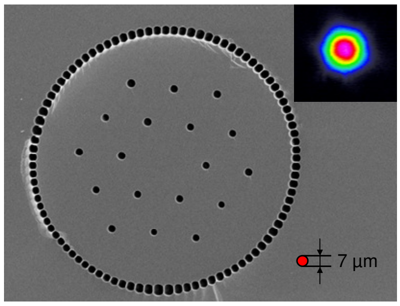

Figure 1: Microscope image of the large-pitch photonic crystal fiber and beam profile at 220 W output power. The core diameter (7 µm) of a standard step-index fiber is shown for comparison (red circle).

References

[1] F. Tavella et al., "Fiber-amplifier pumped high average power few-cycle pulse non-collinear OPCPA", Opt. Express **5**, 4689-4694 (2010).

[2] J. Rothhardt et al., "High average and peak power few-cycle laser pulses delivered by fiber pumped OPCPA system", Opt. Express **12**, 12719-12726 (2010).

[3] S. Hädrich et al., "High harmonic generation by novel fiber amplifier based sources" Optics Express, **18**, 20242-20250 (2010).

[4] T Eidam et al., "Fiber chirped-pulse amplification system emitting 3.8 GW peak power," Opt. Express **19**, 255-260 (2011)

[5] J. Rothhardt et al., "135 W average power femtosecond pulses at 520 nm from a frequency doubled fiber laser system," submitted to Optics Letters

Ultra-high peak power fiber lasers using novel fiber designs

Tino Eidam,[1,2] Jan Rothhardt,[1,2] Fabian Stutzki,[2] Florian Jansen,[2] Steffen Hädrich,[1,2] Henning Carstens,[2] Cesar Jauregui,[2] Jens Limpert,[1,2] and Andreas Tünnermann[1,2]

[1]Helmholtz Institute Jena, Germany; [2]Institute of Applied Physics, Friedrich-Schiller-University Jena, Germany

Fiber based laser systems are known for excellent beam quality, which is nearly independent of the emitted average power. However, fiber based laser systems are restricted by nonlinearities since the light propagates confined in a small core along long distances. In combination with the steady improvements in Chirped-Pulse Amplification (CPA) technology and the increase in the available fundamental mode area, fiber based ultra-short pulse amplifiers have been successfully developed. Today, they deliver pulse peak powers up to 1 GW and found a variety of applications covering e.g. ultra-stable frequency combs [1], high harmonic generation [2] and micro-machining [3]. One integral part in further performance scaling is the development of so-called very large mode area fibers, i.e. single-mode fibers with Mode Field Diameters (MFDs) beyond 50 µm. However, higher order mode discrimination, which is required for single mode operation, is not straightforward in active double-clad fibers, since inside the highly multimode pump cladding every mode of pump and signal propagates, in a good approximation, without losses. Nevertheless, effective single-mode behavior can still be achieved in so called large pitch fibers (LPFs) by exploiting the different overlap of the modes with the doped area.

State-of-the-art-FCPA

Up to now, the highest peak power emitted directly from a fiber chirped pulse amplifier system (FCPA) was demonstrated using an 85 µm rod-type PCF (see Fig. 1b) with a corresponding MFD of 71 µm [4]. This rod-type fiber possesses small air holes that can be described by an effective refractive index slightly lower than that of glass. Therefore, the resulting signal core numerical aperture (NA) can be extremely low. Using this kind of fiber, pulses with an energy of 1 mJ and a peak power of 1 GW were demonstrated [4]. However, in [4] the output pulses were still deteriorated due to the accumulated and uncompensated nonlinear phase despite of the large stretching ratio and core size.

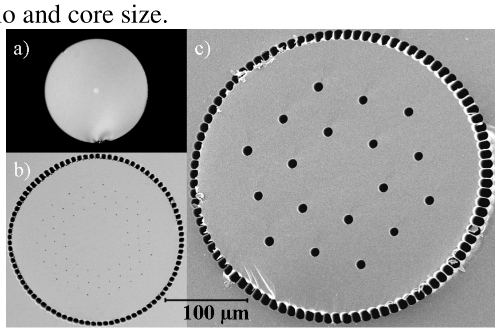

Figure 1: Microscope images (all at the same scale) of a) standard step index fiber with 6 µm core b) 85 µm core rod type PCF and c) 108 µm core LPF.

Performance scaling – 105 µm LPF

The limitations in pulse energy and pulse peak power of FCPA systems have been overcome by using an Ytterbium-doped LPF (see Fig 1c) with a core diameter of 108 µm and an affective MFD of 105 µm as main amplifier. Furthermore, the nonlinear phase acquired during amplification is compensated by using a spatial-light modulator based phase shaping technique. Thus, this FCPA system is able to produce pulses with 2.2 mJ compressed energy and 480 fs duration. The resulting peak power of 3.8 GW is the highest ever reported value directly emitted from a fiber chirped-pulse amplification system.

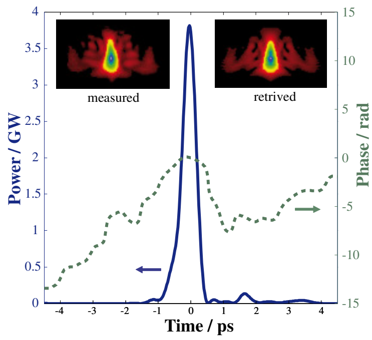

Figure 2: Temporal profile (blue) and phase (green) of the output pulses at a maximum pulse energy of 2.2 mJ measured with a FROG device.

References

[1] D.C. Yost, T.R. Schibli, J. Ye, J.L. Tate, J. Hostetter, M.B. Gaarde, and K.J. Schafer, "Vacuum-ultraviolet frequency combs from below-threshold harmonics," Nature Phys. **5**, 815 - 820 (2009).

[2] S. Hädrich et al., "High harmonic generation by novel fiber amplifier based sources" Optics Express, **18**, 20242-20250 (2010).

[3] A. Ancona, S. Döring, C. Jauregui, F. Röser, J. Limpert, S. Nolte, and A. Tünnermann, "Femtosecond and picosecond laser drilling of metals at high repetition rates and average powers," Opt. Lett. **34**, 3304-3306 (2009).

[4] F. Röser, T. Eidam, J. Rothhardt, O. Schmidt, D. N. Schimpf, J. Limpert, and A. Tünnermann, "Millijoule Pulse Energy high Repetition Rate Femtosecond Fiber CPA System," Opt. Lett. **32**, 3495 (2007),

Research Area 3: Laser-driven particle acceleration, particle diagnostics

Research Area 3 is dedicated to the acceleration of charged particles using high-intensity, high-power lasers with the ultimate goal of merging this novel acceleration technique with the existing RF-technology as it is used in well-established, conventional large-scale facilities. With the Deutsche Elektronen Synchrotron (DESY) in Hamburg and the heavy-ion accelerator facility at GSI in Darmstadt being partners of the Helmholtz-Institute Jena, the institute represents the natural link between these different approaches for particle acceleration and may serve as a first test bed for combining the technologies in the near future.

Having this future goal in mind, a significant number of subprojects within HI-Jena are dedicated to the acceleration of charged particles, i.e. electrons, protons and heavier ions, using the high-power laser facilities which are available within the HI-Jena, namely JETI and POLARIS in Jena and the PHELIX facility at GSI in Darmstadt. Here, investigations aiming at a deeper understanding of the physics underlying the respective acceleration processes have been carried out. This includes variations of the adequate targets used for the acceleration of electrons from He, D_2 or H_2 gas jets (see article by A. Sävert *et al.*) and ions using water and liquid He and H_2 droplets (see article by J. Polz *et al.*). While the influence of different laser parameters has been studied by determining the dependence of their respective variation on the parameters of the accelerated electron pulses (see article by M. Nicolai *et al.*), optical probing techniques have been used to study the laser-target interaction in situ (see articles by M. Reuter *et al.* for electrons and by O. Jäckel *et al.* for ions).

Another approach has been used to further characterize the ion acceleration process by detecting the electromagnetic radiation generated during the acceleration process. For the acceleration of ions from the rear surface of a laser-irradiated thin metal foil the generated radiation lies (among others) in the THz-band, i.e. a characterization of this radiation has the potential to serve as an indirect diagnostic for the ion acceleration process (see article by A. Gopal *et al.*). As a possible future application of laser-driven ion acceleration, the fast ignition of appropriate fuel targets with energetic ions has been investigated numerically (see article by T. Schlegel *et al.*). Here, the difference to previously conducted work lies in the concept of ponderomotive acceleration of ions, which are already available within the high-density core of the pre-compressed fusion pellet, by a high-power laser pulse. Hence, this approach does not rely on the use of additional targets to generate the high-energy ions for ignition, which makes it attractive for high-repetition-rate operation.

Since the detection of the generated particle radiation is another important issue which is often calling for well-adapted solutions to the various situations, specific particle detectors are developed within HI-Jena. The layout, the characterization and the testing of a novel Thomson-parabola design have been done at HI-Jena (see article by B. Aurand *et al.*). A specific form adapted from a design from the Rutherford Appleton Laboratory (UK) has been used, which combines a high energy range and resolution for the ion radiation due to a special electric field geometry realized in the spectrometer. Furthermore, the future FAIR facility at GSI in Darmstadt also calls for specific particle detectors for various applications. Here, new ferromagnetic materials for a cryogenic current comparator have been tested for the future use in the FAIR facility (see article by R. Geithner *et al.*).

One of the worldwide first experimental programs aiming at the injection of laser-accelerated ion pulses into the conventional accelerator structure at GSI has been started within HI-Jena, too. Here, a significant amount of infrastructure needed to be prepared and installed, which allows for the generation of laser-accelerated proton beams using the PHELIX facility in a setup enabling the synchronized injection of these particle pulses into the existing ion accelerator beam line at the Z6 experimental area at GSI (see article by B. Zielbauer *et al.*). Since the energy spectrum, the divergence and also the particle fluxes should ideally be adapted to the requirements of the conventional accelerator, a significant amount of numerical simulations has been carried out to design appropriate ion-beam guiding and focusing optics (see article by I. Hofmann *et al.*).

Differences in wake field acceleration of electrons between helium and hydrogen*

A. Sävert[1], M. Schnell[1],M. Reuter[1], M. Nicolai[1],C. Widmann[1], A. Arunachalam, S.P.D. Mangles[3], C. Spielmann[1,2] and M.C.Kaluza[1,2]

[1] Friedrich Schiller Universität Jena, Germany; [2] Helmholtzinstitut Jena, Germany;
[3] Imperial College London, UK

Super sonic helium gas jets have been used for more than 15 years as a reliable target for electron acceleration with high power laser beams [1]. Recent experiments have used hydrogen filled capillary tubes to accelerate electrons to energies to the GeV level via laser wake field acceleration [2]. These electron bunches not only feature high energy but show additionally good pointing and a small divergence, what was attributed to the geometry of the capillary. In an experimental campaign at the JETI laser we have looked into another significant difference, the gas itself.

Laser pulses of a duration of τ=36fs and energies of 650mJ were focused onto the target by a f/20 off axis parabolic mirror. The diameter of the focal spot was 19 µm FWHM. This resulted in a vacuum FWHM intensity of 1.9×10^{18} W/cm^2.

The laser pulse hit a gas jet which is produced by a super sonic nozzle with 3mm exit diameter. The accelerated electrons were monitored on scintillating phosphor screens by 12bit CCDs. The first screen was placed 33cm behind the nozzle to observe the pointing and the beam divergence. When the screen was removed, the electrons could enter the electron spectrometer consisting of a 0.7 T dipole magnet and a 2 mm entrance slit. The electron spectrum was visualized with 2 additional screens, one for the low energy (10 MeV-55 MeV) and one for the high energy (60 MeV- 240 MeV) part. Additionally a side view was installed to measure the electron density by using a Nomarski interferometer for every shot.

The target position was optimized for the helium gas jet to get well-collimated electron bunches with high energy mono energetic features. After this position was found the target was left unchanged during the complete experiment. First a pressure scan for helium was performed and then a pressure scan for hydrogen. Before the hydrogen was filled in, all the tubes were evacuated to ensure no residual gas was left to avoid ionization injection from high z gases like nitrogen. The optimal plasma density was found to be 2×10^{19} cm^{-3} for both gases.

In the beginning we have looked at the pointing of the electron beam on the first scintillator screen. In Figure 1 30 consecutive shots at the optimal pressure were added up and the position of the individual shots are displayed.

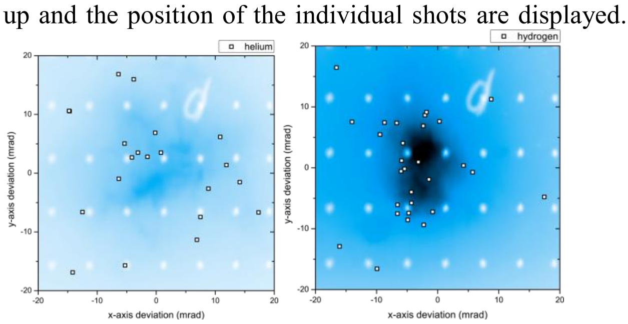

FIGURE 1: Pointing of the electron bunches at the first lanex screen for helium (left) and hydrogen (right).

The color scale is the same in both pictures. The electron bunches from the hydrogen gas jet have a higher charge than those from the helium gas jet. The pointing has also improved by a factor of 2 in the horizontal direction and by a factor of 1.5 in the vertical direction.

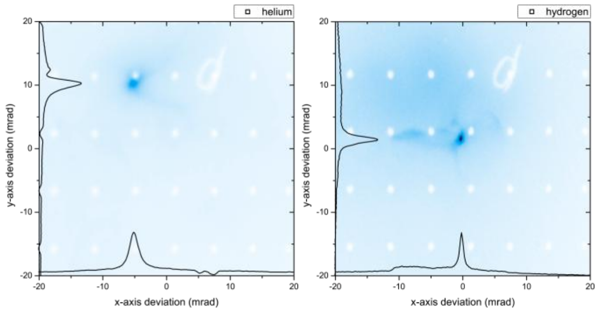

FIGURE 2: Divergence of the electron bunch for a typical shot for helium (left) and hydrogen (right)

The divergence of a single electron bunch has also improved. Figure 2 shows a single electron beam imprint from a helium (left) and from a hydrogen gas jet(right). The result is a well-collimated electron beam with a horizontal divergence of 1.6 mrad and a vertical divergence of 2.3 mrad.

First simulations using a PIC code suggest that the increased mobility of the background ions lead to an increased electrical field strength inside the plasma wave. Therefore a higher number of electrons can be loaded in the plasma wave and accelerated to high energies.

Further experiments related to the geometry of the gas target are in preparation.

References

[1] A. Modena *et al*, Nature 377, 606 (1995)
[2] W.P. Leemans *et al*, Nature Physics 2, 696 (2006)

* This work was supported by the DFG (contract no. TR18) and by the BMBF (contract nos: 03ZIK052 and 05K10SJ2)

A parameter scan for laser wakefield acceleration of electrons

M. Nicolai[*1], *C. Widmann*[1], *M. Reuter*[1], *A. Sävert*[1], *M. Schnell*[1], *O. Jäckel*[1,2], *C. Spielmann*[1,2], *G. G. Paulus*[1,2], *and M. C. Kaluza*[1,2]
[1]IOQ, Jena, Germany; [2]HIJ, Jena, Germany

In the process of laser wakefield acceleration a high intensity laser pulse excites a plasma wave accompanied by huge electric fields. These fields can be utilized to accelerate electrons to relativistic energies over a few mm only. However, the energy and pointing stability of the electron bunches are currently not comparable to conventional accelerators. Therefore experiments which investigate the dependence of the parameters of the electron bunch on experimental parameters were performed at the JETI-Laser.

Influence of a pulse front tilt

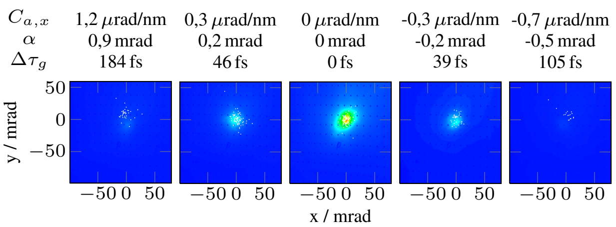

Figure 1: Averaged images of the electron bunch profile for different angular chirps $C_{a,x}$ in the laser pulse and the corresponding pulse front tilt α and group delay $\Delta\tau_g$

A pulse front tilt[1] of a large diameter laser pulse has two main disadvantages. Firstly, it drives an asymmetric plasma density profile[2] and secondly the laser pulse duration increases significantly. A pulse front tilt can originate from a misaligned grating compressor where the two gratings are not parallel. How sensitive the acceleration process is with respect to a compressor misalignment is shown in figure 1. The plots show the electron bunch profiles averaged over 100 single shot while the white dots mark the centers of the single electron bunches which had a circular or elliptical transverse profile. The origin of the axes corresponds to the laser propagation direction. The plot in the middle is for optimal compressor settings. The plots next to it show the averaged electron bunch profile when one compressor grating was tilted by only one step of the motor controlling the grating rotation. This resulted in a pulse front tilt of 0.2 mrad and the pulse duration increased by a factor of approximately two. The plots show that the electron bunches had less charge and the pointing stability was worse. By further detuning the grating the pulse duration became a multiple of the original and almost no electrons were accelerated. In the optimal case 80 % of the electron bunches were in a 20 mrad cone and hit the electron spectrometer. Most of the spectra showed a broad background with a peak between 70 and 90 MeV.

Dependence on laser energy and plasma density

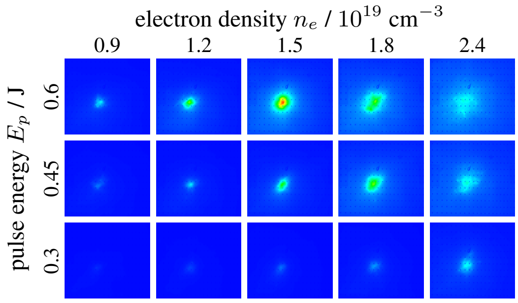

Figure 2: Averaged images of the electron bunch profile for different laser pulse energies and plasma densities

A variation of the laser pulse energy and the plasma density has different effects on the acceleration process. For lower laser energy a higher electron density is necessary to break the plasma wave. But for higher density the plasma wavelength shortens and the laser pulse does not fit into it anymore. So the wakefield excitation is not resonant anymore and acceleration has to rely on nonlinear processes like pulse compression and self focusing. Figure 2 shows the averaged electron bunch profiles for different laser pulse energies and plasma densities. For the highest laser energy the optimal plasma density was $1.5 \cdot 10^{19}$ /cm^3. Here, a lot of electrons were injected into the wakefield and were accelerated in a small cone which led to a high charge density on the fluorescent screen. For higher densities more electrons were accelerated, but they were spread over the whole screen, so the charge density was lower. With reduced laser energy less electrons were accelerated and a higher plasma density was needed to accelerate electrons at all.

The best pointing stability was achieved just above the threshold density for wave breaking and the pointing became worse with further increasing the plasma density. The electron spectra lost their quasi-monoenergetic features and became more and more exponential with higher density.

References

[1] G. Pretzler et al., Appl. Phys. B **70**, 1 (2000).

[2] A. Popp et al., Phys. Rev. Lett. **105**, 215001 (2010).

* maria.nicolai@uni-jena.de

Water and liquid He and H_2 micro droplets as targets for laser ion acceleration*

J. Polz[1], R. Costa Fraga[2], A. Kalinin[2], R. Grisenti[2], O. Jäckel[1,3], S. Herzer[1] and M. Kaluza[1,3,#]

[1]Institut für Optik und Quantenelektronik, Universität Jena, Germany; [2]Institut für Kernphysik, Goethe Universität Frankfurt am Main, Germany; [3] Helmholtz Institut Jena, Germany

Laser matter interactions are able to heat plasma electrons to relativistic temperatures of the order of MeV. These electrons can generate electric fields of the order of TV/m at the rear surface of thin foils. These fields can be utilized to accelerate ions via the TNSA mechanism to several tens of MeV energy [1]. One way to further improve the ion energies is to increase the TNSA fields

$$E = \sqrt{\frac{2}{e_N} \frac{k_B T_e n_{e0}}{\varepsilon_0}}$$

(e_N – Euler's number, k_B – Boltzmann's constant, T_e – electron temperature, n_{e0} – electron density, ε_0 – dielectric constant) [2]. One disadvantage of using flat foils as a target is the fast spreading of the energetic electrons across the back surface, thus decreasing the electron density and the strength of the accelerating fields.

One possibility to prevent this spreading is the use of mass or volume limited targets, where the hot electrons driving the ion acceleration are concentrated on the limited volume of the target. While the production of micrometer sized solid targets using micro lithography always requires a support structure to position the objects in the laser focus, the generation of micro droplets gets by without these and thus represents a method for generating real mass limited targets. Here we present the use of water and liquid He and H_2 micro droplets as targets for laser ion acceleration.

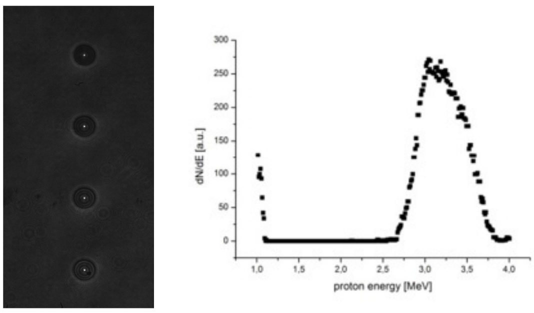

Figure 1: Water droplet beam and typical proton spectrum

Water micro droplets

We used a nozzle with 10 µm aperture, delivering droplets of 25 µm diameter at a repetition rate of 1 MHz. To synchronize the droplets to the laser pulse a piezo actuator was used, stimulating the breakup of the water jet into a chain of equally sized and spaced droplets (see fig. 1).

The ion beam generated during the laser target interaction was detected with a Thomson parabola equipped with an MCP online diagnostic. In contrary to previous publications [3] we were able to improve the peak energy of mono energetic particles from 1 MeV per nucleon (deuterium) to 3.5 MeV per nucleon (see proton spectrum in fig. 1).

Cryogenic micro droplets

Cryogenic helium and hydrogen exhibit particle densities at least one order of magnitude lower than typical solid state targets like metal or carbon foils, which makes them interesting for laser ion acceleration.

A proof of principle experiment with liquid helium droplets analogue to the use of the water micro droplets was performed recently. The diameter of the nozzle exit was 5 µm, delivering droplets of 8 µm in diameter. The source could not be synchronized to the laser due to the absence of a piezo modulator. In the experiment He^{2+} ions with energies up to 4 MeV were generated (see figure 2).

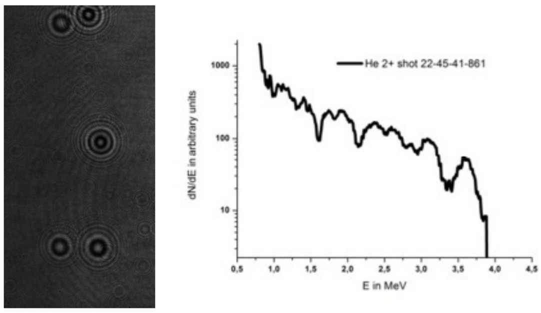

Figure 2: Unsynchronized liquid He droplet beam and He^{2+} spectrum

The experiment showed that even with an unsynchronized source laser acceleration is feasible but at the cost of reproducibility and parameter control. To further improve the performance tests with piezo driven nozzles at liquid helium temperature and to access hydrogen as a target, tests with triple point chambers are currently carried out.

References

[1] Snavely, R. A et al. "Intense high-energy proton beams from petawatt-laser irradiation of solids" Physical Review Letters 85, 2000, p. 2945-2948

[2] Mora, P "Plasma expansion into a vacuum", Physical Review Letters, Vol. 90, 2003, 185002

[3] Ter-Avetisyan et al., "Quasimonoenergetic deuteron bursts produced by ultraintense laser pulses", Physical Review Letters, Vol. 96, 2006, 145006

* The work leading to these results has recieved funding by the Bundesministerium für Bildung und Forschung (under contracts 03ZIK052 and 03ZIK445) and from the Helmholtz Gemeinschaft (under grant VH-NG-331).

Ion acceleration experiments at the JETI laser *

O. Jäckel[1,2], S. M. Pfotenhauer[2], J. Polz[1,2], H.-P. Schlenvoigt[2], J. Heymann[2], H. Schwoerer[2], S. Steinke[3], A. P. L. Robinson[4], and M. C. Kaluza[1,2]

[1]Helmholtz-Institut Jena, Germany; [2]Institut für Optik und Quantenelektronik, Friedrich-Schiller Universität Jena, Germany; [3]Max Born Institut, Berlin, Germany; [4]Central Laser Facility, STFC, RAL, DIDCOT, OX11 0QX, UK

Focusing intense laser pulses on thin target foils leads to the generation of relativistic plasmas and consequently to the presence of a hot electron population with a temperature in the MeV range. These temperatures together with the characteristic screening lengths of such electron distributions at the target back surface cause the occurring field strengths in the TV/m range that give rise to efficient ion acceleration. The experiments performed at the JETI laser system strongly focussed on the characterization of these ion acceleration processes. For this purpose different experiments have been conceived both to directly observe the process as well as to apply laser accelerated ions to laser driven post acceleration [1, 2].

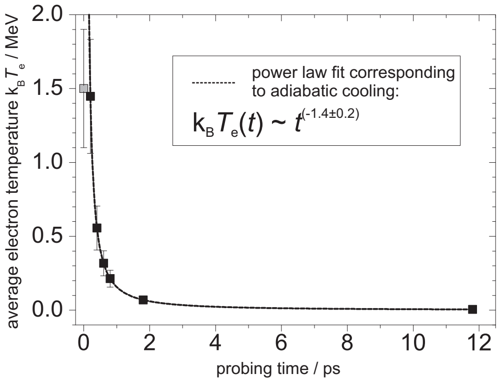

Figure 1: Adiabatic cooling of hot electron distribution driving laser ion acceleration at the back surface of thin foils is highlighted by the dashed fit curve.

For the first approach a pump-probe setup was designed which in combination with a special target design allowed the direct observation of the hot electron distribution at the target back surface. A small fraction of the JETI laser pulses is split off, frequency doubled, and passes the target back surface while it collects a phase shift correlated to the hot electron density present in the ion acceleration region. This region of interest is imaged onto a CCD camera using an f/2 objective for high spatial resolution. To determine the electron density distribution an Nomarski interferometer was implemented into the imaging path. Delaying the probe pulse with respect to the pump pulse enabled a study of the temporal evolution of the electron sheath. In addition to the direct determination of all important properties of the hot electron distribution such as Debye length, temperature, number density distribution, and their energy content also an adiabatic cooling behavior was observed, c.f. Fig. 1.

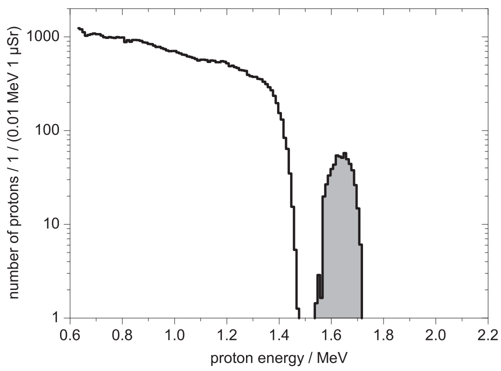

Figure 2: Re-acceleration of protons beyond the high energy cutoff using the double-stage setup results in the grey peak.

A second experiment was performed using a staged laser based ion acceleration setup. The proton bunch accelerated during a first laser plasma interaction is subsequently applied to a second one. The accelerated ions were detected via a Thomson spectrometer equipped with a microchannel plate based ion detector to work online. The measured spectra all showed a characteristic modulation containing signatures of re-acceleration, deceleration and a depletion region in between. A delay stage in use for the second laser pulse driving the second acceleration stage allowed to exactly control the timing and consequently the energy position of the characteristic modulation in the temporally dispersed proton spectrum. Due to this possibility the production of free-standing proton peaks beyond the high energy cut-off became possible (Fig. 2).

References

[1] O. Jäckel, J. Polz, S. M. Pfotenhauer, H.-P. Schlenvoigt, H. Schwoerer, M. C. Kaluza, "All-optical measurement of the hot electron sheath driving laser ion acceleration from thin foils", New Journal of Physics, 2010, **12** 103027

[2] S. M. Pfotenhauer, O. Jäckel, J. Polz, S. Steinke, H.-P. Schlenvoigt, J. Heymann, A. P. L. Robinson, M. C. Kaluza, "A cascaded laser acceleration scheme for the generation of spectrally controlled proton beams", New Journal of Physics, 2010, **12** 103009

* Work supported by BMBF (contract no. 03ZIK052 and no. 03ZIK445) and the EU (Laserlab Europe)

Interferometry of laser generated plasmas for electron acceleration*

M. Reuter[1], A. Sävert[1], M. Nicolai[1], C. Widmann[1], A. K. Arunachalam[2], M. Schnell[1], C. Spielmann[1,2] and M. C. Kaluza[1,2]

[1]Institute of Optics and Quantum Electronics, Jena, Germany, [2]Helmholtz-Institute Jena, Jena, Germany

Introduction

By means of laser generated plasmas immense electric fields can be generated. Therefore, they represent a possible alternative to conventional acceleration systems. An accurate observation of the processes occurring during the acceleration is required in order to control the parameters of the generated particle radiation as accurately as possible. Interferometric measurements using a short, synchronized, optical probe beam are one possibility [1].

Such a probe pulse was set up at the JETI-laser system of the IOQ. Using this probe pulse, the temporal evolution of the plasma density could be investigated during the interaction of the main beam with the plasma. In the course of this the distribution of the refractive index of the plasma is recorded in the phase of the probe beam. Analyzing the interferograms with regard to phase information the electron density distribution can be calculated. During a recent experiment relativistic electron pulses were generated and detected with an electron spectrometer. Simultaneously, the plasma density was determined interferometrically. Comparing the electron spectra with the information yielded from the interferograms knowledge about the acceleration process can be gained.

Experimental Setup

The setup of the probe beam and inside the target chamber is introduced briefly in the following. Due to spatial restrictions the probe beam is set up on two platforms.

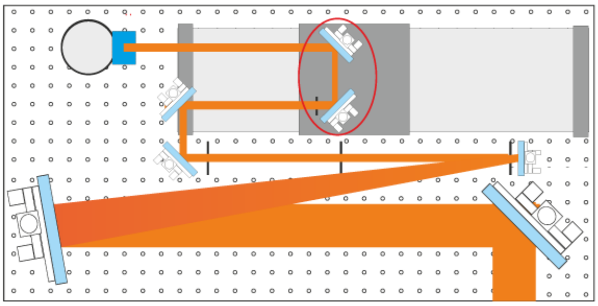

Figure 1: Lower platform of the probe beam.

The main components are a mirror telescope and a linear translation stage. Two mirrors of the linear translation stage situated on the lower platform (Figure 1) are motorized. In addition to the essential components near and far field diagnostics (Figure 2) are installed. In combination with the motorized mirrors, beam displacements due to the movement of the translation stage can be compensated. Using a single shot autocorrelator (Figure 2) the pulse duration of the probe pulse could be measured to 87 fs outside the interaction chamber. To further reduce the pulse duration to its transform limit of 30 fs, dispersive mirrors will be integrated in the future.

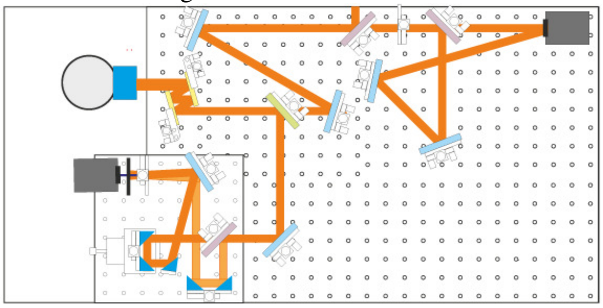

Figure 2: Upper platform of the probe beam.

While the main beam is focussed by means of a parabolic mirror into a gas jet the probe beam propagates nearly perpendicular to the main beam through the plasma. Simultaneously the electron energy is detected in the electron spectrometer.

Results

A characteristic interferogram and the electron density distribution which was deduced assuming cylindrical symmetry are shown in Figs. 3 and 4, respectively. The laser pulse entered the plasma from the left. High-energy electron bunches were observed when a small channel diameter and steep intensity gradients in laser direction are still present at late times during the interaction.

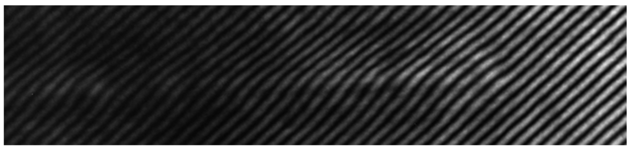

Figure 3: Characteristic interferogram.

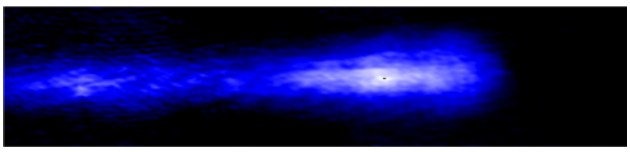

Figure 4: Plasma density (a.u.).

* This work was supported by the DFG (contract no. TR18) and by the BMBF (contract nos: 03ZIK052 and 05K10SJ2).

References

[1] R. Benattar et al., Rev. Sci. Instr. 50, 1583 (1979)

High power T-rays from table top laser plasma accelerators

A. Gopal[*1,2], *T. May*[3], *S.Herzer*[1], *A. Reinhard*[3], *M.Schubert*[3], *M.Kaluza*[1,2], *J.Polz*[1,2], *U.Dillner*[3], *H-G.Meyer*[3], *and G.G. Paulus*[1,2]

[1]Helmholtz Institute Jena, Helmholtzweg 4, D-07743 Jena, Germany; [2]Institute of Optics and Quantum Electronics, Friedrich Schiller University Jena, D-07743 Jena, Germany; [3]Institut für Photonische Technologien, Postfach 100239, 07702 Jena, Germany

Table top relativistic laser plasmas

Plasmas produced by high intensity lasers are highly nonlinear physical systems. They are sources of coherent x-rays [1], extremely powerful bunches of high energy electrons [2] and ion beams [3]. In addition to being a powerful radiation and particle source, the characteristic of the emitted radiation could also provide valuable information about processes occurring during laser matter interaction. The extremely short spatial (few tens of microns) and temporal duration (few hundred picoseconds) makes them difficult to characterise by means of external probes. For this reason, the radiation emitted by the plasmas is usually a suitable diagnostic to explore extremely hot and dense plasmas [4].

The T-ray project

Todate, table top laser driven particle accelerators are capable of accelerating electrons to GeV [2] and ions to several tens of MeV [3] energies. However many applications require increase in particle flux, energy etc. Various schemes have been proposed to address these issues, such as increasing the laser intensity or modifying target properties. Our approach to the optimisation of the laser based ion acceleration scheme relies on a novel diagnostic of the accelerating field based on THz radiation detection. The acceleration process can be simplified as follows. By irradiating a thin metal foil target with infrared laser radiation at intensities greater than 10^{18} W/cm^2, a high density plasma is formed and a bunch of extremely energetic hot electrons (MeVs) is generated. Some of these hot electrons travel through the target and exit at the rear surface thereby generating a micron scale plasma sheath with a space charge field of the order of TV/m. The sheath field is strong enough to pull out the ions from the rear surface by field ionisation. The energetic electrons which are leading the plasma sheath experience deceleration while the ions and protons are accelerated to several MeV energies. Because of the dynamics of charged particles, radiation of electromagnetic waves at the THz frequency (T-rays) is expected. At non-relativistic velocities or β $(\frac{v}{c})$ $<<$ 1, radiation would be emitted mainly perpendicularly to the target normal direction. Because of the acceleration dynamics of the electrons and ions occur on a different time scale (which depends on their mass), can be monitored by spectral analysis of the emitted T-rays.

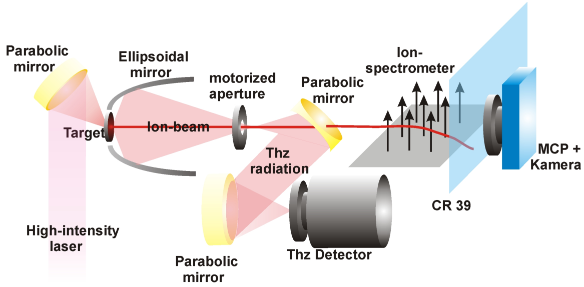

Figure 1: **A schematic of the experimental layout.**

Experiment

The experiment was performed on the onsite JETI laser system. JETI laser delivers 600 mJ pulses of 30 fs duration and 790 nm central wavelength. With state of the art focussing optics an intensity of $\sim 10^{19}\ W/cm^2$ was achieved on target. A schematic of the experimental layout is shown in figure 1. The T-rays were collected using an ellipsoidal mirror and was relayed onto a calibrated hybrid pyroelectric detector placed outside the experimental vacuum chamber. Simultaneously the ion spectra was measured using an ion spectrometer.

Results

The special geometry of our collection optics allowed us to identify the collection angles. In our latest experiment we have detected T-ray pulses of energy no less than 2 μJ. The initial studies on the spectrum reveal that the most of the energy is between $0.3 - 2$ THz region. Angularly resolved measurements show that the detected radiation is non-collinear implying dipole like emission mechanism. Particle In Cell simulations have been carried out to identify the T-ray generation mechanism. Further studies are being performed to correlate the T-ray emission to the underlying laser plasma dynamics.

References

[1] Murnane, M.M. et al. *Science*. **251**, 531 (1991)

[2] Leemans, W.P. et al. *Nature Physics*. **2**, 696 (2006)

[3] Snavely, R.A. *Physical Review Letters*. **85**, 2945 (2000)

[4] Tatarakis, M. et al. *Nature*. **415**, 280 (2002)

[5] Macklin, J.J. et al. *Physical Review Letters*. **70**, 766 (1993)

[6] Kmetec, J.D. et al. *Physical Review Letters*. **68**, 1527 (1992)

[7] Hamster, H. et al. *Physical Review Letters*. **71**, 2725 (1993)

* supported by Carl Zeiss Stifftung

Fast ignition with ponderomotively accelerated ions *

T. Schlegel[1,2], C. Regan[3], and V. Tikhonchuk[3]

[1]GSI, Darmstadt, Germany; [2]Helmholtz-Institute, Jena, Germany; [3]CELIA, Université Bordeaux, France

Contrary to the central spark ignition concept, the fuel of the deuterium-tritium (DT) capsule in a fast ignition (FI) scheme will be compressed at lower implosion velocities to densities of several hundred g/cm^3, what reduces problems with high symmetry and hydrodynamic instabilities [1].

To ignite such a precompressed pellet, additional internal energy must be allocated in a local region of its dense core, the so-called hot spot, at the moment of stagnating implosion. As soon as fusion chain reactions will set in, a burn wave spreads over the whole volume of the target. For this secondary heating, intense beams of fast electrons or ions produced with help of an additional short and intense laser pulse were proposed.

With the advent of ultra-intense laser pulses, a scheme of efficient ponderomotive ion acceleration from overdense plasma regions becomes conceivable, which may provide high particle numbers in the accelerated ion bunch [2]. This regime of hole boring should allow ion acceleration directly inside the fusion pellet without any secondary target (see Fig. 1 (a)), thus enabling fuel ignition and burn in high repetition rate operation [3].

To reduce the needed laser energy and power in a demonstration experiment, a cone-guided DT target could be applied [5], where the laser beam propagates through low-density carbon inside the cone and accelerates carbon ions with high efficiency and small beam divergence, as shown in Fig. 1 (b). The design of the ion beam parameters for such an experiment, based on analytical studies [4], was checked in hybrid numerical simulations. Ion beam propagation and energy deposition in the precompressed DT target were modeled with a two-dimensional kinetic transport code. The successive hydrodynamic evolution of the beam-heated target was calculated with the radiative hydrodynamic code CHIC. For a laser pulse with an intensity $I_{\rm las} \simeq 5 \times 10^{21}$ W/cm^2 and the focal radius $r_{\rm f} \simeq 10\,\mu$m, which propagates through the 200 μm thick overcritical carbon layer of density $\rho_{\rm C} = 0.2$ g/cm^3, the generated beam of 175 MeV carbon ions will deposit 13.5 kJ of energy in the dense core of the pellet. The acceleration efficiency equals 16%. A transverse beam spread of 3° was supposed, which can be evaluated from two-dimensional particle-in-cell simulations. The ion temperature at this stage is shown in Fig. 2 (a). A CHIC simulation starting from these plasma parameter distributions confirmed pellet ignition after about 10 ps. The time delay can be explained by the density and temperature dependence of the DT fusion reaction rate, which describes the efficiency of the α-particle release. The characteristic times for energy equilibration between α-particles and electrons and for the subsequent energy transfer to fuel ions are of the order of 1 ps in the parameter range at hand. The time dependence of the fusion power is depicted in Fig. 2 (b). The integral fusion energy amounts to 20 MJ, the corresponding gain factor is 180. The ignitor laser energy is 100 kJ, its power equals 15 PW and the pulse duration is 7 ps.

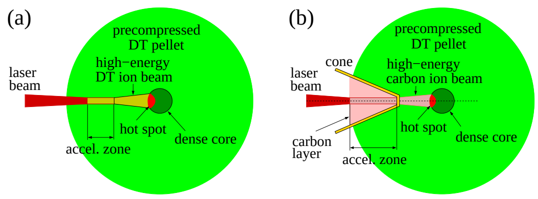

Figure 1: Ponderomotive ion acceleration in the stagnation phase of DT capsule compression. (a) DT acceleration in front of the dense core. (b) Scheme with a low-density carbon layer inside a cone embedded in the DT pellet.

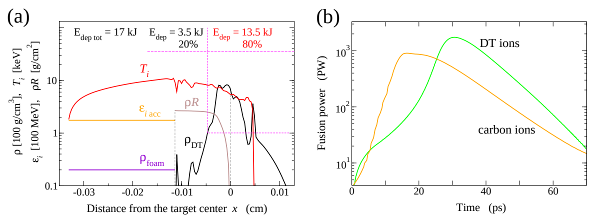

Figure 2: (a) Plasma parameters just after energy deposition of high-energy carbon ions. (b) Fusion power as function of time for both cases discussed in the text.

The pure DT scheme requires higher laser intensity, energy and power because of lower acceleration efficiency, larger ion beam spread and less localized energy deposition. For a large-scale fusion target [6] with an areal mass density $\simeq 2.6$ g/cm^2, a short-pulse laser energy of 180 kJ was needed in simulations to ignite the pellet. The fusion power history is shown in Fig. 2 (b) and yields a gain of 150.

References

[1] M. Tabak et al., Phys. Plasmas 1 (1994) 1626.

[2] N. Naumova et al., Phys. Rev. Lett. 102 (2009) 025002.

[3] V.T. Tikhonchuk et al., Nucl. Fusion 50 (2010) 045003.

[4] T. Schlegel et al., Phys. Plasmas 16 (2009) 083103.

[5] A. Debayle et al., J. Phys.: Conf. Ser. 244 (2010) 022032.

[6] D.S. Clark and M. Tabak, Nucl. Fusion 47 (2007) 1147.

* Work supported by the European support program Marie Curie IRSES project # 230777, by EURATOM in the framework of keep-in-touch activities and by the HiPER European project.

Development and Test of New Thomson-Parabolas for Laser-Ion-Acceleration

B. Aurand[*1,2,3]; *F. Klos*[1]; *M. Weipert*[1]; *P.D. Eversheim*[4] *and T. Kühl*[1,2,3]

[1]GSI, Darmstadt, Germany; [2]EMMI, Darmstadt Germany; [3]Johannes Gutenberg University Mainz, Germany; [4]Rheinische-Friedrich-Wilhelms University, Bonn, Germany

Thomson parabolas [1] (TP) have become a standard diagnostic tool for laser-ion-acceleration experiments. A particularly compact and versatile version has been designed and was tested and calibrated using a cyclotron.

The design (Fig. 1) is similar to the TPs developed at Rutherford-Appleton-Laboratory [2]. Permanent magnets create a magnetic field of up to 0.7 T. In combination with the variable electric field applied by tilted potential plates, the energy acceptance is in the range between 0.7 and 16 MeV per nucleon (Fig. 2). For diagnostics we use re-usable Image Plates (IPs) mounted on a rotatable drum. In this way, the device is capable of measuring four consecutive shots before the experimental chamber has to be opened to exchange the IPs.

The IP mount can be replaced by a pre-aligned laser diode holder, which in combination with the fully adjustable baseplate allows for a quick alignment inside the target chamber.

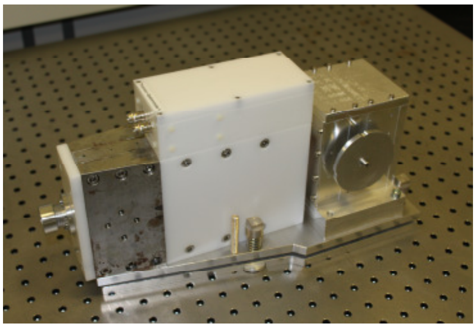

Fig.1: Picture of the fully equipped Thomson spectrometer

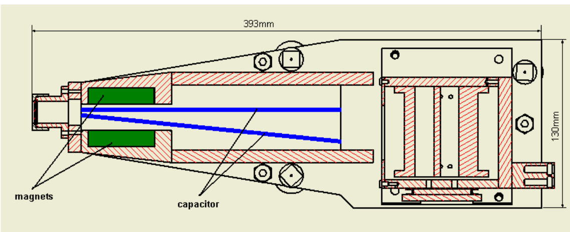

Fig.2: Scheme of the magnets and the capacitor inside the spectrometer

Calibration

After construction and assembly of the TP, the magnetic field distribution was mapped with a Hall probe to determine the distribution of the field strength along the ion trajectories. The data obtained were used to simulate the ion trajectories using the ion-optics computer program SIMION 8.0 [3].

A helium beam from the cyclotron of the Helmholtz Institut für Strahlen- und Kernphysik at Bonn University was used for an absolute calibration of one of the parabolas.

Up to now, for five different energies in the range of 6-14MeV per nucleon – $^{4}He^{2+}$ -ion trajectories were measured with different high-voltage settings, resulting in a varying E-field deflection. Simulation results and measured values are in good agreement.

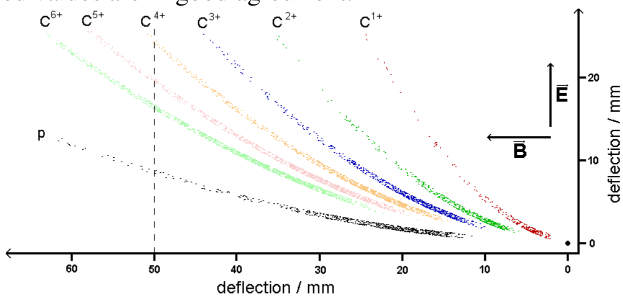

Fig.3: Simulated signal of relevant ion species in the energy range from 0-200MeV. The active detector size is 50x50mm

Outlook

A further improvement will be a new data acquisition by a micro-channel-plate (MCP) based imaging system. By the use of fiber-connectors the design could be small enough to replace the existing image-plate box without changing the dimensions of the parabola.

In addition, using the feature of a gateable MCP with a rise time in the few-ps-range would lead to an effective suppression of background radiation, by the short acceptance time window for accumulating particles.

Acknowlegements

We would like to thank D.Carroll and D. Neely from Rutherford-Appleton-Laboratory for their support concerning the parabola design.

Also we thank the staff of the cyclotron of the "Helmholtz Institut für Strahlen- und Kernphysik" at Bonn University for their support during the calibration experiment.

References

[1] J.J. Thomson; Phil. Mag. 21 225 (1911)
[2] D.C. Carroll et al.; Central Laser Facility Annual Report 2005/2006
[3] D.A. Dahl; Int. J. Mass. Spectrom. 200 (2000)

* B.Aurand@gsi.de

New ferromagnetic materials for an improved Cryogenic Current Comparator for FAIR

R. Geithner[1], W. Vodel[1], R. Neubert[2], and P. Seidel[2]

[1]Helmholtz-Institut Jena, Germany, [2]Institut für Festkörperphysik, Friedrich-Schiller-Universität Jena, Germany.

For the recently launched FAIR (Facility for Antiproton and Ion Research) project [1] at GSI Darmstadt an improved low temperature dc Superconducting Quantum Interference Device (LTS SQUID) based Cryogenic Current Comparator (CCC) for non-destructive beam monitoring should be developed.

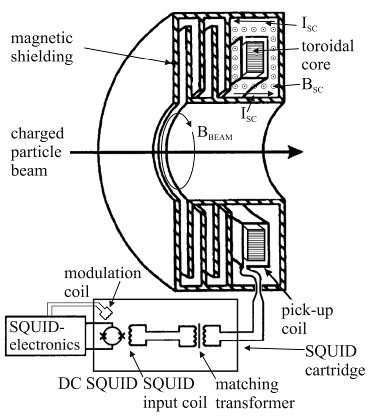

Figure 1: Schematic diagram of the CCC. The superconducting hollow cylinder with magnetic shielding, the superconducting toroidal pick-up coil with ferromagnetic core, the superconducting matching transformer and the SQUID read-out components are all shown.

In the CCC, an ion beam current I_{Beam}, which flows through a superconducting hollow cylinder is transformed via a superconducting toroidal pickup coil with a ferromagnetic core and a matching transformer into a current which is fed through the input coil of the readout DC SQUID UJ 111 [2], [3].

The sensitivity ultimately depends on the pickup coil. It was demonstrated [4] that the use of a ferromagnetic core leads to a possible optimization for better noise performance using materials with a high relative permeability μ_r.

The temperature and frequency dependent measurements of the relative permeability μ_r and the noise contribution of several samples of ferromagnetic materials have shown that the nanocrystalline Nanoperm [5] has some advantages over amorphous Vitrovac and nanocrystalline Vitroperm [6] regarding the usage as core material for the pickup coil of a CCC. Referring to our measurements [4], Nanoperm shows a higher relative permeability μ_r which is less frequency dependent and has a lower noise contribution than Vitrovac or Vitroperm. Although the measurements were done on small samples, we needed cores with much larger dimensions for the CCC in the FAIR project. In this CCC the core for the pickup coil will have an outer diameter of 260 mm, an inner diameter of 205 mm and a height of 97 mm. Three cores with these dimensions were delivered by Magnetec and the magnetic properties were measured in a wide neck cryostat at GSI Darmstadt. The measurements were done at room temperature, in liquid nitrogen at 77 K and in liquid helium at 4.2 K.

The change of the inductance factor A_L, which means inductance of a coil on the tested core divided by the square of the number of turns, is very low in the frequency range between 20 Hz and 10 kHz. The inductance factor A_L decreased to 65 % with decreasing temperature from 300 K to 4.2 K (see Fig. 2).

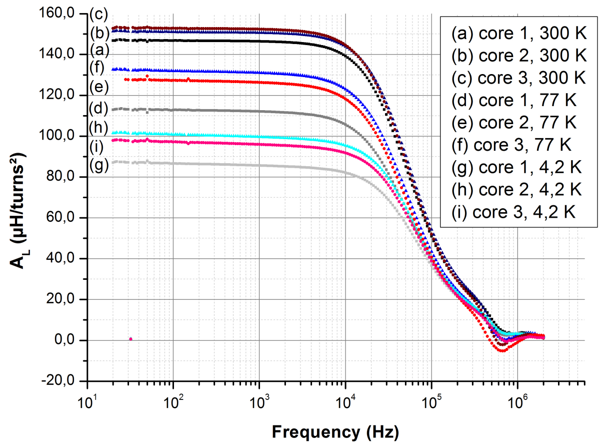

Figure 2: Frequency dependent inductance factor A_L of the Nanoperm cores at different temperatures.

Furthermore the intrinsic noise of the magnetic material influences the achievable signal-to-noise ratio. For that reason the noise contribution of the cores will be measured in a magnetic shielded room in Jena.

Nevertheless the ferromagnetic core material Nanoperm M-764-01 will provide further improvements for the new version of the CCC.

References

[1] Facility for Antiproton and Ion Research (FAIR), homepage available: http://www.gsi.de/fair/.

[2] W. Vodel et al., Supercond. Sci. Technol. 20 (2007), 393.

[3] W. Vodel, K. Mäkiniemi, Meas. Sci. Technol., 3, (1992), 1155-1160.

[4] R. Geithner et al., Applied Supercond. Conf., (2010), Washington, USA, accepted.

[5] MAGNETEC GmbH, Industriestrasse 7, D-63505 Langenselbold, Germany.

[6] VACUUMSCHMELZE GmbH & Co. KG, Gruener Weg 37, D-63450 Hanau, Germany.

LIGHT Update: A laser-based ion-source at Z6

B. Zielbauer[1], A. Almomani[2], V. Bagnoud[1, 3], A. Blazevic[3], C. Brabetz[2, 3], S. Busold[4], O. Deppert[4], H. Eickhoff[3], U. Eisenbarth[3], O. Kester[2, 3], T. Merz-Mantwill[3], F. Nürnberg[4], M. Roth[4], T. Stöhlker[1, 3, 5]

[1]Helmholtzinstitut Jena, Germany; [2]Goethe-Universität Frankfurt, Germany; [3]GSI, Darmstadt, Germany; [4]Technische Universität Darmstadt, Germany; [5]Ruprecht-Karls-Universität Heidelberg, Germany

Introduction

The LIGHT[*,1] project was officially started in 2010 as a collaborative effort between GSI, the Helmholtz Institute Jena and surrounding universities. The project aims at injecting laser-accelerated ions into conventional accelerator structures and later at manipulating them. The first year of the project has dealt with the necessary infrastructure preparation, namely the installation of the laser-based ion-source at the Z6 experimental area, which led to the successful commissioning of our ion source.

In parallel, the collaboration has worked at strengthening the theoretical studies done on the subject, as was highlighted by the large and lively audience to the LIGHT summer workshop, held at GSI.

Short-pulse infrastructure development at the Z6 experimental area

The largest task for the project has been the development of short-pulse laser capabilities at the Z6 experimental area. For this, the addition of a short-pulse compressor and its diagnostics suite to the existing laser hardware was necessary. This so-called "100-TW" subproject was conducted as a joint-effort between the PHELIX team, the HI-Jena, the TU-Darmstadt and the plasma physics department of GSI.

For the short pulse compressor, two options have been pursued in order cope with the somehow aggressive schedule of the project. At first, a compressor equipped with already existing gold-coated diffraction gratings has been designed and fabricated. This 12-cm aperture short-pulse compressor allows for compressing 20-joule pulses while maintaining the laser fluence below 300 mJ/cm^2, i.e. twofold below the laser-induced damage threshold of the gratings. The compressor can also easily accommodate for an upgrade to a larger clear aperture with a consequent increase of the maximum energy to 31 Joules.

Together with the compressor, a short pulse diagnostic package has been developed for both the compressor alignment and the on-shot control of the laser parameters. The diagnostics include near field and far field beam measurements, pulse energy and duration, and wavefront measurements. The diagnostic package was designed, and fielded in 2010. Its integration in the general laser control system of PHELIX will be continued in 2011.

The transport of the short pulses in a vacuum beam line between the compressor located in the south tower clean room of the Z6 experimental area and the target area has been another major step. The beamline is 20 m long and includes 5 turning boxes to drive the laser beam into the Z6 target chamber.

In parallel, several steps had to be taken to comply with radiation safety regulations: The concrete-block walls of the Z6 target area were made higher where possible, and an additional 50-mm thick iron wall was built around the target area to protect the visitor gallery.

Commissioning of the ion source

Recently, a two-week experiment has been conducted to demonstrate the generation of laser-accelerated ions at Z6. The laser beam was focused using a 30-cm focal distance parabola to a ~10 µm spot on a 10-µm thin gold foil. Together with the beam-handling equipment, precise target positioning tools have been validated in our setup. During the experiment, 10 MeV protons have been observed for a laser-pulse energy of 5 J and pulse duration equal to 700 fs +/-100 fs. The Figure 1 shows a photographic picture of the target at the time of laser impact together with the particle beam generated at the foil.

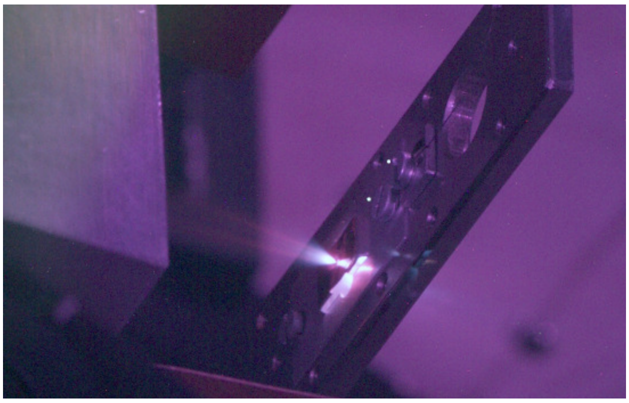

Figure 1: Image of the backside of a target shot by PHELIX. The laser pulse comes from the right and the plasma beam escaping from the back of the target can be seen on the picture.

Outlook for 2011

Based on the successful commissioning of the ion source, we will proceed with the next steps, namely the collimation of the ion beam using a pulsed solenoid and the preparation of the ion beam optics.

[1]https://www.gsi.de/documents/DOC-2010-Nov-36-1.pdf

[*] The acronym stands for **L**aser **I**on **G**eneration, **H**andling and **T**ransport.

Collection and focusing of laser accelerated protons *

I. Hofmann[1], *J. Meyer-ter-Vehn*[2], *X. Yan*[3], *A. Orzhekhovskaya*[4], *and S. Yaramyshev*[5]
[1]Helmholtz-Institut Jena, Jena, Germany; [2,3]MPQ, Garching, Germany; [1,4,5]GSI, Darmstadt, Germany

We study collection and focusing of laser produced protons for therapy applications using simulation data from the radiation pressure acceleration (RPA) model by Yan et al.[1], and assuming particles are collected and focused with a solenoid magnet (details see Ref. [2]).

The energy dependent focusing leads to a chromatic effect, which spoils the achievable emittance - here called "chromatic emittance" depending on the energy window $\Delta E/E$ and production opening angle Ω. We have applied the DYNAMION code [3] to a solenoid of 36 cm length. In Fig. 1 we show how the focal spot (at 1.7 m) of a beam with $\Omega = \pm 40$ mrad and $\Delta E/E = \pm 0.05$ is enlarged by the chromatic effect.

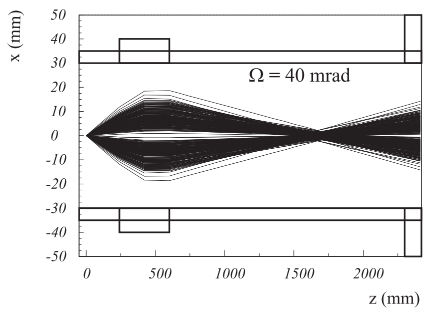

Figure 1: Sample rays from laser source (at $z = 0$) through solenoid showing chromatic blow-up at focal spot.

For this chromatic emittance we find a scaling law

$$\epsilon = \alpha_c \Omega^2 \frac{\Delta E}{E}, \qquad (1)$$

where α_c is a constant for a given geometry and in our case $\alpha_c \approx 0.3$ m/rad.

Concerning laser proton simulation by RPA we have assumed a circular polarized laser pulse with wavelength $\lambda = 1\mu$m and assumed the following parameters: spot radius 10 μm, pulse duration 66 fs, specific power 3×10^{21} W/cm^2, peak power 10 PW, pulse energy 620 J and average power 6 kW (10 Hz). The spectral yield of particles as function of energy E and within a given production divergence angle Ω, $dN(E,\Omega)/dE$ $[MeV^{-1}]$ describes the number of particles in a small energy interval dE and within $\pm\Omega$ as shown in Fig. 2. For the above parameters it is "quasi-monoenergetic" with a peak at about 225 MeV.

It is convenient to display the spectral yield of protons by color codes in a contour plot in the plane of $\Delta E/E$ and Ω as shown in Fig. 3. Beam transport and focusing of particles on the tumor require a beam not exceeding a certain upper limit of emittance - here the chromatic emittance - that needs to be defined according to the final transfer optics. As example we show 2 curves of constant emittance following Eq.1. The dashed curve ($\epsilon = 50$ mm mrad) allows transport to the tumor over 1-2 m distances, whereas the solid curve ($\epsilon = 5$ mm mrad as usual for synchrotrons) would be appropriate over distances of 10-20 m. The color code indicates the number of particles available within the respective emittances. For $\epsilon = 50$ mm mrad the yield can be as high as 3.5×10^{10} particles for $\Delta E/E = \pm 0.1$ and $\Omega = 40$ mrad, which is found a factor 10 above the single shot requirement for therapy.

* Work supported by EURATOM, IFE-KiT-Program.

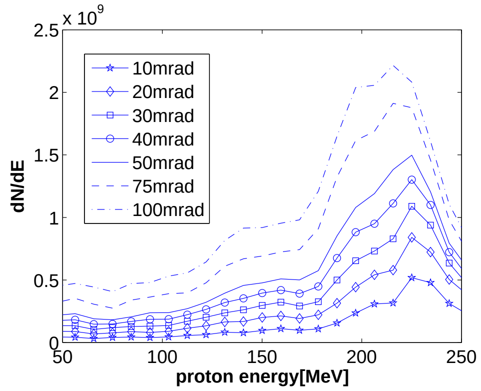

Figure 2: Spectral yield of RPA accelerated protons.

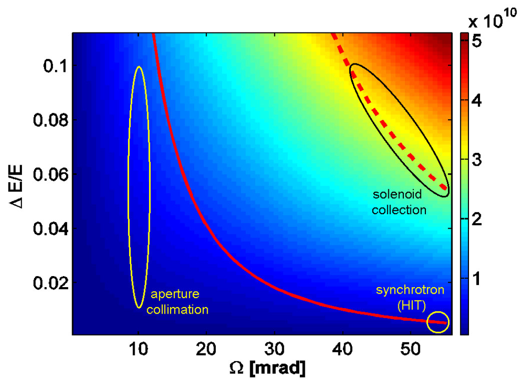

Figure 3: Contour plots for available intensities.

References

[1] X.Q. Yan et al., Phys. Rev. Lett. **103** (2009) 135001-1.

[2] I. Hofmann et al., accepted for publication in Phys. Rev. ST Accel and Beams (2011).

[3] S. Yaramishev et al., Nucl. Instrum and Methods A **558** (2005) 90.

Research Area 4: X-ray science including high-resolution x-ray spectroscopy, polarimetry and laser-based x-ray generation

Research Area 4 is committed to the development of ultra-high-sensitivity crystal and semi-conductor polarimeters and of focusing high-resolution crystal x-ray optics and spectrometers along with the advancement of x-ray generation and x-ray-laser spectroscopy and Thomson-scattering diagnostics.

High-definition X-ray polarimetry with the highest purity is needed for the investigation of vacuum birefringes predicted by the QED theory. Within the present Research Area, the performance of polarizers based on channel-cut single crystals has been dramatically improved and first tests have yielded very promising results.

Position-sensitive solid-state x-ray detectors have been employed as Compton polarimeters in an experiment at the ESR storage ring for the direct determination of the M2 magnetic quadrupole contribution to the Lyman-α_1 transition in U^{91+}. With a similar technique the linear polarization of electron–nucleus bremsstrahlung has been investigated at the polarized electron source at the TU-Darmstadt. These processes are also important in high-energy ion–atom collisions. In a pilot experiment, polarization of elastic scattering processes in the hard x–ray regime were investigated at the synchrotron facility DORIS III making use of the same Compton polarimeters. Within the High Data Rate Initiative of the Helmholtz research program “Photons, Neutrons and Ions” the working package “Real Time Data Processing” was established for advanced detector readout systems also serving the efforts in optimizing the electronic readout for Compton polarimeters.

Within the course of the developments for crystal optics and high-resolution spectrometry also the spectroscopy of helium-like argon has been prepared and reference spectra have been recorded with a Johann spectrometer set up for this purpose. X-ray reflection properties of two-dimensionally bent crystals were studied entailing small systematic corrections important for accurate spectroscopy.

The generation of high harmonics was investigated at the JETI laser in Jena and at the PHELIX laser at GSI and the efficiency of the process was measured for the first time. The efficient generation of high harmonics plus the overlap with x-ray laser transitions is the prerequisite for applications as a coherent XUV and x-ray source and for seeding free-electron lasers. In addition, x-ray parametric amplification was demonstrated at both facilities.

Time resolved XUV Thomson scattering was investigated at FLASH demonstrating the ability of diagnosing the fundamental plasma parameters - density and temperature - for conditions of warm dense matter. Laser–plasma acceleration experiments have been conducted at the LOASIS Ti:sapphire laser, where the x-ray flux was measured by a filtered CCD camera. Diagnostics for the strong electric fields present in target normal sheath acceleration (TNSA) have been set up at JETI making use of the Si-K_α radiation of a thin seeding layer of SiO.

High definition X-ray polarimetry

K.S. Schulze[1,2], *B. Marx**[2], *I. Uschmann*[1,2], *E. Förster*[1,2], *T. Stöhlker*[2,3], *and G.G. Paulus*[1,2]

[1]Helmholtz Institute Jena, Helmholtzweg 4, D-07743 Jena, Germany; [2]Institut of Optics and Quantum Electronics, Friedrich Schiller University Jena, D-07743 Jena, Germany; [3]GSI Helmholtzzentrum für Schwerionenforschung, Planckstraße 1, 64291 Darmstadt

Quest for a ultrahigh purity of polarization

The goal of the high-definition X-ray polarimetry is achieving the highest possible purity of the polarization state of X-rays. Ultra-high purity can be exploited to detect new or insufficiently investigated phenomena, e.g. birefringence of vacuum in the framework of quantum electrodynamics. To this end, an X-ray polarimeter based on channel-cut crystals was developed by B. Marx during her diploma thesis. The polarizer and the analyzer consist of monolithic silicon crystals into which a trench ("channel") is cut. At the walls of this channel, 4 reflections at an angle of 45° can take place. The state of the art have been purities between 10^{-7} and 10^{-8} (the literature does not show the corresponding extinction curves). We were able to improve this result by two orders of magnitude. The paper of B. Marx [1] shows the properties of the polarimeter and the results of the purity measurement at three different x-ray photon energies. During a further measuring campaign in September we were able to improve the purity by approximately one additional order of magnitude by using 6- and 8-reflection channel-cuts in silicon monoliths. The new purities are

- $2.4 \cdot 10^{-10}$ at 6.457 keV
- $6.2 \cdot 10^{-10}$ at 12.914 keV

This is an improvement of our own data by one order of magnitude at 6.4 keV and by a factor of 15 at 12.9 keV. Fig. 1 shows the suppression of the x-rays from the polarizer by rotating the analyzer at 6.4 keV. In order to achieve these results, simulation were performed. The corresponding results helped to orient the crystals such as to minimize Umweg excitations.

Application of the X-ray polarimeter

Due to the high purity of the polarimeter, one can observe very small ellipticities and rotations of the polarization of X-rays induced by birefringent or optically active media. Therefore, it is conveivable that phenomena can be observed that are well investigated in the visible range but not in the X-ray range. Examples are optical activity, birefringence, and field-induced birefringence. We have investigated a sucrose solution between crossed polarimeters and observed a rotation of the polarization plane of 1.0 ± 0.9 arcsec and an ellipticity of $(6 \pm 3) \cdot 10^{-10}$ (Fig. 2). The solution has been in a cuvette with polyimide windows. Further investigations are needed to clarify the origin of this effect. Other kinds of sugar, e.g. glucose and fructose, have to be investigated, too. In another first application experiment we demonstrated that one can use a crystalline quartz crystal as an X-ray phase plate to vary the polarimeter transmission by 6 orders of magnitude. Applying a voltage to the quartz can change the phase of the X-ray wave by structural modification of the crystal via the piezo effect. Such phenomena will be used in the future for fast X-ray switching.

* supported by the DFG TR 18

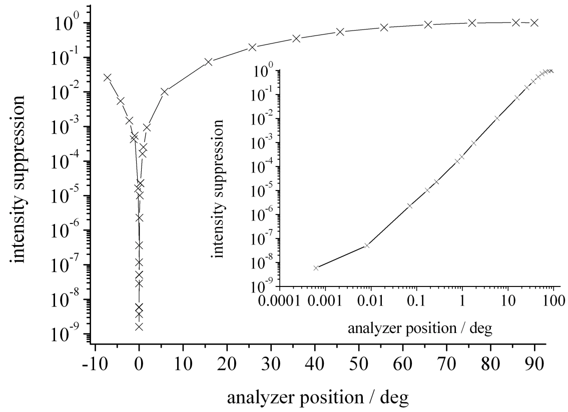

Figure 1: Extinction curve for $\hbar\omega$=6457 eV after four 400-reflections at a silicon channel-cut crystal.

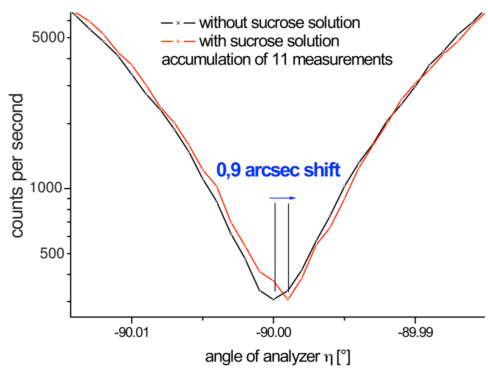

Figure 2: The classic example of optical activity of sucrose measured in the X-ray spectral region.

References

[1] B. Marx, I. Uschmann, S. Höfer, R. Lötzsch, O. Wehrhan, E. Förster, M. Kaluza, T. Stöhlker, H. Gies, C. Detlefs, T. Roth, J. Härtwig, and G.G. Paulus, "Determination of high-purity polarization state of X-rays", Optics Communications 284 (2011), 915-918

Polarimetry: Direct Determination of the Magnetic Quadrupole Contribution to the Lyman-α_1 Transition in U^{91+}

G. Weber[1,2], *H. Bräuning*[1], *A. Surzhykov*[1,3], *S. Fritzsche*[1], *S. Hagmann*[1,4], *C. Kozhuharov*[1], *R. Märtin*[1,3], *N. Petridis*[4], *R. Reuschl*[1], *U. Spillmann*[1], *S. Trotsenko*[1,2], *D.F.A. Winters*[1], *and Th. Stöhlker*[1,2,3]

[1]GSI, Darmstadt, Germany; [2]Helmholtz Institute Jena, Jena, Germany; [3]University of Heidelberg, Heidelberg, Germany; [4]University of Frankfurt, Frankfurt, Germany

Hydrogen-like ions are the simplest and most fundamental atomic systems whose study along the isoelectronic sequence provides detailed information about the effects of relativity and quantum-electrodynamics on the atomic structure. Since these effects are largest for the 1s ground-state, experimental studies of L $\rightarrow$ K transitions are of paramount importance for such investigations. This is in particular true for the domain of high-Z ions where precision measurements of the Lyman-α_1 (Ly-α_1: $2p_{3/2} \rightarrow 1s_{1/2}$) transition energies are a powerful technique to test the theory of strong field QED [1]. However, due to the lack of efficient polarimeter systems for the hard x-ray regime, previous studies were restricted to measurements of the spectral and angular distribution of the emitted radiation [2].

The experiment was performed at the internal gasjet target of the ESR where bare uranium ions at an energy of 96.6 MeV/u interacted with H_2 molecules. Via the radiative electron capture process, excited U^{91+} ions in the $2p_{3/2}$ state were formed which subsequently decayed to the ground state. The emitted photons were detected by an array of standard solid state x-ray detectors at various observation angles and by two novel-type double-sided segmented x-ray detectors at 35° and 90° with respect to the beam axis. By applying the position sensitive x-ray detectors as Compton polarimeters we performed the first linear polarization measurement of the Ly-α_1 radiation in a high-Z system, namely in U^{91+}. Here, we observed an interference between the electric-dipole (E1) and the magnetic-quadrupole (M2) transition amplitudes leading to a significant depolarization of the Ly-α_1 radiation, see Fig. 1.

Both, studies of the Ly-α_1 angular distribution and its linear polarization, can be utilized in order to derive information about the M2 amplitude relative to the E1 amplitude while relying on a theoretical estimate for the population of the $2p_{3/2}$ magnetic sub-levels, which is characterized by the alignment parameter $\mathcal{A}_2$ (see [3] and [4] for details). However, in our recent work [5] we show that a combination of both measurements enables a very precise determination of the ratio of the E1 and the M2 transition amplitudes and the corresponding transition rates without any assumptions concerning the population mechanism for the excited $2p_{3/2}$ state, see Tab. 1. This finding opens a new route to disentangle the population process of the excited ionic state from the subsequent decay. The accuracy of the obtained amplitude ratio will stimulate more detailed quantum-electrodynamical investigations on the transition amplitudes of highly-charged ions beyond Dirac's theory.

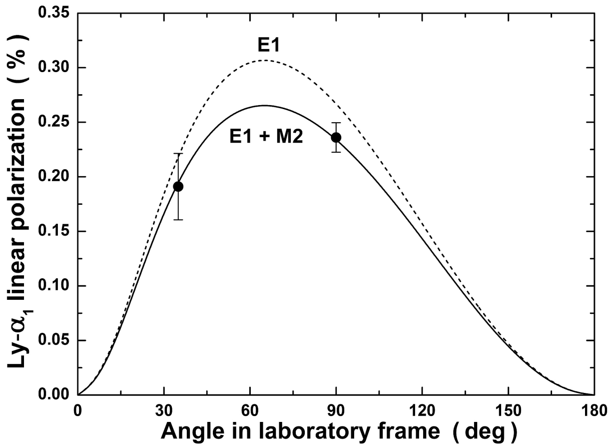

Figure 1: Measured linear polarization of the Ly-α_1 line following the REC into initially bare uranium projectiles with energy 96.6 MeV/u in comparison to theory with (—) and without (- - -) taking into account the E1-M2 interference [5].

Alignment parameter $\mathcal{A}_2$		Amplitude ratio a_{M2}/a_{E1}	
Experiment	Theory	Experiment	Theory
-0.451 $\pm$ 0.017	-0.457	0.083 $\pm$ 0.014	0.0844

Table 1: Comparison of the measured and the theoretical alignment parameter $\mathcal{A}_2$ for the $2p_{3/2}$ level and the M2/E1 amplitude ratio of the Ly-α_1 decay in H-like uranium. The theoretical values also include the cascade feeding due to capture into high-lying levels [5]. See text for further discussion.

References

[1] A. Gumberidze et al., Phys. Rev. Lett. **94**, 223001 (2005).

[2] Th. Stöhlker et al., Phys. Rev. Lett. **79**, 3270 (1997).

[3] A. Surzhykov et al., Phys. Rev. Lett. **88**, 153001 (2002).

[4] A. Surzhykov et al., Hyperf. Interact. **146-147**, 35 (2003).

[5] G. Weber et al., Phys. Rev. Lett. **105**, 243002 (2010) .

Target effects on the linear polarization of electron-nucleus bremsstrahlung*

R. Märtin[1,2], *R. Barday*[3], *J. Enders*[3], *Y. Poltoratska*[3], *U. Spillmann*[1], *G. Weber*[1,4], *and Th. Stöhlker*[1,2,4]

[1]GSI Helmholtzzentrum für Schwerionenforschung GmbH, Darmstadt, Germany; [2]Physikalisches Institut, Universität Heidelberg, Heidelberg, Germany; [3]Institut für Kernphysik, Technische Universität Darmstadt, Darmstadt, Germany; [4]Helmholtz-Institut Jena, Jena, Germany

The polarization properties of electron-nucleus bremsstrahlung occurring both in electron-atom collisions and, in inverse kinematics, in ion-atom collisions have continuously attracted strong theoretical interest [1, 2]. Due to the recent development of efficient Compton polarimeters precise studies of photon linear polarization in the energy region from roughly 70 up to a few hundred keV have become possible [3]. However, for the correct interpretation of bremsstrahlung polarization measurements using solid state targets one has to consider the electron transport properties within the target. As for high-Z materials the mean free path length of electrons with energies below a few hundred keV is in the order of a few nm, target effects can be expected even for the thinnest target foils that can be used practically.

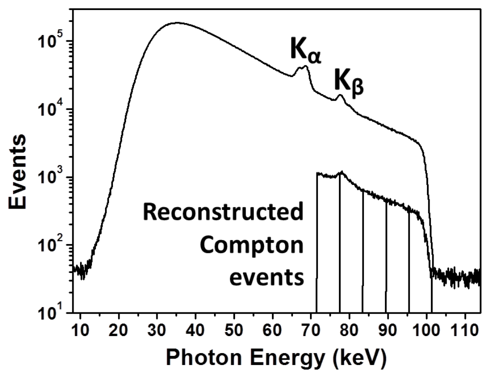

Figure 1: Bremsstrahlung distribution of 100 keV unpolarized electrons impinging on a gold target (90 $\frac{\mu g}{cm^2}$) recorded at 130° observation angle. The bottom curve shows the fraction of the reconstructed Compton events which can be used for the polarization analysis.

We performed a bremsstrahlung measurement at the polarized electron source SPIN at the TU Darmstadt [4, 5] using gold targets of different thicknesses (90 $\frac{\mu g}{cm^2}$ and 178 $\frac{\mu g}{cm^2}$, respectively). The available electron energy of 100 keV is well suited for the use of our novel-type Si(Li) Compton polarimeter, which we applied for x-ray detection. Fig. 1 shows the bremsstrahlung distribution recorded at 130° observation angle. The bottom curve shows the fraction of reconstructed Compton scattering events within the detector crystal from which one can obtain the linear polarization properties.

* Work supported by DFG through SFB 634 and by the state of Hesse through the LOEWE centre HIC for FAIR

Fig. 2 shows the degree of linear polarization of bremsstrahlung measured for the two different gold targets. The polarization has been evaluated for different photon energies reaching from the endpoint of the distribution down to 71.5 keV. As seen, the degree of linear polarization is reduced for the thicker target. This is due to the deflection of electrons inside the target, mainly due to elastic scattering in the field of the nucleus, which leads to a superposition of different observation angles with respect to the electron momentum direction at the detector position.

Currently, we are developing an electron transport Monte-Carlo code to estimate the effects of the finite target thickness on bremsstrahlung polarization. Preliminary results already indicate that the bremsstrahlung polarization is much more sensitive to target effects than the spectral distribution, which has been studied extensively in the past.

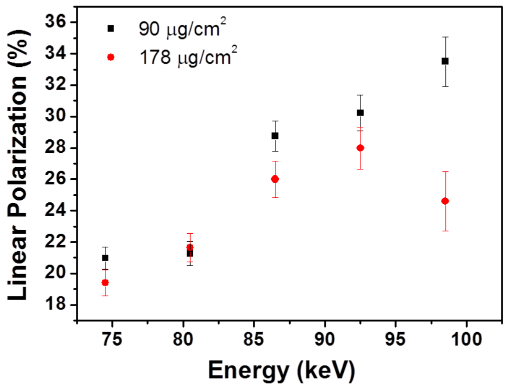

Figure 2: Preliminary: Degree of bremsstrahlung linear polarization for two different target thicknesses as a function of the energy of the emitted photon. Here only the statistical uncertainty is considered for the error bars.

References

[1] D. Jakubaßa-Amundsen, J. Phys. B: At. Mol. Opt. Phys. **40** (2007) 119

[2] V. A. Yerokhin and A. Surzhykov, Phys. Rev. A **82**, 062702 (2010)

[3] G. Weber *et. al*, JINST **5** C07010 (2010)

[4] C. Heßler, Conf. Proc. EPAC08, 1482-1484 (2008)

[5] R. Märtin *et. al*, GSI Scientific Report 2009, ATOMIC-PHYSICS-01

Polarization properties of elastic scattering processes in the hard x–ray regime investigated at the synchrotron facility DORIS III

M. Schwemlein[1,2], *T. Groß*[1,2], *U. Spillmann*[1], *G. Weber*[1,3], *R. Märtin*[1,2], *M. von Zimmermann*[4], *and Th. Stöhlker*[1,2,3]

[1]GSI, Darmstadt; [2]University of Heidelberg; [3]Helmholtz Institute Jena; [4]DESY, Hamburg

The elastic (Rayleigh) scattering of polarized energetic photons by atoms has attracted continuous theoretical and experimental interest [1, 2]. Observations under large scattering angles are of particular importance as they are well resolved from Compton scattering contributions and, in case of high-Z targets, are most sensitive to relativistic effects on the K-shell electrons. In addition, the theoretical description of Compton to Rayleigh differential cross section is of particular challenge. The recent development of efficient and precise Compton polarimeters for the energy region between 70 keV and a few hundred keV [3] together with the availability of intense beams of polarized hard x–rays at synchrotron facilities enables for differential cross section measurements of Rayleigh scattered photons. Furthermore, for best of our knowledge, no experimental data for the degree of linear polarization of elastic (Rayleigh) scattered photons are available, up to now.

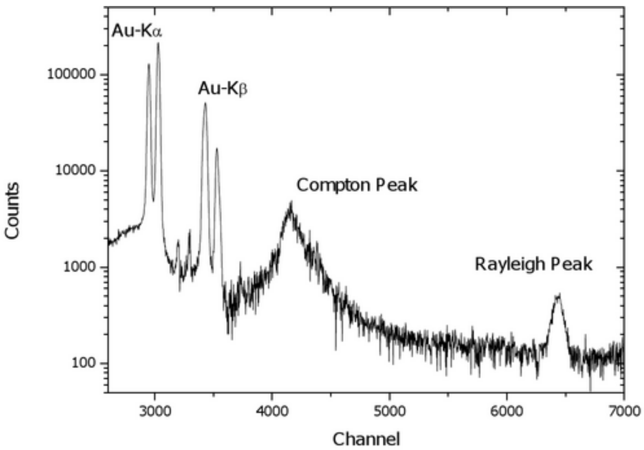

Figure 1: A linearly polarized photon beam with an energy of 147 keV, is backscattered from an Au-target. The spectrum was measured with a standard Germanium detector under a scattering angle of 156 °.

Therefore, we performed a first test experiment at Helmholtz Centre DESY in Hamburg. The synchrotron DORIS III provides us with both, a high intensity as well as a 92 % linearly polarized photon beam. Despite a high detector efficiency, a low count rate was expected because of low cross section under large scattering angles Θ. With three days of test–beamtime, the goal was to explore count rate, background radiation and the property of DORIS III for x–ray spectroscopy and polarimetry at the energy range of 100 keV.

In our experimental setup we investigated backscattered Compton and Rayleigh photons from a primary beam with an energy of 147 keV. A typical spectrum is given by figure 1, which shows the Compton– and Rayleigh–Peak at a scattering angle of $\Theta = 156\,^\circ$ as well as the $K_{\alpha_{2,1}}$ and $K_{\beta_{1,2}}$ radiation of a thin Au target. Points of interest are the Compton and Rayleigh cross sections at high energies and large scattering angles Θ. A preliminary analysis yields in Compton to Rayleigh count rate of 22 ± 5 (Au–target) and 230 ± 20 (Ni–target).

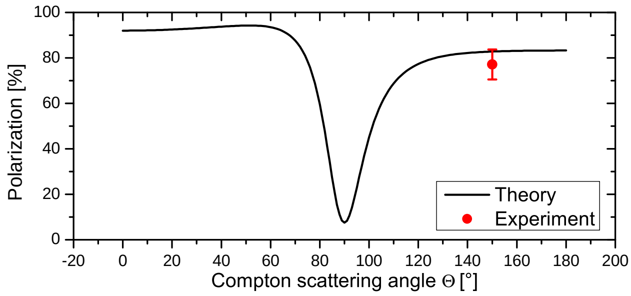

Figure 2: Expected degree of linear polarization of Compton scattered photons.

After the installation at the beamline, we started a proof–of–principle measurement with a 2D Si(Li) Compton–Polarimeter [4] to figure out, if a polarization study with low count rate of scattered photons and a high intensity of background radiation was feasible in general. Figure 2 shows the theoretical polarization of Compton scattered photons, calculated for a 92 % linearly polarized primary beam [5]. Polarization analysis leads us to a $77.1 \pm 6.6\,\%$ linear polarization of the Compton scattering peak, which fits to theory.

In this first pilot experiment, counting statistics of Au–Compton and Au–Rayleigh is low. But based on existing data we are now applying for an extended run. This future experiment, planned for 2011, will make use of an improved target chamber. This intends to reduce background radiation, which enables polarization studies of Rayleigh scattering.

References

[1] P.P. Kane *et al.*, Phys. Rep. **140** 75 (1986)

[2] A. Hopersky *et al.*, JETP **105** 549 (2007)

[3] U. Spillmann *et al.*, Rev. Sci. Instrum. **79** 083101 (2008)

[4] G. Weber *et al.*, JINST **5** C07010 (2010)

[5] F. Lei *et al.*, Space Sci. Rev., **82** 309 (1997)

High Data Rate Initiative: Electronic Readout for a Si(Li) – Compton – Polarimeter

U. Spillmann[1], E. Badura[1], K.H. Blumenhagen[2], H. Bräuning[1], J. Hoffmann[1], K. Koch[1], N. Kurz[1], R. Märtin[1,2], S. Minami[1], W. Ott [1], Th. Stöhlker[1,2,3], G. Weber[3], M. Weber[4]

[1]GSI, Darmstadt, Germany; [2]PI, University of Heidelberg, Germany; [3]HI Jena, Germany;
[4]IPE, KIT, Karlsruhe, Germany

Within the High Data Rate Initiative (HDRI) [1] of the Helmholtz research program "Photons, Neutrons, and Ions" KIT and GSI collaborate closely within the working package "Real Time Data Processing" bringing together the expertise of the partners in the development of advanced detector readout systems. As one of the first common projects between KIT, GSI and Helmholtz-Institute Jena we started the development of a self-triggering 2-dimensional position-, time-, and energy sensitive Si(Li)-strip detector read out with modern custom designed FPGA-based signal digitizer hardware as a demonstrator system. This project is of great importance for future x-ray spectroscopy and polarimetry experiments of the SPARC collaboration [2] at GSI and FAIR.

As detector platform we have chosen an already existing Si(Li)-strip detector [3] that has worked reliable in several beam times at the ESR as well as external places, e.g. TU Darmstadt and DESY, Hamburg, and has produced excellent results [4]. Up to now it was equipped with standard NIM and VME electronic. The outcome of this project using custom designed FPGA-based signal digitizer hardware will serve as a blue print for the next generation of readout electronics of thick planar strip detectors with the collaboration.

The concept is based on the fast digitizing of the preamplifier signals coming from the detector to acquire the small signals directly. The consecutive employment of pulse shape analysis techniques will show the energy and timing information of an event.

For this first demonstrator we profit from recent developments of the Experiment Electronics department of GSI. They provide us with a set of 8 FEBEX2 – ADC boards [5] with 8 input channels each. Sampling the data is performed with a frequency of 65 Ms/s and a resolution of 12 bit at an input range of +/-1V. A 1.6 GBit fiber link connects the digitizer board with the PLEXOR3-PCIe Interface hosted by a commercial PC that manages the event building and data transport by ethernet. In addition a TRIXOR1-PCIe board takes over the trigger handling and the dead time locking. The PC runs a LYNX RT-operating system and as DAQ we employ MBS [6] to take advantage of the GSI data acquisition and storage environment. To adapt the signal output of the preamplifier to the input of the FEBEX2 board the fast linear amplifier SiLiVer was developed. It has a single ended input and gives a differential output. The two consecutive amplifier stages provide a voltage gain of forty. The small form factor of the amplifier boards allows us to mount them inside the preamplifier housing to avoid losses on the signal cables.

In a first step the pulse shape analysis of the event data will be managed by PC hardware. It allows us to optimize the algorithms within a short time. The main goal of this first step is to rebuild the functionality of the NIM and VME hardware and to be able to handle photo effect and Compton events. From this point on we can make use out of the system in atomic physics experiments. In collaboration with the KIT we will refine the algorithms for the digital pulse shape analysis with the aim to manage more complex event histories like two or three Compton events for one incident photon. We plan to meet the demand of increased computing power by dedicated hardware solutions designed by KIT.

Most parts of the hardware for the demonstrator have been produced and tested already. A few parts are still in the assembly phase. First tests of the complete system are planned for March 2011.

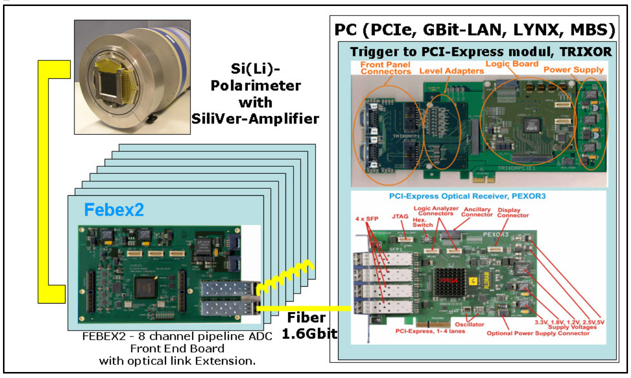

Figure 1: Sketch of the new readout chain of the Si(Li)-Polarimeter Demonstrator

References

[1] http://www.hdri-pni.de
[2] Technical Report of the SPARC collaboration http://www.gsi.de/fair/experiments/sparc/index_e.html
[3] G. Weber et al., "Performance of a position sensitive Si(Li) x-ray detector dedicated to Compton polarimetry of stored and trapped highly-charged ions", JINST 5,C07010 (2010)
[4] Th. Stöhlker et al., "Polarization and angular correlation studies of X-rays emitted in relativistic ion-atom collisions", EPJ-ST 169, 5-14 (2009)
[5] http://www.gsi.de/onTEAM/grafik/1130845854/febex2.pdf
[6] http://www-win.gsi.de/daq/

Development of a crystal spectrometer for studies with helium-like argon

N. Winters[1,2,3], Z. Yin[1,2], H.F. Beyer[1,4], D.F.A. Winters[1,2], E. Förster[4], and Th. Stöhlker[1,2,4]*

[1]GSI Darmstadt; [2]Universität Heidelberg; [3]EMMI; [4]Helmholtz-Institut Jena

Introduction

We report on the development of a crystal spectrometer for experiments with helium-like argon ions as a target. The spectrometer will be used as a precise diagnostic tool to study a) collisions between relativistic highly charged ions and argon atoms at the ESR; b) the interaction between pulses from the PHELIX laser and large argon clusters; and c) studies of He-like argon as created in the SPARC EBIT. The spectrometer is optimised for accurate x-ray spectroscopy of inner-shell transitions in He-like argon (Ar^{16+}) with an energy of about 3 keV.

Crystal spectrometer

The Bragg crystal spectrometer is arranged in the Johann geometry with a Rowland circle diameter of 1.28 m. A Monte Carlo simulation program (*MacRay*, see e.g. [1]) was used to obtain the optimum geometry. We use a cylindrically bent InSb (220) crystal with outer dimensions of 20x15 mm^2 and a lattice constant of $2d$ =4.58 Å. Bragg's Law for diffraction states that $n\lambda = 2d\sin\theta$, where λ is the wavelength of the impinging radiation according to $E = hc/\lambda = hc/(2d\sin\theta)$. First order diffraction then gives an energy of E = 3.129 keV. The diffraction angle θ=59.9° can then be related to a position X by focussing the diffracted x-rays onto a CCD camera. The size of the CCD is 26.6x6.6 mm^2, and the pixel size is 26x26 μm^2. The quantum efficiency is about 95% for ~3 keV x-rays. The spectrometer's total detection efficiency and resolution depend on the size of the x-ray source and its distance from the crystal.

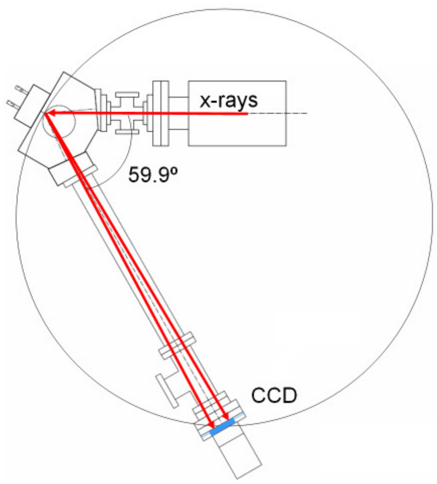

Figure 1: Schematic of the crystal spectrometer. The x-rays are diffracted from a InSb(220) crystal and detected by a CCD camera. The Bragg angle is 59.9°. The spectrometer is optimised for resolving the 1s2p → $1s^2$ ($^3P_1$, $^3P_2$, $^1P_1$) transitions in He-like argon ions at ~3.13 keV.

First results: reference spectra

For the first tests, we used the $L_{\alpha1,2}$ lines from cadmium (Cd) and terbium (Tb) at around 3.13 keV as a reference. These lines were obtained by irradiating solid state Cd and Tb targets with an x-ray tube.

The background-subtracted CCD data were analysed using a program that features *cluster analysis* (see e.g. [2]). Clusters are caused by charge splitting on the CCD, *i.e.* one photon hits more than one pixel. In the analysis, the 2D position data from the CCD is converted into an energy spectrum, which can be used to determine transition energies and line intensities.

Figure 1 shows a reference spectrum of Cd, as obtained with the crystal spectrometer. One can clearly separate the $L_{\alpha1}$ from the $L_{\alpha2}$ line, and the lines have an almost perfect Lorentzian profile, as expected.

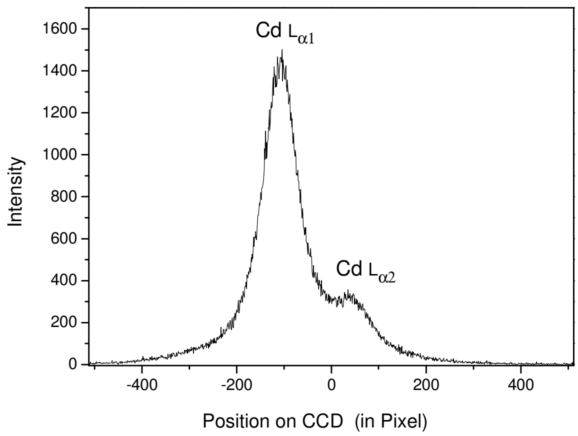

Figure 2: Cd reference spectrum recorded with the CCD camera of the crystal spectrometer.

Planned experiments

The spectrometer is designed to spectrally resolve the 1s2p → $1s^2$ ($^3P_1$, $^3P_2$, $^1P_1$) inner-shell transitions in He-like argon ions, see *e.g.* [3]. In the beginning of 2011, first tests at the SPARC EBIT are foreseen. Later, in spring 2011, experiments in the PHELIX laser bay are planned. At a later stage, the spectrometer can be installed at the internal target at the ESR.

References

[1] H.F. Beyer, Nucl. Instrum. Meth. Phys. Res. A **400**, 137 (1997).

[2] M. Trassinelli *et al.*, GSI Scientific Report 2006, atomic-physics-19, 263 (2006).

[3] R.D. Deslattes, H.F. Beyer and F. Folkmann, J. Phys. B: At. Mol. Phys. **17** L689 (1984).

On the X-ray Reflection Properties of Perfect Elastically Bent Crystals

R. Loetzsch[12] *, I. Uschmann*[2] *and E. Förster*[1,2]

[1]Helmholtz Institute Jena; [2]IOQ,Friedrich-Schiller-Universität Jena;

Elastically bent crystals are widely used as monochromators [1], spectrographs [2] and imaging devices [3] for X-rays. Thus their reflection properties have to be known precisely.

Elastically bent crystals have usually three kinds of strain: bending of net planes, gradients of the net plane distances as well as fans of net planes. If the crystal is bent in two dimensions an additional laterally varying strain gradient occurs. This effect was never studied theoretically or experimentally. But especially for very precise measurements the influence would not be negligible.

Here we report on measurements of lateral deviations of the reflection properties of two dimensionally bent crystals.

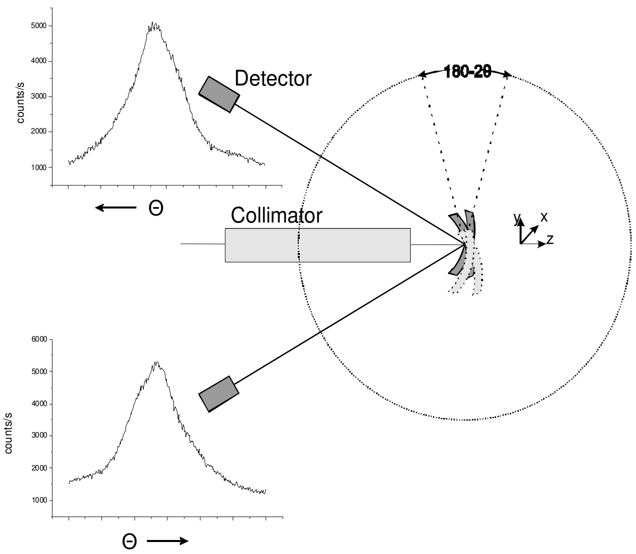

Fig. 1: Bond method: the X-ray beam from a tube is collimated and is reflected at two symmetric positions. Rocking curves are recorded.

The measurement scheme is shown in Fig. 1. It employs a modified Bond method [4] at high Bragg angles. We measure the diffracted intensity curves at the two positions were a selected net plane of the crystal reflects. The angular difference of these two positions is 180°-2 Θ, were Θ is the Bragg angle for the reflection. At different spatial crystal positions we measure the variations of the kinematical Bragg angle.

To obtain precise results one has to take a few measurement details into account. First a goniometer with steps of 0.9” (1” = $4.8 \cdot 10^{-6}$ rad is combined with an angular encoder with an accuracy of 0.18”. This allows to measure small variations of lattice constants ($\Delta d/d \sim 10^{-6}$). Since the thermal expansion of the crystal is also in the order of 10^{-6}/K the temperature during the measurement has to be stabilised. Further, if a bent crystal is moved laterally (x and y-direction), also the distance z from the reflecting point on the crystal to the rotation axis of the goniometer changes. This would introduce an error to the measurement, thus the z value has to be held constant during the measurement. This change of z value with the lateral movement is observed by a simple imaging technique, based on the limited depth of image sharpness. Then the position is corrected during the x-ray measurement.

The measurement system employs a standard X-ray tube, whose radiation is collimated by fine slits. The crystal mount consists of the goniometer combined with the encoder, a translation and a rotation stage to vary the lateral position on the crystal and a translation stage to hold the distance between rotation centre and crystal surface constant. The diffracted radiation is registered with two scintillation counters. The whole apparatus is mounted on a stone plate to stabilize it. Since the temperature in the laboratory is oscillating with amplitude of more than 1 K a Styrofoam box is covering the whole apparatus, thus the temperature during a measurement could be held constant within a few tenth Kelvin.

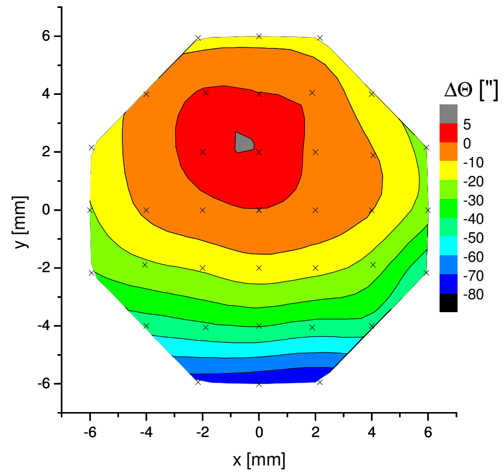

Fig. 2: Measurement of laterally varying Bragg angle. The crosses denote the measuring positions. The colors show Bragg angle deviations.

In Fig. 2 we show the first results for a spherically bent silicon crystal, whose bending radius is 206 mm. We used the 444 reflection of Cu $K_{\alpha 1}$ at a Bragg angle of 79.3°. The measuring spot on the crystal was 0.5x0.5 mm². It shows a symmetrically varying Bragg angle shift along the crystal surface with a maximal shift of 70”. For comparison: the rocking curve width for a flat silicon crystal in this reflection is 5” and for the bent one it is 90”. These variations would correspond to a spectral shift of $\Delta\lambda/\lambda=3x10^{-4}$ at 45° Bragg angle, which was never considered before as a correction in x-ray spectroscopy. But it is an additional effect on the reflection properties of two dimensionally bent crystals, which is in the same order as the Johann error and thus has to be taken into account for interpreting high resolution spectroscopy data.

[1] A. Rousse, C. Rischel, S. Fourmaux, I. Uschmann, S. Sebban, G. Grillon, Ph. Balcou, E. Förster, J. P. Geindre, P. Audebert, J. C. Gauthier, D. Hulin, “Non-thermal melting in semiconductors measured at femtosecond resolution“, Nature 410, 65 (2001)

[2] Golovkin, R. Mancini, S. Louis, Y. Ochi, K. Fujita, H. Nishimura, H. Shirga, N. Miyanaga, H. Azechi, R. Butzbach, I. Uschmann, E. Förster, J. Delettrez, J. Koch, R.W. Lee, L. Klein, “Spectroscopic Determination of Dynamic Plasma Gradients in Implosion Core”, PRL 88, 045002 (2002)

[3] E. Förster, K. Gäbel, and I. Uschmann, “X-ray microscopy of laser-produced plasmas with the use of bent crystals”, Laser Part. Beams 9, 135 (1991)

[4] Bond, W. L., “Precision lattice constant determination”, Acta Cryst. 13, 814 (1960)

SHHG report (2010): efficiency of relativistic surface harmonic generation

C. Rödel,[1,2] J. Bierbach,[1] O. Jäckel,[1,2] and G. G. Paulus[1,2]

[1] *Institute of Optics and Quantum Electronics, Friedrich Schiller University Jena, D-07743 Jena, Germany*
[2] *Helmholtz Institute Jena, Helmholtzweg 4, D-07743 Jena, Germany*

Generation of high harmonics at surfaces is a promising source of coherent XUV- and X-ray radiation. Applications range from nonlinear XUV optics to seeding of free-electron X-ray lasers. However, progress in realizing this potential is still clearly behind expectations. This project seeks to identify and remove these roadblocks. For the first time, the efficiency of surface high-harmonic generation (SHHG) was measured with a calibrated spectrometer.

INTRODUCTION

Current high intensity lasers deliver a peak power of tens or even hundreds of terawatts. The focused intensity can exceed $10^{21}\,\mathrm{W/cm^2}$. When such a laser pulse interacts with a solid target, a plasma is created and the electrons quiver in the driving field of the laser. Electrons are accelerated to relativistic energies such that $\gamma = \sqrt{1 - v^2/c^2} \approx \sqrt{1 + a_0^2}$ where a_0 is the normalized vector potential of the incident laser.

When the laser pulse is focused on a solid surface at oblique angles of incidence, the laser field causes relativistic oscillations of the vacuum-plasma boundary. The mirror-like reflection at the oscillating surface is the basis of an intuitive model of a relativistically oscillating mirror (ROM) that modulates the phase of the reflected beam. Because of the coherence of this process, XUV pulses are created harmonically when the plasma surface moves with the highest γ towards the direction of the incident wave. Therefore attosecond pulses are created within each cycle leading to a harmonic comb in the spectral domain. The XUV pulses are shorter than the driving laser pulse because of the high nonlinearity of the process. A thorough analytical model of surface high harmonic generation (SHHG) process predicts a power law of the emitted harmonics

$$\eta(\omega) = \left(\frac{\omega}{\omega_0}\right)^{-\frac{8}{3}} \tag{1}$$

up to a roll-off frequency $\omega_{ro} \approx 8\gamma^3\omega_0$.

Using these equation as an estimate for the spectral properties of the generated harmonics with a driving laser of $a_0 = 10$, the surface harmonic emission should be a competitive XUV source as compared to FLASH and even more powerful free-electron X-ray lasers. Due to their coherence and their diffraction limited beam

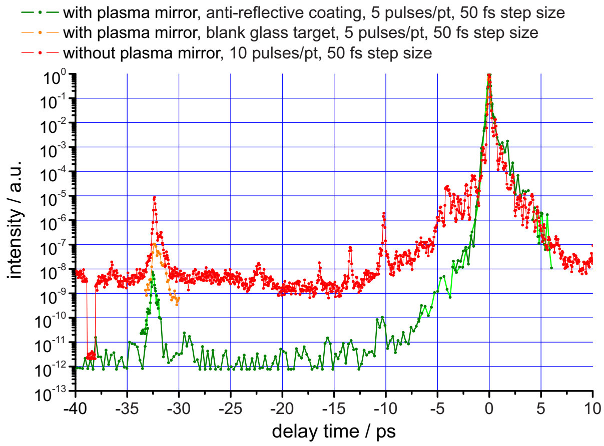

Figure 1. contrast enhancement using different plasma mirror targets: red) without plasma mirror, orange) with blank glass (BK7) plasma mirror target, green) with anti-reflective (AR) coated plasma mirror target

quality, surface harmonic radiation seems to be an ideal candidate for seeding free-electron lasers like FLASH or XFEL. Surface harmonic radiation is not limited in intensity as it is the case for gas harmonics and intense harmonic emission in the keV range should be feasible with current laser systems.

Notwithstanding theoretical predictions on the efficiency of SHHG, experimental results are below expectations so far. For a long time, the laser pulse contrast has been believed to be the decisive problem. Due to often ineluctable technical limitations of ultrahigh power laser systems, there is a certain laser intensity level before the main pulse. Accordingly, a plasma is created even before the main pulse arrives and causes a pre-plasma. The respective electron density as a function of space decreases exponentially

$$N(x) = N_{\max} \exp\left(-\frac{x}{L_p}\right) \tag{2}$$

on the plasma scale length L_p. Current theoretical models, however, assume a step-like plasma density and thus are not dependent on parameters like $N_{\max}$ or L_p. It turns out that this assumption is valid only in the ultra-relativistic limit, i.e. the power law (1) is universal and indepent on $N_{\max}$ or L_p in this limit. Experimentally, the laser pulse contrast and the plasma scale length can be controlled using a plasma mirror [1]. A contrast measurement is shown in Fig. 1.

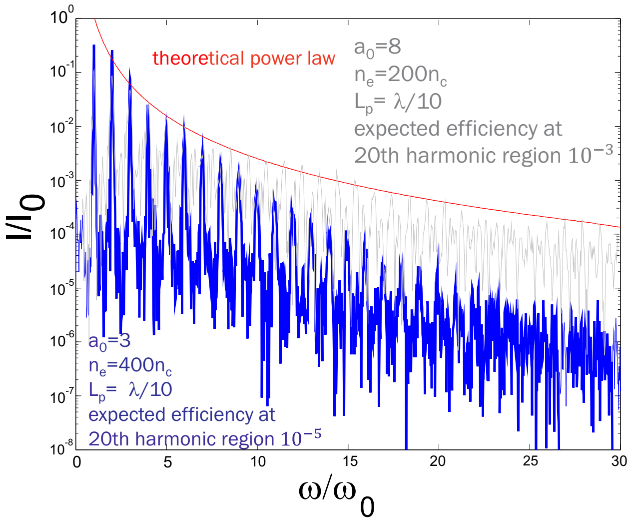

Figure 2. one-dimensional particle-in-cell simulation with LPIC code: blue) JETI experiment $a_0 = 3$, $\tau = 80\,\mathrm{fs}$, $L_p = 0.1\lambda$, $N_{\max} = 400n_c$), grey) conditions with upgraded JETI laser and plastic coated targets $a_0 = 8$, $\tau = 30\,\mathrm{fs}$, $L_p = 0.1\lambda$, $N_{\max} = 200n_c$

SIMULATIONS

In order to include realistic plasma conditions, we performed one-dimensional simulations of the emitted surface harmonics using the particle-in-cell code LPIC. Using actual laser pulse parameters ($a_0 = 3$, $\tau = 80\,\mathrm{fs}$) and plasma parameters, it shows that the simulated efficiency at the 20th harmonic is some orders of magnitude below the predictions of the theoretical power law, see Fig. 2. An increase of the laser amplitude from moderate relativistic values of $a_0 = 3$ to strongly relativistic values $a_0 = 8$ results in a significant increase of harmonic intensity and in spectra fitting perfectly to the predicted power law as seen at the grey curve of Fig. 2. The corresponding laser and plasma parameters can be achieved with the upgraded JETI laser system. The predicted efficiency at the 20th harmonic increases from 10^{-5} to 10^{-3} as a_0 is increased from 3 to 8.

The simulations exhibit a few other interesting features. The double line structure, e.g., in relativistic SHHG spectra can be explained by spectral modulations caused by an unequal spacing of the emitted attosecond pulse train. This effect can be attributed to a denting of the emitting surface. The light pressure pushes the oscillating surface and leads to different emission points from the surface. Hence the attosecond pulse train has an unequal spacing and a negative chirp. This line structure was observed experimentally and is in good agreement to the theoretical modeling [2].

The efficiency of SHHG also depends on the plasma scale length in a moderate relativistic regime. In particular the efficiency drops down for scale length shorter than $\lambda/5$ and high values of $N_{\max}$. An optimization of these parameters should affect the stability of the harmonic generation which is essential for future applications.

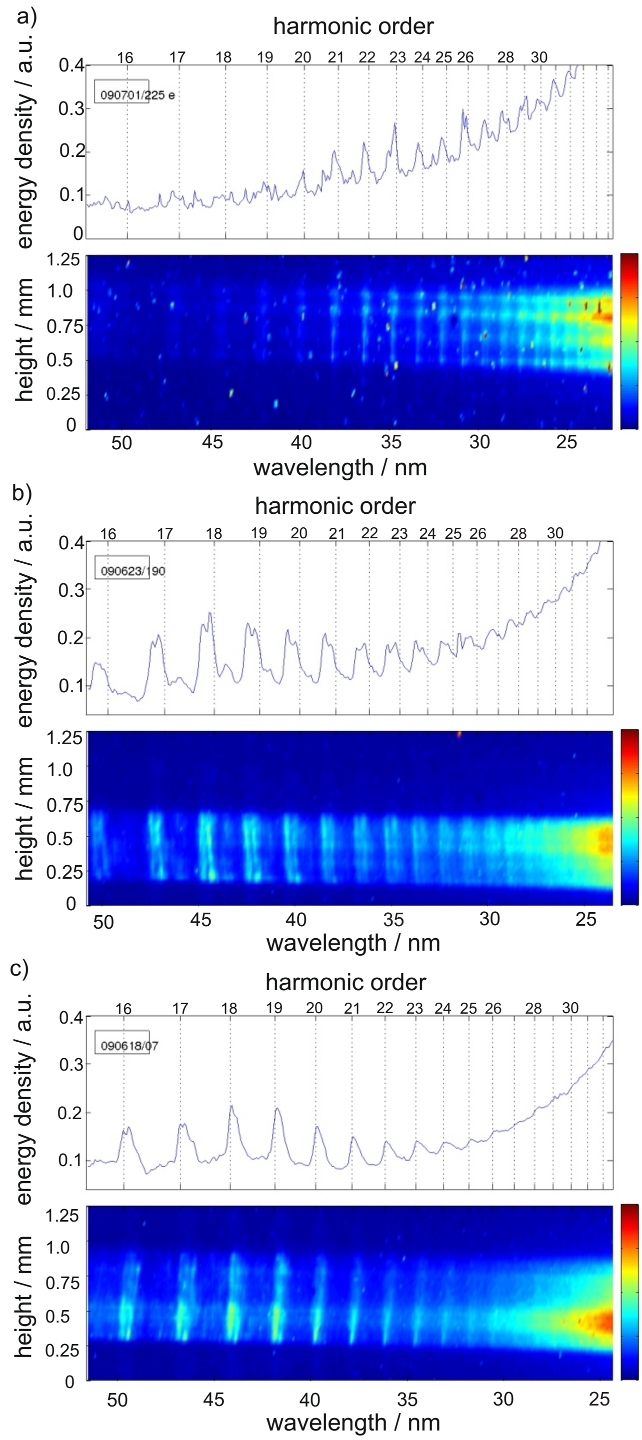

Figure 3. experimental raw spectra with different laser pulse contrast: a) without plasma mirror b) with intermediate contrast enhancement c) with best contrast enhancement

EXPERIMENTS AT JETI LASER

Surface high harmonic emission was recorded with a single-shot XUV spectrograph that has been calibrated regarding the incident photon flux at the ELETTRA synchrotron. Typical raw spectra and lineouts for different contrast conditions are shown in Fig. 3. The strongest harmonic emission was found at intermediate contrast. However, the reproducibility of the harmonic emission suffers considerably if an intermediate or bad pulse contrast is used. For estimating the energy that is contained in each harmonic line, it is necessary to include the beam characteristics of the XUV pulses. We assume a divergence of the relativistic harmonic emission by using the numerical values of a similar SHHG experiment at the ASTRA laser. Based on this, we conclude that the 17th harmonic contains $2\,\mu$J, the 21th 100 nJ, and the 25th 10 nJ. The conversion efficiency drops exponentially and is 10^{-5}, 10^{-6}, and 10^{-7}, respectively. This agrees quite well with the simulations. A further increase of intensity, as it will be the case for the upgraded JETI, will improve the efficiency by more than one order of magnitude.

Another approach to improve the stability and our understanding of SHHG comprises the systematic investigation of the dependence of SHHG on the plasma similarity parameter

$$S = \frac{N_{\max}}{a_0 \cdot n_c}. \tag{3}$$

By using efficient second order harmonic generation with a ultra-thin KDP crystal, the contrast and the critical plasma density n_c will be improved. Targets with a low density will be used to reduce $N_{\max}$.

[1] C. Rödel, M. Heyer, M. Behmke, M. Kübel, O. Jäckel, D. Ehrt, M. C. Kaluza, G. G. Paulus, *High repetition rate plasma mirror for temporal contrast enhancement of terawatt femtosecond laser pulses by three orders of magnitude*, Applied Physics B (accepted)

[2] M. Behmke, D. an der Brügge, C. Rödel, M. Cerchez, D. Hemmers, M. Heyer, O. Jäckel, M. Kübel, G. G. Paulus, G. Pretzler, A. Pukhov, M. Toncian, T. Toncian, O. Willi, *Controlling the spacing of attosecond pulse trains from relativistic surface plasmas*, (submitted)

[3] C. Rödel, M. Behmke, M. Heyer, S. Fuchs, E. Eckner, J. Bierbach, W. Ziegler, O. Jäckel, G. Pretzler, G. G. Paulus, *Efficiency of surface high harmonic radiation generated with a table-top terawatt laser*, (in preparation)

Generation and tuning of high-order harmonic radiation for x-ray-laser seeding using the Phelix shortpulse-frontend

D. C. Hochhaus[1,2,3], J. Seres[4,5], B. Aurand[1,3,7], B. Ecker[1,6,7], B. Zielbauer[1,6], D. Zimmer[1,7,8], C. Spielmann[4,5], T. Kühl[1,7]

[1]GSI Helmholtzzentrum für Schwerionenforschung, Darmstadt, Germany; [2]Johann-Wolfgang von Goethe Universität, Frankfurt, Germany; [3]ExtreMe Matter Institute, Darmstadt, Germany; [4]Friedrich Schiller Universität, Jena, Germany; [5]Universität Würzburg, Würzburg, Germany; [6]Helmholtz Institut Jena, Jena, Germany; [7]Johannes Gutenberg Universität Mainz, Mainz, Germany; [8]Université Paris-Sud 11, Orsay, France

.

Over the last years the x-ray laser team of GSI developed a good expertise in the generation of x-ray lasers in Ni-like media using the travelling wave excitation in the in-house developed double-pulse single beam grazing incidence pumping (DGRIP) scheme [1]. Amelioration of the beam quality and the spatial coherence as well as the pointing stability of plasma-based soft x-ray lasers (XRL) has been successfully demonstrated by using high-order harmonic (HH) radiation for injection-seeding [2, 3].

The proposed usage of soft x-ray lasers at GSI (XRL) for spectroscopy of heavy ions in the experimental storage ring (ESR) and in the upcoming storage ring at FAIR (NESR) will benefit from the capability of using a seeded XRL. A successful seeding process demands amongst others a perfect spectral match between the XRL lasing transition and the seed harmonic. The pump-laser dependent HH wavelength ($\lambda_k = \lambda_1/k\,, k = 2n+1,\ n \in \mathbb{N}_0$) can be tuned by controlling the process of high-order harmonic generation in the gas medium even if the pump laser wavelength is fixed, as it is the case for the Phelix Nd:glass laser system.

In the experiments performed, we focused the 350 fs long laser pulses into a nickel tube which was connected to a pulsed gas valve delivering ms-long He, Ne or Ar gas pulses. The nonlinear interaction of the intense laser pulses with intensities of 10^{14}-10^{15} W/cm² with the gas lead to high harmonic emission in the soft x-ray regime.

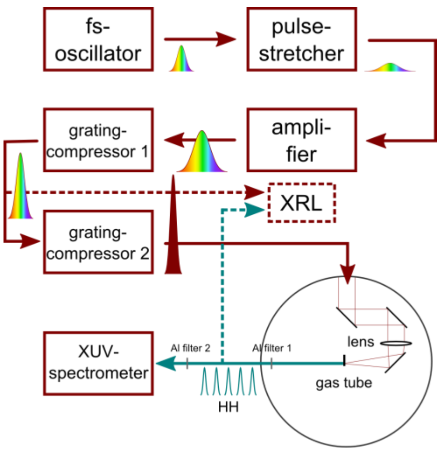

Figure 1: Schematic of the HH setup.

The HH radiation was analyzed by an in-house developed XUV-spectrometer using a flat-field grating and a XUV-charge coupled device resulting in a spectral resolution of ≈ 0.02 nm/px.

To extend the accessible XRLs for injection seeding, we mixed the Phelix frontend beam with its second harmonic to be able to create not only odd but also even order harmonic radiation up to the 59th harmonic at 17.86 nm. The lines were spectrally tuned by taking advantage of the non-adiabatic frequency shift applying quantum-path control [4].

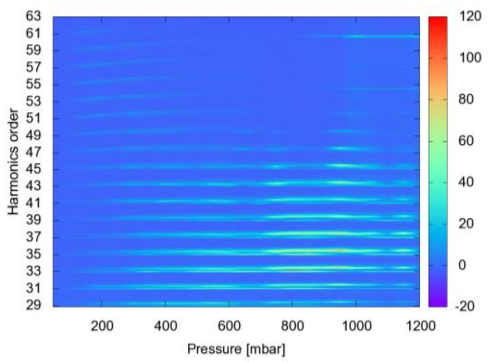

Figure 2: Broadening of the spectral coverage by the non-adiabatic blueshift

Results

We were able to extend the spectral coverage of the HH radiation created by the Phelix-fs-frontend to cover a large spectral portion of the XUV/soft x-ray regime between 18 nm and 35 nm allowing spectral overlap with many XRL transitions such as Ni-like Y (24.01 nm), Zr (22.02 nm) and Mo (18.9 nm) X-ray lasers. Ni-like Nb (20.33 nm) as well as Ne-like Mn (26.9 nm), Fe (25.49 nm), Ge (23.2 nm) and Se (20.6 nm) are in reach.

References

[1] D. Zimmer.et al., Opt. Express 16, 10398 (2008)
[2] Ph. Zeitoun et al., Nature 431, 426 ff (2004)
[3] Y. Wang et al., Nature Photonics. 2008;2(2):94-98
[4] D. C. Hochhaus et al., Appl. Phys. B (to be published)

High Brightness Coherent X-ray Sources by High-Order Harmonic Generation and Parametric X-ray Amplification

B. Ecker[1,3,5], B. Aurand[1,4,5], V. Bagnoud[1], D.C. Hochhaus[1,4,6], T. Kuehl[1,4,5], B. Zielbauer[3], D. Zimmer[1,5], J.Seres[2], E.Seres[2], C. Spielmann[2]

[1]GSI, Darmstadt, Germany; [2] Friedrich-Schiller-Universität Jena, [3] Helmholtz Institut Jena, [4]ExtreMe Matter Institute, [5]Johannes Gutenberg-University Mainz, [6]JohannWolfgang von Goethe-University Frankfurt

Progress in HH Generation at GSI

The development of high-order harmonic (HH) generation at GSI aims at creating a seed source for soft X-ray lasers (SXRL) that are based on amplification of spontaneous emission. It has been demonstrated that a seeded SXRL possesses a higher beam quality in terms of spatial homogeneity and spatial coherence [1]. In combination with the narrow spectral bandwidth, seeded SXRL represent attractive diagnostic tools for highly charged heavy-ion spectroscopy experiments [2].

In 2010 the investigations on HH generation at GSI succeeded in shifting the HH radiation in a large spectral range, covering 50% of the spectrum between 17 nm and 35 nm [3]. Furthermore, a new process called x-ray parametric amplification (XPA) was discovered, demonstrating an exponential increase of the XUV pulse energy by three orders of magnitude [4].

HH- / XPA-Setup and Experimental Results

The HH and XPA experiments utilize the front-end of the PHELIX laser system, which delivers up to 10 mJ of pulse energy compressed to 350 fs FWHM pulse duration at a repetition rate of 10 Hz. The beam is focused by either a 40 cm or 60 cm focal length lense to an almost diffraction-limited focal spot of 50 µm FWHM in diameter, resulting in an intensity of up to 1.5e15 W/cm². The gaseous medium used to create the XUV radiation is provided by a Ni tube backed by an electronic valve. The combination with a precision valve controller allows for applying a well-defined pressure in the range between 50 mbar and 1200 mbar. Further parameters to optimize the XUV signal are the IR laser pulse energy and the position of the gas tube relative to the focal spot. The XPA and HH radiation is directed to an in-house developed XUV diagnostics chamber, providing both a XUV footprint camera and a spectrometer. The first is used to measure the spatial profile of the XUV beam, allowing the estimation of the XUV pulse energy, the beam divergence and the spatial energy distribution. The latter consists of a 1200 l/mm flat-field gold grating and a back-illuminated CCD camera, recording the XUV spectrum in the range between 17 nm and 35 nm. To separate the XUV and the IR light two separate Al filters of 200 nm thickness are used.

Figure 1 shows the measured beam profile of the 41st harmonic at 25.7 nm, integrated over fifty XUV pulses. The FWHM beam diameter of 0.6 mm x 0.8 mm corresponds to a divergence of 0.9 mrad x 1.1 mrad, respectively. The ellipticity can be related to a spatial chirp of the IR pump laser, which was caused by a misalignment of the pulse compressor and resulted in an elliptical focal spot.

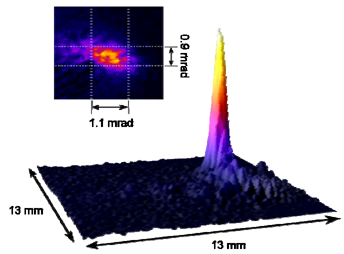

Figure 1: Spatial profile of the XUV beam at 25.7 nm in 2D and 3D integrated over fifty consecutive shots. The FWHM spot size of 0.6 x 0.8 mm² corresponds to a divergence of 0.9 x 1.1 mrad.

Summary and Outlook

The demonstrated the spectral overlap of the HH radiation and several SXRL transitions has been the key prerequisite for carrying out future SXRL seeding experiments at GSI. In addition, the newly discovered XPA process has been studied in experiments performed at GSI and at the JETI laser system in Jena. The data obtained from the latter is currently being evaluated. Further experiments utilizing the PHELIX and JETI lasers are planned for 2011.

References

[1] Ph. Zeitoun et al., “A high-intensity highly coherent soft X-ray femtosecond laser seeded by a high harmonic beam”, Nature 431, 426-429 (2004)

[2] A. Gumberidze et al., Nucl. Instrum. Methods Phys. Res., Sect. B, Beam Interact. Mater. Atoms 267, 248 (2009)

[3] D. C. Hochhaus et al., “Tuning the high-order harmonic lines of a Nd:Glass laser for soft x-ray laser seeding”, Appl. Phys. B 100, 711-716 (2010)

[4] J. Seres et al. , Nature Physics 6, 455-461 (2010)

Time-resolved XUV Thomson Scattering at FLASH

U. Zastrau[2], E. Förster[1], V. Hilbert[2], S. Toleikis[3], and P. Neumayer[4]

[1]Helmholtz Institute Jena; [2]IOQ, Friedrich-Schiller-Universität Jena;
[3]HASYLAB, DESY Hamburg; [4]EMMI and GSI Darmstadt;

Thomson scattering in the XUV or x-ray regime using free electron laser (FEL) radiation provides a diagnostic method for the determination of important plasma parameters such as temperature and density. Such a diagnostic is of crucial interest for the investigation of so-called Warm Dense Matter (WDM) with free electron densities of n_e=10^{21}-10^{26} cm^{-3} and temperatures of several eV. Using XUV radiation at 92 eV photon energy, provided by the FLASH facility at DESY Hamburg, we gain access to the WDM regime at near-solid density (n_e=10^{21}-10^{22} cm^{-3}). The experimental parameters enable to investigate a regime where the transition from ideal plasma to degenerate, strongly coupled plasma occurs [1]. A systematic understanding of this largely unknown WDM domain is crucial for the modeling and understanding of contemporary plasma experiments, like laser shock-wave or Z-pinch experiments as well as for inertial confinement fusion (ICF) experiments, as the plasma evolution follows its path through this domain.

In order to study basic plasma properties from scattered spectra, it is necessary that the respective radiation source is able to penetrate through dense plasmas, i.e. the frequency of the probing radiation ω_{rad} has to be larger than the density dependent electronic plasma frequency ω_{pe}. Available sources to probe such plasmas are x-ray backlighter systems as well as FEL radiation currently available in the XUV at FLASH or the x-ray regime at LCLS (California).

Within the last four years, an international group of scientists bundled their expertise, aiming for the realization of XUV Thomson Scattering on liquid hydrogen droplets at FLASH. The X-ray Optics Group Jena coordinated a capacious BMBF project for "Innovative instrumentation at FLASH", which has been extended for another three years funding period, starting from July 2010. Together with several subcontractors, such as the "Fraunhofer Institut für Optik und Feinmechanik Jena" (Dr. Torsten Feigl) and the "FIAS Frankfurt" (Dr. Paul Neumayer), we are developing sophisticated XUV spectrometers, imaging systems, and interferometers for the Thomson Scattering experiment.

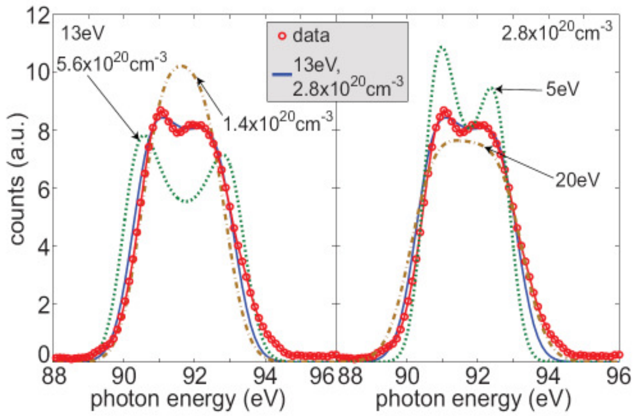

Fig. 1: Self-Thomson Scattering Spectra obtained with HiTRaX spectrometer at FLASH in 2009 [2].

In former experiments, we successfully demonstrated "self-Thomson Scattering" on liquid hydrogen [2]. That is, the liquid hydrogen sample is hit by the intense XUV pulse with pulse duration of about 15 fs. While the first part of the pulse mainly heats the droplet via photoionization, the later part of the pulse scatters off a heated plasma at warm dense matter conditions. We used the very successful "HiTRaX" spectrograph, which was developed, built, and calibrated by a Jena-DESY joined team [3]. From XUV spectra obtained using this instrument, we were able to determine the fundamental plasma parameters, density and temperature (see Fig. 1). This outstanding result was published in Physical Review Letters in 2010 [2].

A second XUV spectrometer, using a Hitach flat-field grating, was built by our subcontractor Dr. P. Neumayer from FIAS Frankfurt. It is named "Flatfield Forward Scattering Spectrometer (FFSS). This spectrometer will be upgraded by a large-aperture multilayer reflection mirror to cover several angles simultaneously.

It is in this context that we report on first time-resolved experimental data obtained in a recent experimental campaign at FLASH in October 2010. For the first time, the highly demanding task of overlapping three beams in space and time was achieved. The hydrogen droplet beam, a pumping 100-fs Ti:Sapphire laser pulse (800 nm wavelength), and the probing 30-fs XUV pulse (92 eV photon energy) where overlapped with 5 µm spatial and 500 fs temporal precision.

The Ti:Sapphire laser reached an intensity of several 10^{13} W/cm² in the focus, ionizing the hydrogen droplet mainly by tunnel-effect and barrier-suppression [4]. The generated hot electrons heat the target homogeneous by collisions. Within the first picoseconds after excitation, the atoms and ions (protons) gain the thermal energy from the hot electron gas. The Thomson-scattered signal is observed by two independent XUV spectrometers at 20° (FFSS) and 90° (HiTRaX) degrees scattering angle. As sketched in Fig. 2, we observe a strong increase in direction of smaller scattering angles after 5 ps. These results are currently under detailed analysis. In the next years, the complex plasma dynamics of laser-excited hydrogen will be investigated by time-resolved XUV Thomson Scattering at several angles simultaneously.

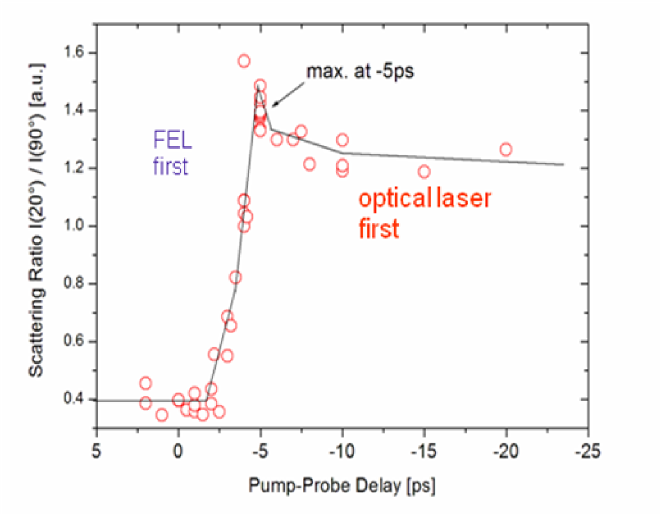

Fig. 2 The ratio of Rayleigh-scattered photons as function of the pump-probe delay.

References

[1] R.W. Lee, et al., *J. Opt. Soc. Am.* **B20**, 770 (2003)
[2] R. Fäustlin, U. Zastrau, E. Förster, et al., *J. Inst.* **5** P02004 (2010)
[3] R. Fäustlin, …, U. Zastrau, E. Förster, et al., *Phys. Rev. Lett.* **104**, 125002 (2010)
[4] P. Gibbon and E. Förster, *Plasma Phys. Contr. Fusion* **38** 769 (1996)

X-ray emission from laser-plasma acceleration experiments

S. Trotsenko[1,2], D. B. Thorn[2,3], G. R. Plateau[4,5], C. G. R. Geddes[4], N. H. Matlis[4], E. H. Esarey[4], M. Battaglia[4], C. B. Schroeder[4], S. Shiraishi[4], Th. Stöhlker[1,6], S. Tashenov[2,6], C. Tóth[4], and W. Leemans[4]

[1]Helmholtz Institute Jena, 07743 Jena, Germany; [2]GSI, 64291 Darmstadt, Germany; [3]ExtreMe Matter Institute EMMI/GSI, 64291 Darmstadt, Germany; [4]Lawrence Berkeley National Laboratory, Berkeley, CA 94720, USA; [5]École Polytechnique, 91128 Palaiseau, France; [6]University of Heidelberg, 69120 Heidelberg, Germany;

Laser driven plasma-based accelerators [1,2] have been shown to generate quasi-monoenergetic electron beams with energies up to GeV [3,4]. The studies have shown a big potential of this accelerators to become a cost efficient alternative to the conventional linear accelerators. In such accelerators, a femtosecond laser pulse drives a plasma wave whose space charge field accelerates electrons from the plasma. Even though, for the replacement of conventional linear accelerators with the laser-plasma accelerators requires further development, the latter offer several unique applications. In particular, x-ray emission from oscillations of the electrons (betatron motion) in the intense focusing field of a laser-plasma accelerator show promise for use in femtosecond-scale time-resolved radiography of ultrafast processes. However, the spectral characteristics of this betatron emission have been so far characterised only from filter pack measurements.

In order to achieve higher resolution in spectroscopy of betatron radiation, we used an x-ray charge-coupled device to record the spectrum of betatron radiation, with a full width at half maximum resolution of ≤ 250 eV. Moreover, simultaneous measurements of x-ray and electron spectra has been performed along with x-ray images that allowed for determination of the betatron emission source size. This allows for a determination of differences in the x-ray spectra as a function of the energy spectrum of accelerated electrons.

Details of the experimental setup are shown in Fig. 1. Here, a pulse from Berkeley's LOASIS Ti:sapphire laser was focused above a gas-jet nozzle oriented transversely to the beam line. The peak power was 10 TW [0.45 J in 45 fs FWHM] and was focused onto a 7.5 μm FWHM spot. The plasma density profile had a peak density of $3 \cdot 10^{19}$ cm^{-3}. For a characterization of the electron beam a combination of integrating current transformer (ICT), phosphor screen and an optical CCD was used.

For the x-ray imaging as well as measuring their energy distribution, a 1024x256 pixel back-illuminated CCD camera was used with 26 μm square pixels and a 40 μm deep depletion region. The CCD was placed 220 cm from the laser/gas-jet interaction region and was operating under a high vacuum. A thin window (0.1 μm Al, 14 μm polycarbonate, 18 μm Kapton) was installed between the CCD and the laser interaction chamber, because of the different vacuum requirements for them.

For the measurements of the betatron emission source size, few fiber wires with different thicknesses (and materials) were fabricated in order to form crosshairs that were placed between the laser/gas-jet interaction region and the CCD.

In order to reduce background from high energy photons (resulting from stopping many MeV electron beams in the magnetic spectrometer) the CCD was placed in a lead brick enclosure. In addition, the line of sight of the camera was restricted by a rectangular stainless steel pipe that was fitted to the size of the CCD chip (~25x7 mm^2). Also the part of the aluminium target chamber on the CCD side was covered with plastic in order to reduce on-axis hard x-ray bremsstrahlung. For further details of the experiment we refer to [5].

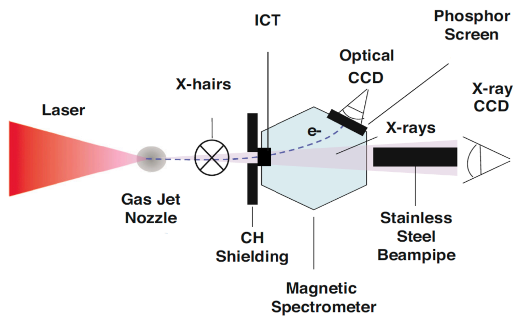

Figure 1: Schematic of the experimental setup.

The studies were extended to the higher energy region, well above the Si *K*-edge of the synchrotron radiation. The second amplifier of the LOASIS laser system (<60 TW) was used. The higher energy region was chosen in order to avoid uncertainties related to the low-energy features of the photon spectrum [5]. In addition, this measurements were supplemented by use of filter packs.

From a preliminary data analysis one can conclude that a high flux (~10^6) of ~5 keV collimated photons (~2.7x0.7 mrad) was achieved. Also correlation of the x-ray flux with the electron beam charge was observed with insensitivity of the first to other accelerator parameters. The data analysis is in progress.

The support by the US Department of Energy, NA-22 and NSF is gratefully acknowledged..

References

[1] T. Tajima and J. M. Dawson, Phys. Rev. Lett. 43, 267 (1979).
[2] E. Esarey *et al.*, IEEE Trans. Plas. Sci. 24, 252-288 (1996).
[3] K. Nakamura *et al.*, Physics of Plasmas 14, 056708 (2007).
[4] J. Osterhoff *et al.*, Phys. Rev. Lett. 101, 085002 (2008).
[5] D. B. Thorn *at al.*, Rev. of Scient. Instr. 81, 10E325 (2010).

Measurement of Strong Electric Fields in Target Normal Sheath Acceleration*

R. Loetzsch[1,2], S. Höfer[1,2], T. Kämpfer[1,2], J. Polz[2], O. Jäckel[2], I. Uschmann[2], E. Stambulchik[3], E. Kroupp[3], I. Maron[3], and E. Förster[1,2]

[1]Helmholtz Institute Jena; [2]IOQ, Friedrich-Schiller-Universität Jena; [3]Weizmann Institute of Science , P.O.Box 26, Rehovot 76100, Israel

During the interaction of an intense laser pulse with solid targets, electrons are accelerated to relativistic energies. This is accompanied by the creation of strong electric and magnetic fields reaching TV/m and tens of kT. Especially at the rear side of laser irradiated foils this strong electric fields lead to acceleration of ions to MeV energies, known as target normal sheath acceleration (TNSA) process. Although the effects of these strong fields are well known and used, most information about the fields is gained through simulations, since they are hard to measure. But measurements would be very helpful to verify and benchmark these simulations which are important not only to understand laser foil experiments but also astrophysical and fusion plasma processes.

Our tool for measuring these electric fields is K-shell spectroscopy, since the emission of an atom in such a field is altered due to the Stark effect. Thus we use a tracer layer at the backside of the irradiated foil to deduce the TNSA fields. The tracer should be a light element where the Stark effect is greater than in high Z elements, but on the other hand the K-shell emission of very light elements is harder to detect. Therefore the chosen compromise is silicon with its K-shell emission around 1740 eV. Strong electric fields alter this emission in two ways: first one of the three K-α components is shifted to higher energies. This shift depends quadratically on the field strength. And secondly the dipole forbidden L1-K transition at 1680 eV becomes allowed, and the ratio of its intensity to the intensity of the other K-α components depend quadratically on the field strength. For electric field strengths of 1 TV/m this ratio is approximately 1/1000. Especially the second effect is a unique evidence for the fields, since it is not affected by magnetic fields or emission by higher ionized atoms as it is the case for the first effect.

To measure these rather weak signals one needs a spectrometer with a high luminosity which has to cover a fairly great wavelength range. Thus a cylindrically bent PET crystal spectrometer in von Hámos geometry with an opening angle of 20 degree was used. Since one can expect a large background from scattered and direct high energetic photons to this signal, it is necessary to detect single photons to have a chance to distinguish between the background and the signal. Therefore a CCD camera is used to detect the signal. Additionally a careful shielding is necessary. To provide a correlation between x-ray signal and TNSA accelerated ions, we simultaneously measure the ion spectra for each shot.

* Work supported by Laserlab Europe and the DFG (TR18)

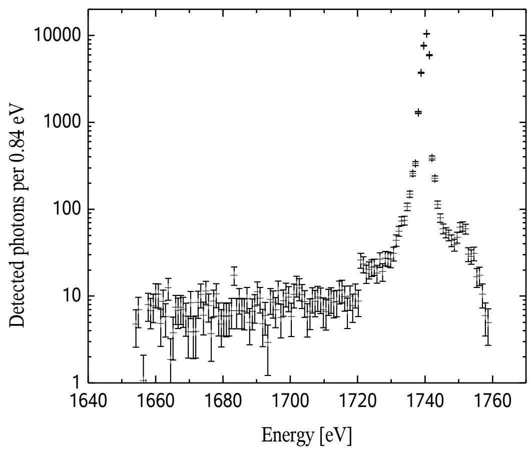

Figure 1: Silicon K-shell spectrum accumulated over 120 shots from a 25 µm thick Ti foil coated by 1 µm SiO.

The experiment was carried out on the JETI laser system in Jena, delivering pulses of 30 fs pulse duration with energy of approx. 800 mJ on the target. The targets used were Ti foils of either 5 or 25 µm thicknesses, coated by 1 µm SiO.

In Fig.1 we show the spectrum from the 25 µm Ti foil. This spectrum is obtained by utilising the single photon counting regime of CCD. Thus only photons in the right energy range were taken into account. The images from 120 shots are accumulated. It shows the capability to measure the K-shell emission almost background free. The dynamic range achieved is better than 3 orders of magnitude.

Unfortunately in this measurement campaign the laser had a prepulse problem, so the electric field strengths were not that high as possible. Therefore we only measured protons with energies up to 0.4 MeV for 5 µm thick Ti foils and even smaller proton energies for the 25 µm thick Ti foils. In the thicker foils we also detected protons only in a few shots. Thus we were not able to detect the forbidden L1-K transition this time. The other problem was that the 5 µm thin Ti foils are too transparent to the Bremsstrahlung emitted from the front-side plasma. This might be different with better prepulse conditions, if not, one could use targets with higher Z than Ti, that would absorb the Bremsstrahlung more efficient.

Research Area 5: QED and relativistic ionization

The future facilities of photon heavy-ion science are opening up a new frontier for studies of the structure of matter and its interactions. In this research area, relativistic ionization by ultrahigh-intensity lasers probe the quantum many-particle dynamics in atoms. A combination of heavy-ion beams at GSI and FAIR with high-intensity lasers provide a novel approach to investigate highly relativistic single-electron ionization. They may also give access to the regime of QED-induced nonlinearities of the quantum vacuum and pave the way towards new tests of fundamental symmetries such as atomic parity violation. Our joined projects offer unprecedented studies of fundamental physics complementary to collider experiments, realizing the vision to establish high-intensity lasers as a new tool for fundamental physics.

Research in the project EBIT focuses on setting up and testing an electron beam ion trap for future experiments targeting the investigation of relativistic ionization dynamics. Of particular interest are relativistic and QED corrections of the photoionization process.

Further research concentrates on developing a Penning-trap-based tool for advanced studies of multiphoton ionization of confined particles and other reactions by highly intense laser light. Particularly, the control of the particles' localization and spatial density helps to optimize the laser-particle interaction in highly focused fields.

The QED theory project has developed several experimental scenarios for testing long-standing predictions from quantum electrodynamics as well as advancing the search for hypothetical new particles beyond the standard model.

We have proposed a new mechanism to search for spontaneous vacuum decay in strong fields in terms of pair production. This catalysis mechanism relies on the unprecedented combination of high-intensity lasers and X-ray probe photons. Furthermore, we have proposed the first scenario where high-intensity lasers could contribute to search for unexpected optical signals that would point to new particle candidates such as axion-like particles (ALPs).

Finally, we have contributed to the investigation of parity violation in atomic transitions, which provide for a complementary lever arm on physics beyond the particle standard model. Parity-violating effects originating from electroweak neutral currents can become visible in transitions induced by high-intensity lasers. Our research has identified suitable atomic transitions and helped determining the required laser intensity relying on state of the art EUV laser sources.

EBIT report (2010): relativistic ionization dynamics

T. Rathje[1,2], *D. Hoff*[2], *A. M. Sayler*[2], *N. Shvetsov-Shilovsky*[2], *T. Stöhlker*[2,3], *and G. G. Paulus*[1,2]

[1]Helmholtz Institute Jena, Helmholtzweg 4, D-07743 Jena, Germany; [2]Institut of Optics and Quantum Electronics, Friedrich Schiller University Jena, D-07743 Jena, Germany; [3]GSI Helmholtzzentrum für Schwerionenforschung, Planckstraße 1, 64291 Darmstadt

Research in the project EBIT focused on setting up and testing an electron beam ion trap for future experiments targeting the investigation of relativistic ionization dynamics.

Introduction

Intense ultra-short lasers enable ionization of heavy ions to very high charge states. The ionization dynamics is characterized by by absorption of hundreds of photons and emission of many electrons. The electron dynamics is dominated by relativistic kinematics. Upcoming petawatt-class laser facilities will also lead to relativistic heavy ion kinematics. Of particular interest are relativistic and QED corrections of the photoionization process.

Electron Beam Ion Trap EBIT

The investigation of the ionization dynamics at ultrahigh intensities has always been hampered by ionization of background gas: All atoms ionize within a fraction of the duration of a femtosecond laser pulse as soon as the intensity exceeds a few times $10^{14}\ \mathrm{W/cm^2}$. Terawatt or even petawatt lasers can be focused to intensities six orders of magnitude higher. However, the focal volume where the intensity reaches these values is by orders of magnitude smaller than the focal volume where ionization of atoms saturates. As a consequence, even for the best vacua feasible, experiments performed so far were dominated by ionization of background gas.

The goal of our approach is to separate ionization events from the species of interest from ionization of background gas in space and time thus allowing a very efficient discrimination of background events. This goal can be accomplished using a fast ion beam that is crossed by the intense laser beam at right angles. The ions, further ionized and slightly deflected by the laser, are detected down-streams by a time and position resolving detector.

The ion beam is produced by an EBIT (Electron beam ion trap), which enables the investigation of ions in a wide range of charge states. The dynamics of ionization can be studied in dependence of the initial charge state of the ions. In addition, it is possible to measure the sum momentum of the electrons which is determined by the the recoil momentum of the ion. The use of laser fields with relativistic intensities eliminates the possibility of rescattering, thereby enabling a clean study of possible correlations during optical tunnel ionization even with linearly polarized light.

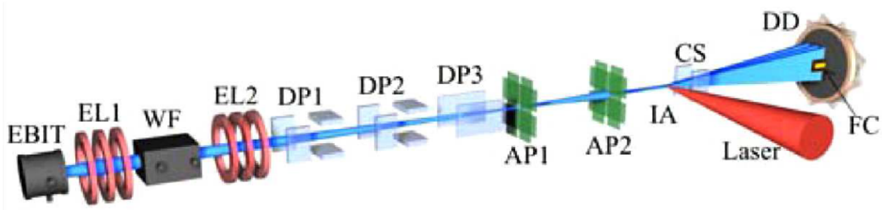

Figure 1: Experimental setup of the ion beam apparatus, which includes an electron beam ion trap (EBIT), two Einzel lenses (EL1, EL2), a Wienfilter (WF), three deflector plates (DF1, DF2, DF3), two adjustable pinholes (AP1, AP2), an interaction region (IA), a charge seperator (CS), a faraday cup (FC) and a delay- line detector (DD). The laser beam is focused vertically linear polarized into the ion beam.

Theoretical Modeling

We have modeled multiple-electron multiphoton ionization based on the theory of optical field ionization. In this investigation, sequential ionization is assumed, i.e. after each ionization step the ion core relaxes to its ground state before the next electron is ionized. The goal this work is to establish a baseline based on the null-hypothesis that ionization proceeds purely sequential, i.e. there are no correlations involved. Experimental results will be confronted with the theoretical predictions. This will allow identifying correlations in the ionization dynamics. Also not included in our present model are relativistic and QED effects. However, at the intensities at which the first experiments will be performed, such effects are not expected to play a significant role.

In contrast to earlier work, we also model the ionization dynamics on a sub-cycle basis, i.e. the possibility that more than one electron ionizes per optical cycle is included. This is important in order to predict the recoil on the ions correctly. The latter can in fact be measured by the deflection of the ions which can be recorded on the positionsensitive detector. Surprisingly, we observed that the recoil on highly charged ions has a strong dependence on the absolute phase (also known as CE phase) and may even be measurable for 20-fs pulses.

References

[1] N. I. Shvetsov-Shilovski, A. M. Sayler, T. Rathje, G. G. Paulus, *Momentum distributions of sequential ionization generated by an intense laser pulse*, Physical Review A (accepted)

Figure 2: T. Rathje and D. Hoff working on the ion beam apparatus.

A Penning trap for multiphoton ionization studies in extreme laser fields

M. Vogel[1], *W. Quint*[1,2], *Th. Stöhlker*[1,2,3], *and G. Paulus*[4]

[1]GSI, Darmstadt; [2]Ruprecht Karls-Universität Heidelberg; [3]Helmholtz-Institut Jena; [4]Universität Jena

We are presently developing a Penning-trap based tool for advanced studies of multiphoton ionization of confined particles and other reactions by highly intense laser light. Particularly, ion manipulation techniques allow control over the particles' localization and spatial density. It is thereby possible to optimize the laser-particle interaction which is of special importance when laser foci are small. Non-destructive detection of reaction products in the trap supports advanced studies by maintaining the products for further studies at extended confinement times of up to hours. The interaction of highly intense radiation

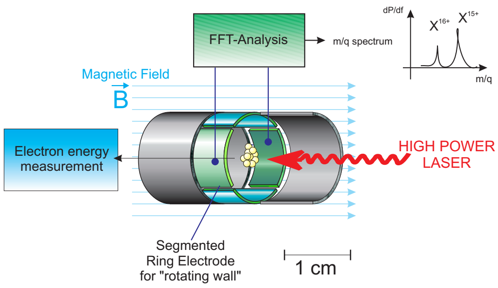

Figure 1: Schematic view of the open-endcap Penning trap with segmented ring electrode for non-destructive mass spectrometry.

with matter and the corresponding non-linear effects have been subject of lively research, both theoretical and experimental, especially in the infrared and visible photon energy regimes. Laser systems capable of producing high intensities also at photon energies in the EUV and (soft) X-ray regime open access to novel effects like non-linear Compton effects or simultaneous elastic and inelastic photon scattering, and allow multiphoton-ionisation experiments in a new domain. Recently, exceptionally strong non-linear photoionization has been observed using high-intesity EUV laser light and been connected with the excitation of collective giant resonances. However, most experiments have so far relied on time-of-flight mass spectrometry or related methods and have been unable to analyse the reaction products with high accuracy, nor were they able to select or prepare products for further studies in a well-defined way.

The present development is a Penning-trap-based experiment for the advanced investigation of multiphoton-ionisation of confined particles by highly intense laser light, e.g. from free-electron lasers. Focus is on control over the confined particles' localization and optimized overlap with the laser light by Penning trap techniques like the use of trap electrodes as "electrostatic tweezers" and by applying a "rotating wall", respectively. Also, the non-destructive detection of reaction products is a central property.

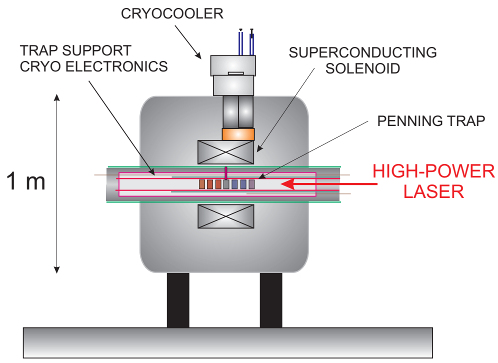

Figure 2: Schematic view of the setup. The Penning trap is located inside a horizontal superconducting magnet and traversed by the laser light. Cryogenic electronics is used for non-destructive spectrometry of confined mass and charge states.

As an application example, the FLASH laser facility at DESY, Germany, is currently capable of producing light down to 4.5 nm (275 eV) in pulses of few fs length with peak powers of around 5 GW with repetition rates of 10 Hz [1]. This laser has previously been used for example to perform soft X-ray laser spectroscopy on highly charged ions, photo-ionization studies [2], photo-dissociation of molecular ions, and in studies of the photoelectric effect at ultra-high intensities. As a user facility, FLASH is capable of providing light under well-controlled conditions to guest experimental setups like the present one. The same is true for the PHELIX laser at GSI, Darmstadt, which can be used for studies with highly charged ions from the HITRAP facility. The potential for further studies with the same setup at even more brilliant light sources is huge, both with regard to the current upgrades to FLASH, the POLARIS laser in Jena, the future XFEL facility [3] with photon energies up to 12.4 keV and other facilites [4].

References

[1] K. Tiedtke et al., New J. Phys. **11** 023029 (2009).

[2] M.C. Simon et al., Phys. Rev. Lett. **105**, 183001 (2010).

[3] XFEL technical design report at http://www.xfel.eu.

[4] W. Ackermann et al., Nature Photonics **1** 336 (2007).

QEDTH report (2010): fundamental physics in strong fields

B. Döbrich[*1,2], *H. Gies*[†1,2], *M. Ipinza*[‡1,2], *F. Karbstein*[1,2], *and L. Roessler*[§1,2]
[1]Helmholtz Institute Jena, Helmholtzweg 4, D-07743 Jena, Germany; [2]Theoretisch-Physikalisches Institut, Friedrich-Schiller-Universität Jena, Max-Wien-Platz 1, D-07743 Jena, Germany

Research in the project QEDTH focused on two major research lines: Spontaneous vacuum decay and high-intensity lasers as a probe for fundamental physics. We summarize our major results and new conceptual developments in the quantum theory of strong electromagnetic fields.

Introduction

Upcoming high-intensity laser systems will be able to probe the quantum-induced nonlinear regime of electrodynamics. So far unobserved QED phenomena such as the spontaneous decay of the quantum vacuum in strong electromagnetic fields in terms of pair production can become accessible. In addition, such laser systems provide for a flexible tool for investigating fundamental physics [1]. Primary goals consist in verifying so far unobserved QED phenomena. Moreover, strong-field experiments can search for new light but weakly interacting degrees of freedom and are thus complementary to accelerator-driven experiments. We review our recent contributions to this field, focusing on spontaneous vacuum decay and a new suggestion for a search experiment for "New Physics" facilitated by high-intensity lasers.

In both subprojects, the principal goal was to predict fundamental physical phenomena that will become accessible in upcoming high-intensity laser facilities. As the ultimate aim is the first discovery of these phenomena, experimentally optimized setups need to be worked out which can become realizable in the near future. Very naturally, this type of research requires a close collaboration and echange of knowledge with experimental groups – a combination which is provided by the Helmholtz Institute Jena and also by a close collaboration with GSI (Darmstadt) and DESY (Hamburg).

On the other hand, theoretical methods for realistic configurations are often not available within the conventional textbook approaches to quantum field theory. This makes conceptual developments necessary on which new powerful and efficient computational methods can be built. Research in this direction is therefore an important cornerstone of this project.

Spontaneous vacuum decay

The instability of the quantum vacuum towards pair production in strong external electric fields is in many respects a paradigmatic phenomenon in quantum field theory going back to the work of Sauter, Heisenberg, Euler, and Schwinger initiating quantum field theory. It is nonperturbative in the coupling times the external field strength. It exemplifies the nontrivial properties of the quantum vacuum, as it manifests the instability of the vacuum against the formation of many-body states. In general, it depends strongly on the spacetime structure of the external field, such that the pair production process is expected to exhibit features of nonlocality, final state correlations and real-time dynamics. Moreover, it is a non-equilibrium process in quantum field theory and as such belonging perhaps to the least-well understood branch of modern field theory. Whereas pair proliferation is expected to occur at the critical Schwinger field strength $E_{\rm cr} = m^2/e \simeq 1.3 \times 10^{18}\mathrm{V/m}$, recent studies have suggested that pair production might become observable already at lower but dynamically modulated field strengths [2, 3, 4, 5, 6, 7, 8]. These estimates of the required field strengths indicate that pair production might already become accessible at future high-intensity laser systems such as ELI or the European XFEL at DESY.

Based on Catalyzed pair production – a mechanism that can significantly enhance pair production suggested earlier by our group [3], we have predicted the probability for vacuum decay for the specific case of the ELI-NP project. This project involves high-intensity lasers and an electron beam line. Our proposal has contributed as a building block to the fundamental physics program of the ELI-NP White Book [9] on the basis of which the first step in the European approval process has been taken.

The new catalysis mechanism for non-perturbative vacuum electron-positron pair production relies on superimposing a plane-wave X-ray probe beam with a strongly focused optical laser pulse, such as is planned at the Extreme Light Infrastructure (ELI) facility. For field strenths below the critical field $E_{\rm cr}$, the standard pair production rate is exponentially suppressed as is typical for a tunneling phenomenon. The crucial point is that the superimposed plane-wave X-ray probe can catalyze vacuum decay by effectively reducing the tunnel barrier. This leads to an exponential enhancement compared to the classic predictions.

Figure 1 shows the number of pairs produced by an incident high-energy photon, traversing a strong electric field of 1 μm length, as a function of incoming photon frequency ω during one day of operation. The strong field is assumed to be produced in a standing-wave mode of a focussed laser beam at an intensity of $I = 10^{24}\mathrm{W/cm}^2$. The two curves correspond to two sets of parameters: 10^{13} high-energy photons per pulse with 1 shot per minute repetition

* Supported by DFG-TR18
† Supported by DFG Gi328/5-1
‡ Supported by DAAD
§ Supported by Carl-Zeiss foundation

rate (lower curve), and 10^{15} high-energy photons per pulse with 100 kHz repetition rate (upper curve). We observe that the threshold of 1 pair per day is crossed right near $\omega \simeq 10\ldots20$MeV. Beyond this threshold, i.e. for higher photon frequency or higher field strength, pair production increases exponentially as is characteristic for a nonperturbative phenomenon.

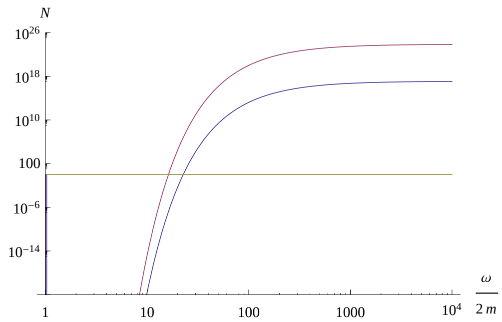

Figure 1: Number of pairs produced by an incident high-energy photon of frequency ω, traversing a strong electric field of 1 μm length, during one day of operation. The strong field corresponds to a laser intensity of $I = 10^{24}$W/cm^2. Parameter sets: 10^{13} high-energy photons per pulse with 1 shot per minute repetition rate (lower curve), and 10^{15} high-energy photons per pulse with 100 kHz repetition rate (upper curve).

Another important progress in this context was the rederivation of the so-called Dirac-Heisenberg-Wigner formalism [10] that allows for a real-time treatment of pair production in arbitrarily time-dependent and inhomogeneous fields. In our work [11], we showed the theoretical equivalence to the widely used quantum kinetic theory in the limit of a purely time-dependent field. Most importantly, our work provided for a first full analysis of this important non-equilibrium process in quantum field theory. In addition to exactly solvable benchmark solutions, we have performed first steps in the direction of a full numerical code which is currently under development.

High-intensity lasers as a probe of fundamental physics

The discovery of the quantum-induced nonlinearities of electrodynamics or vacuum decay as outlined above would verify our most successful theory QED in a parameter region which has been little explored so far. It would complete a quest which has begun in the 1930's. But beyond this, there is another strong motivation to investigate strong-field nonlinearities, since these experiments have a discovery potential of new fundamental physics. This is because the source of fluctuation-induced nonlinear self-interactions of strong electromagnetic fields in vacuum is not restricted to electrons and positrons. Any quantum degree of freedom that couples to photons can lead to modifications of Maxwell's electrodynamics. Strong-field experiments therefore also investigate the general field content of fluctuating particles in the quantum vacuum. If so far unknown particles mediate apparent photon self-interactions in a manner similar to electron-positron fluctuations, they can generate nonlinear corrections analogous to QED processes. Moreover, such hypothetical particles could even be created from strong fields. As high-intensity lasers such as POLARIS at Jena and ELI will substantially push the frontier of strong fields available in a laboratory, they have the potential to search directly and indirectly for new fundamental particles.

In this subproject, we have studied the discovery potential of high-intensity lasers searching for (Pseudo-)scalar particles or corresponding bound states. Such hypothetical particles are often intimately related with the realization of global symmetries in particle physics. They can play the role of condensation channels of symmetry-breaking condensates as well as occur as (pseudo-)Goldstone bosons. A particularly prominent example is given by the axion, which so far provides for the only viable solution to the strong CP problem.

Even though the axion or more generally, axion-like-particles (ALPs), generically develop couplings to photons by means of a dimension-5 operator, giving rise to an effective action of the type

$$\mathcal{L}_{\mathrm{P}} = -\frac{1}{4}F_{\mu\nu}F^{\mu\nu} + \frac{1}{2}\partial_\mu\phi\partial^\mu\phi - \frac{1}{2}m^2\phi^2 + \frac{1}{4}g\phi F_{\mu\nu}\tilde{F}^{\mu\nu} \,, \tag{1}$$

where, ϕ is the axion-like field with mass m and coupling g, direct axion searches are inflicted by a presumably extremely small coupling g. Strongest bounds on this coupling for a wide mass range exist typically in the sub-eV regime and are provided by astrophysical arguments related to stellar cooling or direct solar observation, constraining g to lie below $g \lesssim 10^{-10}\mathrm{GeV}^{-1}$. As these bounds are afflicted by potential model-dependencies, laboratory experiments based on direct and model-independent optical probing have become of particular interest. Most commonly, laboratory searches for ALPs are based on the mixing between axions and photons induced by a macroscopic external magnetic field. In particular, so-called "Light-shining-through-walls" (LSW) setups, where probe photons are converted into ALPs in front of the light-blocking wall and reconverted into photons behind that wall, constitute a promising scheme that is used in many experiments worldwide, as recently reviewed in [12].

On the other hand, the highest field strengths which are obtainable nowadays in a laboratory are present within the focal spots of high-intensity laser systems, calling for proposals of ALP search within high-intensity laser-based setups.

In [13], we have investigated the feasibility of a search for axion-like-particles in a purely laser-based setup. In particular, we have concentrated on modern high-intensity laser systems, since the available field strengths can serve as a lever arm for probing the weak coupling g of axions and axion-like-particles (ALPs) to electromagnetism. We have proposed an unprecedented experimental scheme, which relies on the conversion of a probe beam into an ALP beam in an external laser and its reconversion into a photon beam by a second external laser for Gaussian beam profiles. Taking constraints from possible experimental realizations carefully into account, we have suggested a specific set-up where the ALP induces frequency shifts which are reminiscent to sum-frequency generation and difference-frequency generation known from Nonlinear optics.

The amplitudes of these processes depend sensitively on a resonance condition which can serve as a precise probe of the ALP masses. For optical lasers, such an experimental scheme holds the prospect of providing the strongest laboratory bounds on axion-like-particles in the $\mathcal{O}(\mathrm{eV})$ mass range. In Fig. 2 we display the discovery potential of laser based scenarios. We have concentrated on two setups: one involving the lasers available at the HI Jena (POLARIS and JETI++). The second scenario would involve ELI combined with a present-day optical-parametric-amplification (OPA) system. The latter could be used for frequency tuning such that larger mass ranges can be studied. As laboratory searches with dipole magnets generically probe only lower mass ranges, purely laser-based experiments could complement them in an essential manner.

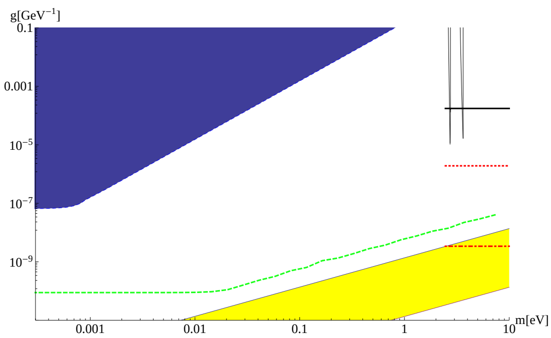

Figure 2: Axion-like-particle exclusion bounds [13] for purely laser-based setups in comparison to searches with dipole magnets. The dark-shaded area in the upper left corner gives the currently best laboratory bounds on axion-like-particles from the ALPS collaboration [14] at DESY, while the best limits on solar axions are provided by the CAST experiment [15], denoted by a green-dashed line. The black wedges denote the exclusion limits for a setup involving the JETI++ and POLARIS laser systems at Jena for one shot at single photon detection. The black line indicates the principle exclusion bounds at this setup by frequency-tuning through optical parametric amplification. The red dotted line corresponds to an estimate for the best obtainable bounds with ELI with a present-day OPA system. The red dot-dashed line suggests the necessary requirements at ELI for testing the parameter regime of typical QCD axion models, which are plotted as a light-shaded band.

In summary, our work suggests that high-intensity lasers are about to evolve into a new tool for fundamental physics.

Conclusions

The prospect of high-intensity laser systems being currently worldwide under intense development is a strong motivation for reconsidering aspects of fundamental physics in strong fields. In particular, the long-standing prediction of quantum-induced nonlinear self-interactions of macroscopic electromagnetic fields and nonperturbative vacuum decay is still awaiting its experimental verification. High-intensity laser systems are good candidates for completing this quest.

In addition to confirming our expectations about quantum properties induced by known degrees of freedom of particle physics, strong-field experiments have recently proved useful to explore new regions in the parameter space of hypothetical new-physics degrees of freedom. Strong fields in combination with optical probes have turned out to be particularly sensitive to weakly coupled particles with light masses in the sub-eV range. High-intensity lasers can add a new chapter to this story by giving experimental access to unprecedented field-strength values. In this project, we have worked out concrete proposals demonstrating that such laser systems may not only discover the QED-induced phenomena for macroscopic fields for the first time, but also search for unexpected optical signals that would point to new particle candidates such as axion-like particles (ALPs). In fact, optical probing using strong fields based on the scheme [13] as reviewed here is presently the only proposal that has the potential to access the QCD axion parameter range in the eV mass range.

References

[1] H. Gies, Eur. Phys. J. D **55**, 311 (2009).

[2] R. Schutzhold, H. Gies, and G. V. Dunne, Phys. Rev. Lett. **101**, 130404 (2008).

[3] G. V. Dunne, H. Gies and R. Schutzhold, Phys. Rev. D **80**, 111301 (2009).

[4] A. Monin and M. B. Voloshin, Phys. Rev. D **81**, 025001 (2010); Phys. Rev. D **81**, 085014 (2010).

[5] T. Heinzl, A. Ilderton and M. Marklund (2010), arXiv:1002.4018.

[6] A. Di Piazza et al., Phys. Rev. Lett. **103**, 170403 (2009).

[7] S. S. Bulanov et al., Phys. Rev. Lett. **104**, 220404 (2010).

[8] V. N. Baier and V. M. Katkov, Phys. Lett. A **374**, 2201 (2010).

[9] http://www.eli-np.ro/documents/ELI-NP-WhiteBook.pdf

[10] I. Bialynicki-Birula, P. Górnicki and J. Rafelski, Phys. Rev. D**44**, 1825 (1991).

[11] F. Hebenstreit, R. Alkofer and H. Gies, Phys. Rev. D **82**, 105026 (2010) [arXiv:1007.1099 [hep-ph]].

[12] J. Redondo and A. Ringwald, arXiv:1011.3741 [hep-ph].

[13] B. Dobrich and H. Gies, JHEP **1010**, 022 (2010).

[14] K. Ehret *et al.*, [ALPS collaboration], Phys. Lett. B **689**, 149 (2010); Nucl. Instrum. Meth. A **612**, 83 (2009).

[15] E. Arik *et al.* [CAST Collaboration], JCAP **0902**, 008 (2009) [arXiv:0810.4482 [hep-ex]].

Atomic Parity–Violation in Highly–Charged Ions*

F. Ferro[†1,2]*, A. N. Artemyev*[1,2]*, A. Surzhykov*[1,2]*, and Th. Stöhlker*[1,2,3]
[1]University of Heidelberg, Germany; [2]GSI, Darmstadt, Germany; [3]Helmholtz-Institut Jena, Germany

The investigation of parity–violation (PV) in atomic transitions between opposite–parity levels is an active and fundamental research area, especially for its implications on the physics beyond the particle Standard Model [1]. In particular, atomic transitions represent the one way to study PV effects originating from neutral currents, i.e. due to the exchange of a Z^0 boson between a nucleon of the nucleus and a bound electron.

Experiments with He–like heavy ions in interaction with high-intensity polarized lasers have the potentiality to further increase the measurement accuracy reached so far. The facilities of GSI, combining the Experimental Storage Ring (ESR) together with the Petawatt High–Energy Laser for Heavy–Ion Experiments (PHELIX) and taking advantage of the precision spectroscopy techniques available for highly-charged ions, offer suitable conditions for future PV experiments.

Effects of the atomic PV Hamiltonian H_{PV} manifest themselves in the mixing η of levels of opposite parity $|\pm>$:

$$i\eta = \frac{< -|H_{PV}|+ >}{E_+ - E_-}\,, \qquad (1)$$

resulting in a state of non-definite parity $|+> + i\eta|->$, that gives rise to observable forbidden transitions.

A precise theoretical knowledge of the level energy splitting $\Delta E = E_+ - E_-$, including its isotopic dependence is the starting point for the design of any forthcoming experiment. In fact, as it straightforwardly follows from Eq. (1), energy degeneracy can amplify the evanescent PV mixing. Since, among the first excited levels of He–like ions, $2^1S_0 \equiv 1s2s^1S_0$ and $2^3P_0 \equiv 1s2p^3P_0$ are closely–lying in energy in ions with atomic number $54 \leq Z \leq 93$ [2], we performed a calculation of electron correlations for several isotope in this Z–interval.

Our theoretical treatment is based on relativistic many–body perturbation theory to all–orders, as a mean to treat electron–electron correlations. We found that $2^1S_0 - 2^3P_0$ degeneracy occurs in the stable isotopes A = 155, 156 of gadolinium (Z = 54), and in the radioactive isotopes A = 219, 220 of protoactinium (Z = 91) [3]. He–like ^{238}U, with ΔE = 2.793 eV, represents an excellent alternative to the short–lived protoactinium nuclides (τ = 2.9 ms), also considering the significant overlap between its atomic wave–functions and the nucleus, which implies a large matrix element $< -|H_{PV}|+ >$.

Among several proposed experimental set–ups, the PV mixing can be measured by means of a stimulated two–photon 2E1 transition from state 2^1S_0 to 2^3P_0, induced by a polarized laser–light. In this specific case, the two levels cannot be degenerate; Rather, their separation should match twice the energy of the photon employed. We found [3] that the He–like isotopes of radon (Z = 86) with $A \leq 212$ and the one isotope of francium (Z = 87, A = 207) allow using laser light in the optical regime. We should mention that also the transuranic isotope of neptunium (Z = 93) with $A \geq 237$ offers these conditions, and is long–lived ($\tau = 2 \cdot 10^6$ yr). The extremely high laser intensity $I \sim 10^{21}$ W/cm^2 makes PV experiments with heavy–ions a rather complicated task, although high–power laser facilities (e.g. PHELIX, POLARIS) are getting closer to the required conditions.

In Ref. [4], we showed that also the levels 2^1S_0 and $2^3P_1 \equiv 1s2p^3P_1$ get rather close in energy (down to a minimum separation $\Delta E \sim$ 0.1eV) for $28 \leq Z \leq 35$, although they are never totally degenerate. The energy splitting of these levels is also affected, in nuclides of nonzero nuclear spin (I $\neq$ 0), by the hyperfine splitting, that reaches its maximum of 150 meV in ^{71}Ga.

A PV mixing between the levels 2^1S_0 and 2^3P_1 is possible through the nuclear–spin dependent component of the weak interaction (dominated by the anapole moment [5]), that connects states of different total angular momentum. By stimulating the transition between the hyperfine levels 2^1S_0 $(F = I)$ and $2^3S_0 \equiv (1s2s)^3S_1$ $(F = I-1, I, I+1)$ with circularly–polarized laser light, an interference term between the allowed M1 multipole and the E1 parity–violating multipole may be observed in the cross section. We theoretically estimated that, by performing such an experiment alternatively with left– and right–polarized light, an asymmetry of order 107 may be expected [6].

The transition energy $2^3S_1 - 2^1S_0$, for Z = 33 is $\sim$ 43eV, thus requiring Extreme Ultra–Violet (EUV) light. The laser intensity needed for such studies is moderate ($\sim 10^{14}$ W/cm^2) and is already achievable with today's EUV laser sources.

References

[1] J. S. M. Ginges and V. V. Flambaum, Phys. Rep. **397** 63 (2004).

[2] F. Ferro et al., Journal of Instrumentation **5** C08006 (2010).

[3] F. Ferro et al., Phys. Rev. A **81** 052112 (2010).

[4] F. Ferro et al., Can. J. Phys. **89** 73 (2011).

[5] V. V. Flambaum et al., Phys. Lett. B **146** 367 (1984).

[6] F. Ferro et al., to be submitted to Phys. Rev. A (2011).

* Work supported by the Helmholtz Gemeinschaft under the project VH–NG–421.

† f.ferro@gsi.de

Effect of the parity nonconservation with laser-induced $2^3S_1 - 2^1S_0$ transition*

V. M. Shabaev[1,2], *A. V. Volotka*[1,3], *C. Kozhuharov*[2], *G. Plunien*[3], *and Th. Stöhlker*[2,4,5]

[1]St. Petersburg State University, Russia; [2]GSI, Darmstadt, Germany; [3]Technische Universität Dresden, Germany; [4]Universität Heidelberg, Germany; [5]Helmholtz-Institut Jena, Germany

Investigations of parity nonconservation (PNC) effects with heavy few-electron ions can provide new opportunities for tests of the Standard Model at low-energy regime. This is mainly due to the fact that, in contrast to neutral atoms, in highly charged ions the electron-correlation effects are suppressed by a factor $1/Z$ and, therefore, can be accounted for by perturbation theory to a high accuracy. Theoretical investigations of the PNC effects with highly charged ions started with Ref. [1], where it was proposed to use close opposite-parity levels 2^1S_0 and 2^3P_1 in He-like ions for $Z \approx 6$ and $Z \approx 29$. Various scenarios appeared later (see, e.g., Ref. [2]) exploited the near-degeneracy of the 2^1S_0 and 2^3P_0 states in He-like ions at $Z \approx 64$ and $Z \approx 90$, where the PNC effects are strongly enhanced.

Here we report the recently suggested scenario [3], where it has been proposed to consider the PNC effect on the laser-induced $2^3S_1 - 2^1S_0$ transition in heavy He-like ions nearby $Z = 64$ (transition energy of about 114 eV) and $Z = 90$ (transition energy of about 240 eV). Because of a large transition energy, until recently the experiments with the laser-induced $2^3S_1 - 2^1S_0$ transition in heavy He-like ions were far from being possible. However, the situation has changed in view of the very significant progress in X-ray laser development. Already now, first X-ray lasers, where photon energies of up to 200 eV can be reached, are getting developed at the PHELIX facility at GSI [4] as well as at the Helmholtz-Institute in Jena. As an alternative scenario, the excitation energy can be obtained by counter-propagating the ultraviolet laser beam with the photon energy in the range from 4 to 10 eV and the He-like ion beam with the energy up to 10.7 GeV/u, which will be available at the FAIR facility in Darmstadt [5].

The cross section for the absorption of a photon with nearly resonant energy $\omega \approx E_{2^1S_0} - E_{2^3S_1}$ and a circular polarization $\lambda = \pm 1$ by a heavy heliumlike ion being initially prepared in the 2^3S_1 state can be written as

$$\begin{aligned} \sigma^{(2^3S_1\to 2^1S_0)} &= \sigma_0^{(2^3S_1\to 2^1S_0)} + \sigma_{\rm PNC}^{(2^3S_1\to 2^1S_0)} \\ &= (1+\lambda\varepsilon)\sigma_0^{(2^3S_1\to 2^1S_0)}\,, \end{aligned} \tag{1}$$

where ε is a parameter which characterizes the relative value of the PNC effect. Utilizing the rigorous formulas for the first-order interelectronic-interaction and QED corrections to the transition amplitudes we have shown that for the $E1$ transition between degenerate levels $(2s, 2p_{1/2})$ these corrections can be accounted for within the zeroth-order approximation in the length gauge, provided the transition energy includes the corresponding corrections. Taking this in account, we derive a simple analytical formula for the PNC correction [3],

$$\varepsilon = -2\xi \frac{3(1+\gamma)\sqrt{1+2\gamma}}{\alpha Z(\sqrt{2(1+\gamma)}-2\gamma)}\,, \tag{2}$$

where $\gamma = \sqrt{1-(\alpha Z)^2}$ and ξ is the PNC mixing parameter.

Table 1: The zeroth-order cross section $\sigma_0^{(2^3S_1\to 2^1S_0)}$, the PNC correction $\sigma_{\rm PNC}^{(2^3S_1\to 2^1S_0)}$, and the parameter ε, for the laser-induced $2^3S_1 \to 2^1S_0$ transition in He-like Gd and Th. The cross sections are given in barn.

Ion	$\sigma_0^{(2^3S_1\to 2^1S_0)}$	$\sigma_{\rm PNC}^{(2^3S_1\to 2^1S_0)}$	ε
$^{158}Gd^{62+}$	4084.1	±2.1	−0.00051
$^{232}Th^{88+}$	1217.6	±0.6	−0.00053

The $2^3S_1 - 2^1S_0$ transition energies are taken from Ref. [6], while for the $2^3P_0 - 2^1S_0$ energies we use conservative estimate $0.074(74)$ eV for Gd and $0.44(40)$ eV for Th. The widths of the levels 2^1S_0 and 2^3S_1 have been calculated within the systematic perturbative QED approach. The results of the calculations for Gd and Th are presented in Table 1. As one can see from the table, in both Gd and Th cases the PNC effect amounts to about 0.05%, which is a rather large value for parity-violation experiments.

The PNC effect is to be measured by counting the intensity difference in the 2E1 decay of the 2^1S_0 state for photon polarizations $\lambda = \pm 1$. The background emission can be separated by switching off the laser light. Changing the photon energy allows one to eliminate the interference with a non-resonant transition via the 2^3P_0 state, which could also be evaluated to a good accuracy if necessary. Moreover, since the 2E1 emission can be measured relative to the intensity of the M1 X-ray line (decay of the 2^3S_1 state), such an experimental scenario appears to be quite realistic.

References

[1] V. G. Gorshkov and L. N. Labzowsky, JETP Lett. **19**, 394 (1974); Sov. Phys. JETP **42**, 581 (1975).

[2] L. N. Labzowsky *et al.*, Phys. Rev. A **63**, 054105 (2001).

[3] V. M. Shabaev *et al.*, Phys. Rev. A **81**, 052102 (2010).

[4] V. Bagnoud *et al.*, Appl. Phys. B **100**, 137 (2010).

[5] Th. Stöhlker *et al.*, Nucl. Instr. Meth. Phys. Res. B **261**, 234 (2007).

[6] A. N. Artemyev *et al.*, Phys. Rev. A **71**, 062104 (2005).

* Work supported by DFG and GSI

ISI cited publications 2010

Bagnoud, V.; Aurand, B.; Blazevic, A.; Borneis, S.; Bruske, C.; Ecker, B.; Eisenbarth, U.; Fils, J.; Frank, A.; Gaul, E.; Goette, S.; Haefner, C.; Hahn, T.; Harres, K.; Heuck, H. M.; Hochhaus, D.; Hoffmann, D. H. H.; Javorkova, D.; Kluge, H. J.; Kuehl, T.; Kunzer, S.; Kreutz, M.; Merz-Mantwill, T.; Neumayer, P.; Onkels, E.; Reemts, D.; Rosmej, O.; Roth, M.; Stöhlker, T.; Tauschwitz, A.; Zielbauer, B.; Zimmer, D.; Witte, K.: **Commissioning and early experiments of the PHELIX facility**, Applied physics B **100**(1), 137–150, 2010.

Bellei, C.; Nagel, S. R.; Kar, S.; Henig, A.; Kneip, S.; Palmer, C.; Sävert, A.; Willingale, L.; Carroll, D.; Dromey, B.; Green, J. S.; Markey, K.; Simpson, P.; Clarke, R. J.; Lowe, H.; Neely, D.; Spindloe, C.; Tolley, M.; Kaluza, M. C.; Mangles, S. P. D.; McKenna, P.; Norreys, P. A.; Schreiber, J.; Zepf, M.; Davies, J. R.; Krushelnick, K. and Najmudin, Z.: **Micron-scale fast electron filaments and recirculation determined from rear-side optical emission in high-intensity laser-solid interactions**, New Journal of Physics **12**, 2010.

Dobrich, B. and Gies, H.: **Axion-like-particle search with high-intensity lasers**, Journal of High Energy Physics, arXiv:1006.5579v1, 2010.

Dunne, G. V.; Gies, H.; Schützhold, R.: **Catalysis of Schwinger vacuum pair production**, Phys. Rev. D **80**(11), 2010.

Ferro, F.; Artemyev, A.; Stöhlker, T.; Surzhykov, A.: **Isotope shift of the 1s2p P-3(0)-1s2s S-1(0) level splitting in heavy He-like ions: Implications for atomic parity-nonconservation studies**, Phys. Rev. A **81**(6), 062503, 2010.

Ferro, F.; Artemyev, A.; Stöhlker, T.; Surzhykov, A.: **Isotopic tuning of the 2 P-3(0)-2 S-1(0) and 2 P-3(1)-2 S-1(0) transition energies in He-like ions for future parity-nonconservation experiments**, Journal of Instrumentation **5,** C08006, 2010.

Geyer, S.; Sokolov, A.; Thorn, A.; Vorobyev, G.; Stöhlker, T.; Kester, O.: **Characterization of the SPARCEBIT at GSI**, Journal of Instrumentation **5,** C10003, 2010. DOI:10.1088/1748-0221/5/10/c10003, OPEN ACCESS.

Gies, H.; Weber, A.: **Geometry-Temperature Interplay in the Casimir Effect**, Int. J. Mod. Phys. A **25**, 2279-2292, 2010.

Hädrich, S.; Rothhardt, J.; Krebs, M.; Tavella, F.; Willner, A.; Limpert, J. and Tünnermann, A.: **High harmonic generation by novel fiber amplifier based sources**, Optics Express **18**(19), 20242-20250, 2010.

Hebenstreit, F.; Alkofer, R. and Gies, H.: **Schwinger pair production in space- and time-dependent electric fields: Relating the Wigner formalism to quantum kinetic theory**, Phys. Rev. D, in press, arXiv:1007.1099 [hep-ph], 2010

Herfurth, F.; Barth, W.; Clemente, G.; Dahl, L.; Gerhard, P.; Kaiser, M.; Kester, O.; Kluge, H. J.; Koszudowski, S.; Kozhuharov, C.; Quint, W.; Sokolov, A.; Stöhlker, T.; Vorobjev, G.; Pfister, J.; Ratzinger, U.; Sauer, A.; Schempp, A.; HITRAP Collaboration: **HITRAP - HEAVY, Highly-charged ions and antiprotons at rest**, Acta physica Polonica B **41**(2), 457– 462, 2010. OPEN ACCESS

Hornung, M.; Bödefeld, R.; Kessler, A.; Hein, J. and Kaluza, M. C.: **Spectrally resolved and phase-sensitive far-field measurement for the coherent addition of laser pulses in a tiled grating compressor**, Opt. Lett. **35**, 2073, 2010.

Hornung, M.; Bödefeld, R.; Siebold, M.; Kessler, A.; Schnepp, M.; Wachs, R.; Sävert, A.; Podleska, S.; Keppler, S.; Hein, J. and Kaluza, M. C.: **Temporal pulse control of a multi-10TW diode-pumped Yb:Glass laser**, Appl. Phys. B **101**, 93, 2010.

Jäckel, O.; Polz, J.; Pfotenhauer, S. M.; Schlenvoigt, H.-P.; Schwoerer, H.; Kaluza, M. C.: **All-optical measurement of the hot electron sheath driving laser ion acceleration from thin foils**, New Journal of Physics **12**, 103027, 2010.

Kaluza, M. C.; Schlenvoigt, H.-P.; Mangles, S. P. D.; Thomas, A. G. R.; Dangor, A. E.; Schwoerer, H.: **Measurement of Magnetic-Field Structures in a Laser-Wakefield Accelerator**, Phys. Rev. Lett. **105**, 115002, 2010.

Kaluza, M. C.; Mangles, S. P. D.; Thomas, A. G. R.; Najmudin, Z.; Dangor, A. E.; Murphy, C. D.; Collier, J. L.; Divall, E. J.; Foster, P. S.; Hooker, C. J.; Langley, A. J.; Smith, J. and Krushelnick, K.: **Observation of a Long-Wavelength Hosing Modulation of a High- Intensity Laser Pulse in Underdense Plasma,** Phys. Rev. Lett. **105**(9), 095003**,** 2010.

Kozhedub, Y. S.; Volotka, A. V.; Artemyev, A. N.; Glazov, D. A.; Plunien, G.; Shabaev, V. M.; Tupitsyn, I. I.; Stöhlker, T.: **Relativistic recoil, electron correlation, and QED effects on the 2p(j)-2s transition energies in Li-like ions**, Phys. Rev. A: Atomic, Molecular, and Optical Physics **81**(4), 042513, 2010.

Kuehl, T.; Aurand, B.; Bagnoud, V.; Ecker, B.; Eisenbarth, U.; Guilbaud, O.; Fils, J.; Goette, S.; Habib, J.; Hochhaus, D.; Javorkova, D.; Neumayer, P; Kazamias, S.; Pittman, M.; Ros, D.; Seres, J.; Spielmann, Ch.; Zielbauer, B.; Zimmer, D.: **Progress in the applicability of plasma X-ray lasers**, Hyperfine Interact. **196** , 233–241, 2010.

Neumayer, P. ; Aurand, B.; Basko, M.; Ecker, B.; Gibbon, P.; Hochhaus, D. C.; Karmakar, A.; Kazakov, E.; Kühl, T.; Labaune, C.; Rosmej, O.; Tauschwitz, A.; Zielbauer, B.; Zimmer, D.: **The role of hot electron refluxing in laser-generated K-alpha sources,** Physics of Plasmas **17**(10), 103103, 2010.

Pfotenhauer, S. M.; Jäckel, O.; Polz, J.; Steinke, S.; Schlenvoigt, H.-P.; Heymann, J.; Robinson, A. P. L. and Kaluza, M. C.: **A cascaded laser acceleration scheme for the generation of spectrally controlled proton beams**, New Journal of Physics **12**, 103009, 2010.

Seres, J.; Seres, E.; Ecker, B.; Hochhaus, D.; Zimmer, D.; Bagnoud, V.; Aurand, B.; Zielbauer, B.; Kuhl, T.; Spielmann, C.: **The super-quadratic growth of high-harmonic signal as a function of pressure reply,** Nature Physics **6**(12), 927–928, 2010.

Shabaev, V. M.; Volotka, A. V.; Kozhuharov, C.; Plunien, G.; Stöhlker, T.: **Parity-nonconservation effect with the laser-induced 2(3)S(1)-2(1)S(0) transition in heavy heliumlike ions.** Phys. Rev. A **81**(5), 052102, 2010.

Sokolov, A.; Herfurth, F.; Kester, O.; Stöhlker, T.; Thorn, A.; Vorobjev, G.; Zschornack, G.: **SPARC EBIT - a charge breeder for the HITRAP project,** Journal of Instrumentation **5,** C11001, 2010.

Surzhykov, A.; Volotka, A.; Fratini, F.; Santos, J. P.; Indelicato, P.; Plunien, G.; Stöhlker, T.; Fritzsche, S.: **Angular correlations in the two-photon decay of heliumlike heavy ions**, Phys. Rev. A **81**(4), 042510, 2010.

Tahir, N. A.; Stöhlker, T.; Shutov, A.; Lomonosov, I. V.; Fortov, V. E.; French, M.; Nettelmann, N.; Redmer, R.; Piriz, A. R.; Deutsch, C.; Zhao, Y.; Zhang, P.; Xu, H.; Xiao, G.; Zhan, W.: **Ultrahigh compression of water using intense heavy ion beams: laboratory planetary physics**, New Journal of Physics **12,** 073022, 2010.

Thorn, D. B.; Geddes, C. G. R.; Matlis, N. H.; Plateau, G. R.; Esarey, E. H.; Battaglia, M.; Schroeder, C. B.; Shiraishi, S.; Stöhlker, T.; Toth, C.; Leemans, W. P.: **Spectroscopy of betatron radiation emitted from laser-produced wakefield accelerated electrons**, Review of Scientific Instruments **81**(10), 10E325, 2010.

Tikhonchuk, V. T.; Schlegel, T.; Regan, C.; Temporal, M.; Feugeas, J.-L.; Nicolai, Ph.; Ribeyre, X.: **Fast ion ignition with ultra-intense laser pulses**, Nuclear Fusion 50, 045003, 2010.

Tikhonchuk, V. T.; Schlegel, T.; Naumova, N.; Sokolov, I. V.; Regan, C.; Temporal, M.; Feugeas, J.-L.; Nicolai, Ph.; Ribeyre; Labaune, C.; Mourou, G.: **Relativistic hole boring and fast ion ignition with ultra-intense laser pulses**, J. Phys.: Conf. Ser. **244**, 022069, 2010.

Trotsenko, S.; Kumar, A.; Volotka, A. V.; Banas, D.; Beyer, H. F.; Brauning, H.; Fritzsche, S.; Gumberidze, A.; Hagmann, S.; Hess, S.; Jagodzinski, P.; Kozhuharov, C.; Reuschl, R.; Salem, S.; Simon, A.; Spillmann, U.; Trassinelli, M.; Tribedi, L. C.; Weber, G.; Winters, D.; Stöhlker, T.: **Spectral Shape of the Two-Photon Decay of the 2 S-1(0) State in He-Like Tin.** Phys. Rev. Lett. **104**(3), 033001, 2010.

Tupitsyn, I. I.; Kozhedub, Y. S.; Shabaev, V. M.; Deyneka, G. B.; Hagmann, S.; Kozhuharov, C.; Plunien, G.; Stöhlker, T.: **Relativistic calculations of the charge transfer probabilities and cross sections for low-energy collisions of H-like ions with bare nuclei**, Phys. Rev. A **82**(4), 042701, 2010.

Weber, G.; Brauning, H.; Hess, S.; Martin, R.; Spillmann, U.; Stöhlker, T.: **Performance of a position sensitive Si(Li) x-ray detector dedicated to Compton polarimetry of stored and trapped highly-charged ions**, Journal of Instrumentation **5,** C07010, 2010.

Zimmer, D.; Ros, D.; Guilbaud, O.; Habib, J.; Kazamias, S.; Zielbauer, B.; Bagnoud, V.; Ecker, B.; Hochhaus, D. C.; Aurand, B.; Neumayer, P. ; Kuehl, T.: **Short-wavelength soft-x-ray laser pumped in double-pulse single-beam non-normal incidence**, Phys. Rev. A **82**(1), 013803, 2010.